

Activation and Inactivation of Hydrogenase Function and the Catalytic Cycle: Spectroelectrochemical Studies

Antonio L. De Lacey and Víctor M. Fernández*

Instituto de Catálisis, CSIC, Marie Curie 2, Cantoblanco, 28049 Madrid, Spain

Marc Rousset

Bioenergetique et Ingénierie des Proteins, Institute de Biologie Structurale et Microbiologie, CNRS, Chemin Joseph Aiguier, 13402 Marseille, Cedex 20, France

Richard Cammack

King's College London, Pharmaceutical Sciences Research Division, Franklin-Wilkins Building, 150, Stamford Street, London SE1 9NH, U.K.

Received November 30, 2006

Contents

1. Introduction	4304
2. The Active Site	4305
2.1. Ni–Fe Hydrogenases	4306
2.2. Fe–Fe Hydrogenases	4307
2.3. Fe–S Cluster-free Hydrogenases	4307
3. The Redox States of the Active Sites	4307
3.1. Ni–Fe Hydrogenases	4308
3.2. Fe–Fe Hydrogenases	4311
3.3. Fe–S-Cluster-free Hydrogenase (Hmd)	4312
4. Activation Processes	4313
4.1. Ni–Fe Hydrogenases	4313
4.2. Fe–Fe Hydrogenases	4315
5. Inactivation Processes	4316
5.1. Ni–Fe Hydrogenases	4316
5.1.1. Inactivation by O ₂	4316
5.1.2. Anaerobic Inactivation by Increased Redox Potential	4317
5.1.3. Inhibition by Carbon Monoxide	4318
5.1.4. Other Inhibitors	4319
5.2. Fe–Fe Hydrogenases	4319
5.2.1. Inactivation by O ₂	4319
5.2.2. Anaerobic Inactivation	4319
5.2.3. Inhibition by CO	4319
5.2.4. Other Inhibitors	4320
6. Catalytic Cycle	4320
6.1. Catalytic Mechanism at the Active Site	4323
6.1.1. Ni–Fe Hydrogenases	4323
6.1.2. Fe–Fe Hydrogenases	4324
6.1.3. Fe–S Cluster-free Hydrogenases (Hmd)	4325
7. Concluding Remarks	4326
8. List of Abbreviations	4326
9. Acknowledgments	4326
10. References	4326

1. Introduction

Hydrogen, the most abundant element in the Universe, is considered to be an environmental friendly energy carrier

because its combustion generates water. Nowadays, owing to the intrinsic stability of the hydrogen molecule, efficient catalysts, mostly based on noble metals such as platinum, are required for the production or utilization of hydrogen at ambient temperatures.¹ In the Biosphere, hydrogen is generated by different metabolic processes in a wide range of microorganisms and also is the energy source of many other living species using hydrogenases as catalysts. Hydrogenases are proteins that harbor Fe or Ni metallic clusters with the special property of reacting with or producing H₂.²

The production of hydrogen from biomass and other organic compounds such as wastes is envisaged as a viable alternative energy source.^{3–24} The more direct use of hydrogenases, to produce hydrogen from water, with the energy of sunlight, has been a dream for many years.²⁵ Ni–Fe hydrogenases adsorbed on carbon electrodes displayed H₂ oxidation rates comparable to electrodeposited platinum and with less sensitivity to poisoning by carbon monoxide.^{26,27} Although these catalysts from some microbial species are fairly durable, their intrinsic instability means that in living systems they are constantly renewed, a situation that is difficult to reproduce in a biotechnological process. In spite of this, hydrogenase covalently immobilized onto carbon supports has shown improved operational stability.²⁸ Moreover, by learning from Nature, it may be possible to develop more efficient biomimetic catalysts for hydrogen activation. Such catalysts, made from abundant metals such as Fe or Ni, could be extensively used in a future energy scenario without flames.^{29,30–40}

Our present knowledge on the structure/function relationships of hydrogenases has benefited from a vast amount of spectroscopic information mainly obtained by EPR, ENDOR, HYSCORE, EXAFS, Mössbauer, and FTIR spectroscopy obtained under redox potential control of the samples. Albracht, Bagley, and co-workers were pioneers in the discovery of spectral features in the infrared associated with carbonyl ligands in the active site of Ni–Fe hydrogenase.^{41,42} The sensitivity of FTIR spectra to the redox state of the hydrogenase active site offered a powerful tool to examine species electrogenerated in situ.⁴³ It is the scope of this review to cover the literature dealing with the different redox states of the active sites of the catalysts Ni–Fe, Fe–Fe, and Fe–S



Antonio L. De Lacey was born in 1966 in Bristol, U.K., and grew up in Madrid, Spain. He received his M.Sc. in Chemistry in 1989 from the Universidad Complutense de Madrid. He obtained his Ph.D. in Chemistry from the Universidad Autónoma de Madrid in 1995, working under the supervision of Prof. V. M. Fernandez at the Instituto de Catálisis (CSIC). From 1996 to 1998 he was a Marie Curie postdoctorate in the group of Prof. C. Bourdillon at the Laboratoire de Technologie Enzymatique (CNRS/ Université de Technologie de Compiègne), France. In 2000 he obtained a Ramon y Cajal Tenure Contract at the Instituto de Catálisis (CSIC), and since 2002 he has been a Staff Researcher there. His research interests are focused on metalloenzyme structure/function relationships, bioelectrocatalysis, and electrode modification for biosensor and biofuel cell applications.



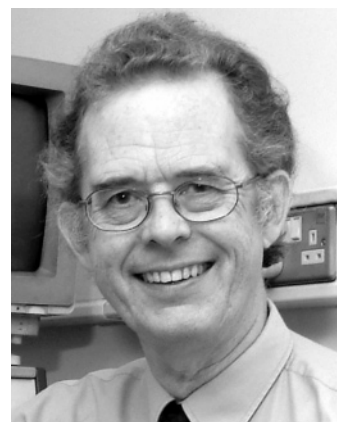
Victor M. Fernández was born in Ronda, Spain, in 1944. He studied Pharmacy at the University of Granada, where he obtained, in 1970, his Ph.D. degree in the Department of Physical Chemistry under the direction of Prof. Dr. J. Thomas. He had postdoctoral stays at the Institute of Physical Chemistry "Rocasolano" of the CSIC in Madrid (Prof. A. Ballesteros), at the Biochemistry Center of the University of Nice (Prof. G. Ailhaud), and at King's College-London (Prof. R. Cammack) with a fellowship from The Royal Society. In 1978 he was appointed as a member of the scientific staff of CSIC at the Department of Biocatalysis of the Institute of Catalysis in Madrid. In 1998 he was promoted to Professor. His main research interest focus is on enzyme redox catalysis. In addition to science, he enjoys family life.

cluster-free hydrogenases, their participation in the activation and inactivation processes of these enzymes, and their participation in the catalytic cycle, with emphasis on the spectroelectrochemical studies. By inactivation we mean the loss of activity, either reversible or irreversible, induced by extrinsic compounds. Activation is often the reversal of this process. For the sake of clarity, Ni–Fe, Fe–Fe, and Fe–S cluster-free hydrogenases will be treated separately although they could be united on the basis of mechanism of reaction and common organometallic chemistry.^{44,45}

The literature citations in the present review will focus on work published since the beginning of the present decade.



Marc Rousset is one of the founders of the BioHydrogen Group of Research, an interdisciplinary federation of forty one French laboratories nationwide specializing in biological hydrogen research. Since 2001, he has been the leader of the Molecular Ecology and Hydrogen Metabolism team, in the laboratory of Bioenergetics and Protein Engineering from CNRS, in Marseille. Since the early 1990s, Dr. Rousset's work has focused on developing genetic tools adapted to *Desulfovibrio* with the aim to study the hydrogen metabolism in this ubiquitous bacteria. These studies resulted in a better understanding of the interconnection of the hydrogen metabolism with the energy generating processes, but the main outcome is most likely the development of the most efficient cellular system for the production of recombinant hydrogenases, making possible molecular studies of these complex metalloenzymes. During the past few years, Dr. Rousset has studied the catalytic mechanism and the proton and electron-transfer processes. Recent work is focused on hydrogenase engineering for biotechnological applications. Dr. Rousset holds a Masters degree in Biochemistry and a Ph.D in Cellular Biology and Microbiology from the University of Provence, Marseille.



Richard Cammack is Professor of Biochemistry at King's College, University of London. At the University of Cambridge he obtained his Bachelor's degree in Biochemistry in 1965 and his Ph.D. in Enzymology in 1968, under the supervision of Malcolm Dixon. At King's College he studies the structure and function of iron–sulfur proteins, using electron magnetic resonance methods.

The multiauthored book *Hydrogen as a fuel. Learning from nature* offers comprehensive reviews of the literature on hydrogenases from the previous century.² We assume these as a starting point, but we will first cover some previous references to provide background for the reader on this very active area.

2. The Active Site

The presence of a redox-active iron–sulfur (Fe–S) cluster at the active site of *Desulfovibrio vulgaris* hydrogenase was proposed by LeGall and co-workers from results obtained by concerted experiments of optical absorption and EPR

spectroscopy on *D. vulgaris* hydrogenases.⁴⁶ Further indirect evidence of the presence of Fe in the active site of *C. pasteurianum* hydrogenase was obtained by experiments by Thauer et al. in which the inhibition of activity by carbon monoxide was reversed by light.⁴⁷

Almost in parallel with the gathering evidence that Fe–S clusters are constitutive redox elements on many hydrogenases, evidence accumulated for the involvement of nickel in the activation of hydrogen by some, but not all, hydrogenases, suggesting the existence of at least two types of active sites in hydrogenases.⁴⁸

2.1. Ni–Fe Hydrogenases

The first crystals of the nickel-containing hydrogenase purified from *D. gigas*, suitable for structure determination, were obtained in the group of E. C. Hatchikian in 1987.⁴⁹ The crystals retained their catalytic activity after incubation under hydrogen, indicating that the crystallization proceeded without damage to the enzyme. This led the way to the first X-ray crystallographic structure of a hydrogenase molecule, in 1995, when Volbeda et al. reported the structure of *D. gigas* hydrogenase at 2.8 Å resolution. The structure revealed the presence of a nickel atom in the active site and eleven iron atoms arranged in a chain of three iron–sulfur clusters: two of cubane type and the middle one a [3Fe-4S] cluster (Figure 1a).⁵⁰

Chemical analyses of unstable metalloproteins are notoriously variable, so it was impressive that the first chemical analysis of the metal content of this enzyme indicated 12 ± 1 Fe atoms per hydrogenase molecule,⁵¹ which proved to be correct. The twelfth Fe atom was found to be associated with electron density located near Ni in the diffraction map.⁵⁰ In a further study, X-ray diffraction data were collected at two wavelengths, just below and above the iron absorption edge, generating a double difference anomalous electron density map. A strong peak was found near the position of the nickel atom and in all positions where Fe have been located in the previous study.⁵² This was a definitive proof of the nature of a dinuclear Fe–Ni center as the active site of nickel-type hydrogenases connected to the surface through the chain of iron–sulfur clusters (Figure 1a). The active site is stabilized in the protein by four cysteine ligands: C530 and C65, which are linked to Ni, and C533 and C68, which are bridging ligands of both Ni and Fe. All of them are strictly conserved, and the two binding motifs CX₂C on the N-terminal side of the peptide and CX₂CX₂H/R on the C-terminal side are always present. These four cysteines play a crucial role in the coordination of the active site, as any attempt to substitute any of them even by serines, the hydroxyl of which is able to link Fe, resulted in an inactive enzyme.^{53–55}

It took one additional year to complete the active site discovery, by FTIR spectroscopy. Using purified *Allochro-matium vinosum* hydrogenase labeled with ¹³C or ¹⁵N, by growth of the bacteria on the appropriate enriched media, it was possible to determine that two cyanides and one carbon monoxide were ligands of the iron atom.^{56,57} The greater mass of ¹⁵N (compared with natural ¹⁴N) led to a shift to lower frequencies of two of the three infrared bands, consistent with the stretching vibration of diatomic molecules containing one nitrogen atom. The greater mass of ¹³C (compared with natural ¹²C) led to shifts in all three bands to lower frequencies. These three diatomic ligands are responsible for the three anomalous bands detected by FTIR, and they are responsible for the low spin character of the ferrous iron

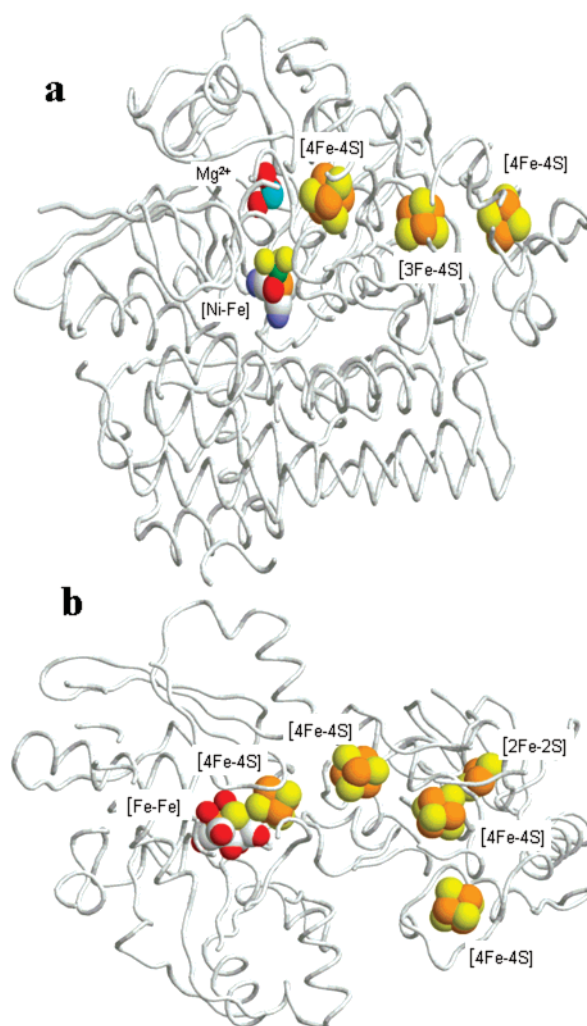


Figure 1. (a) Crystal structure of Ni–Fe hydrogenase from *D. gigas*. The Ni–Fe center is in the center, with the nickel to the front and iron with CN and CO ligands to the back; the peroxo ligand is in red. Coordinates are from the Protein Databank file 1YQ9. Part of the protein has been sliced away to show the metal centers. (b) Crystal structure of *C. pasteurianum* Fe–Fe hydrogenase. Coordinates are from the Protein Databank file 1FEH. The color scheme is as follows: iron, orange; magnesium, cyan; nickel, green; nitrogen, blue; oxygen, red; sulfur, yellow. Plotted with Ras Top 2.1.

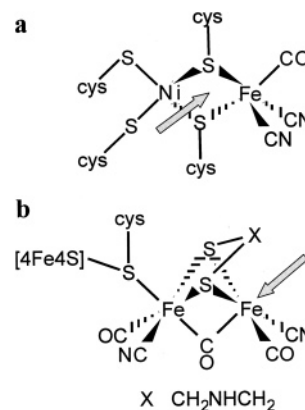


Figure 2. Schemes of the active sites of standard Ni–Fe hydrogenases (a) and Fe–Fe hydrogenases (b). The arrows indicate the vacant coordination site for binding of substrate or inhibitors.

atom of the Ni–Fe center. Figure 2a shows in detail the active site of “standard” Ni–Fe hydrogenases.

Standard Ni–Fe hydrogenases, such as those from *D. gigas*, conserve a histidine residue near to one of the Ni–Fe bridging cysteines. This promotes a hydrogen bond between the histidine and one of the Ni–Fe bridging cysteines, which DFT calculations have predicted would favor the protonation of the N(ϵ) of the histidine.⁵⁸ In bacteria, the synthesis and the building of the Ni–Fe center is a complex process that involves a minimum of seven maturation enzymes plus carbamoyl phosphate, GTP, and ATP.^{59,60} Carbamoyl phosphate is the precursor of the cyanide group, while the origin of the carbonyl is still unknown.⁶¹ Specific enzymes are responsible for nickel transportation and insertion.^{62–64} The loading process of the iron is still unknown, but Fe insertion precedes Ni in the steps of metal center assembly.⁶⁵ Specific chaperones also interact tightly with the large subunit all along the maturation process, especially with one of the active cysteine ligands, cysteine-241 in *E. coli* hydrogenase 3 (C65 in *D. gigas* numbering),⁶⁶ maintaining the active site cavity open and accessible for maturation proteins. This cysteine ligand is released after the completion of the maturation process, which terminates by the cutting of the C-terminal peptide after the histidine or arginine at the terminal coordination motif CX₂CX₂H/R.⁶⁷ This indicates that the final coordination sphere of the active site is generated at the very end of the process.

Some nickel–iron hydrogenases have a cysteine sulfur replaced by a selenium atom.⁶⁸ The first crystal structure of a Ni–Fe–Se hydrogenase isolated from *Desulfomicrobium baculatum* showed the Se atom of a Ni coordinated to selenocysteine instead of the sulfur atom of the equivalent cysteine at the active site in the Ni–Fe enzyme. In addition, the [3Fe-4S] cluster found in Ni–Fe hydrogenases is replaced by [4Fe-4S] in this selenoenzyme, and the putative magnesium ion in the large subunit is replaced by iron.⁶⁹

2.2. Fe–Fe Hydrogenases

Fe–Fe hydrogenases are so-called because they do not contain nickel. They are phylogenetically unrelated to Ni–Fe hydrogenases.⁶³ The Fe–Fe hydrogenases that catalyze H₂ evolution, for example from fermentative bacteria such as *Clostridium pasteurianum*,⁷⁰ have almost identical active sites and proton and electron transfer chains to the enzymes involved in the uptake of H₂, such as those from sulfate-reducing bacteria,⁷¹ despite the differences in their cellular localization, respectively, in the cytoplasmic or periplasmic external spaces (Figure 1b). The active site involved in the activation of H₂ in Fe–Fe hydrogenases consists of a specialized dinuclear iron cluster bonded to the protein backbone through just one cysteine sulfur, which bridges to a [4Fe-4S] cluster. The two iron atoms in the pair are bridged by a ligand (designated “X” in Figure 2b) that appears from the crystal structure to be either 2-azapropane-1,3-dithiol or possibly propane-1,3-dithiol.^{70,71} This ligand has never been isolated, and its biosynthetic pathway is unknown. Fe–Fe hydrogenases also contain a low-spin Fe(II) with CO and CN[−] ligands at the active site (Figure 2b). As Ni–Fe and Fe–Fe hydrogenases are not phylogenetically linked, the strict conservation of low spin Fe(II) with CO and CN[−] coordination indicates that these elements are essential to biological hydrogenase activity.⁷²

2.3. Fe–S Cluster-free Hydrogenases

A totally distinct type of hydrogenase is the enzyme, N⁵,N¹⁰-methylene-tetrahydromethanopterin dehydrogenase

(formerly EC 1.12.99.4, now EC 1.12.98.2), isolated from methanogenic bacteria,⁷³ that also catalyzes the evolution and uptake of hydrogen.⁷⁴ The name is abbreviated to Hmd, for H₂-forming methylenetetrahydromethanopterin dehydrogenase. The enzyme is phylogenetically unrelated to the Fe–Fe hydrogenases and Ni–Fe hydrogenases and is formed by two identical subunits of 38 kDa.⁷⁴ The mechanism of reaction of this enzyme is completely different from those of the other transition-metal-containing hydrogenases discussed above, as it catalyzes the specific, direct reduction of N⁵,N¹⁰-methylene-tetrahydromethanopterin with hydrogen.⁷⁵ In contrast to the Ni–Fe and Fe–Fe hydrogenases, the Fe–S cluster free hydrogenase is highly active in the catalytic dehydrogenation of N⁵,N¹⁰-methylene-tetrahydromethanopterin, (methylene-H₄MPT) although it does not catalyze the reduction by hydrogen of NAD⁺ or NADP⁺ or conventional hydrogenase acceptors such as viologen dyes.⁷³ It also differs from Ni–Fe and Fe–Fe hydrogenases in that the purified enzyme *per se* did not catalyze the conversion of *para*-H₂ to *ortho*-H₂ or the D/H exchange reaction; these reactions specifically require the presence of methylene-H₄MPT.⁷⁶ The specific activity of Hmd purified under anaerobic conditions is very high, about 12.5 μ mol of methylene-H₄MPT reduced per second per milligram of protein.⁷³ The purified enzyme was stable in aerobic conditions, but in cell extracts, it was rapidly inactivated under oxidizing conditions,⁷⁷ which explains why no iron was initially detected in this enzyme and it was formerly described as a “metal-free” hydrogenase.⁷⁴ Later, Thauer and co-workers confirmed that the enzyme from *Methanobacter marburgensis* does not contain iron–sulfur clusters although it harbors an iron-containing cofactor.^{77,78} The Hmd is dimeric and contains two iron atoms per homodimer with the cofactor essential for activity.⁷⁹ FTIR spectroscopy revealed the presence of two CO's bound to the iron at an angle of 90°.^{77,80} The crystal structures of the enzyme from *Methanocaldococcus jannaschii* and *Methanopyrus kandleri* have been recently reported.⁸¹ An interesting feature is that, in the apoprotein–cofactor complex model, the cofactor points to the –SH of the Cys 176, which is essential for the enzyme activity.⁸¹ Recent X-ray absorption spectroscopy of the *M. marburgensis* and *M. jannaschii* hydrogenases indicates the presence of two CO's, one or two N/O atoms coordinated to each Fe, and one S, probably provided by a cysteine.^{80,82} After exposure of the enzyme to CO, the number of iron ligands increased, suggesting that in the native enzyme there is one vacant coordination site on the iron, which is presumably the site of H₂ binding.⁸³

3. The Redox States of the Active Sites

The bimetallic complexes, Fe–Fe or Ni–Fe, that form the active site in the two main types of hydrogenases are able to acquire several stable structures, either catalytically active or inactive, within a relatively narrow range of redox potentials. This functional property is probably due to the combination of different types of ligands that coordinate to the metals: thiolates (good π -donors), cyanides (good σ -donors), and carbonyls (good π -acceptors). Their special coordination may act as an electronic buffer that facilitates the entry and exit of electrons in the active site. However, biomimetic compounds of the active site of hydrogenases with this type of ligation do not share this characteristic to the same extent.^{35,37–38,84–87} A possible explanation for this is that the flexible environment generated by the protein matrix around the active site does not stabilize a particular

redox state but facilitates redox transitions. Besides, the acid–base functional groups of adjacent amino acid residues should allow the coupled transfer of protons and electrons at the active site that favors the thermodynamics of the redox transitions.⁸⁸

Although the kinetics of the hydrogenase reaction itself are too rapid to be examined, different redox states of the active site of hydrogenases have been identified by redox titrations of hydrogenases followed by different spectroscopic techniques. EPR spectroscopy gave the first hints of the existence of redox chemistry of the active site, with the detection of several states with a paramagnetic metal. The introduction of FTIR spectroscopy for hydrogenase characterization was a great step forward, as all redox states of the active site can be detected and usually distinguished by this technique, and the enzymes are amenable to examination by *in situ* spectroelectrochemistry.⁴³ Other spectroscopic techniques, such as EXAFS, ENDOR, and Mössbauer, have given valuable information on structural and electronic aspects of the active site, and the changes upon oxidation and reduction.⁸⁹

3.1. Ni–Fe Hydrogenases

With the irrefutable demonstration of Ni as a component of hydrogenase by the observation of hyperfine splittings in the EPR spectrum of ⁶¹Ni -substituted enzyme,⁹⁰ three different laboratories almost simultaneously submitted three reports in 1982, on the redox-sensitivity of nickel in hydrogenases as seen by EPR spectroscopy.^{90–92} Two types of EPR signals are detected for the oxidized active site of “standard” Ni–Fe hydrogenases (such as those from the *Desulfovibrio* genus—*D. gigas*, *D. fructosovorans*, and *D. vulgaris*—and others from the purple photosynthetic bacteria *A. vinosum* and *Thiocapsa roseopercina*). The EPR signals were designated Ni-A (or Ni_u by some authors; *g*-values for *D. gigas*: 2.31, 2.23, 2.01) and Ni-B (or Ni_r by some authors; *g*-values for *D. gigas*: 2.33, 2.16, 2.01). A third EPR signal, named Ni-C (*g*-values for *D. gigas*: 2.19, 2.16, 2.01) appeared gradually upon reduction with H₂ or chemical reductants. These names, which originally referred to EPR signals, became attached by extension to particular *states* of the nickel and, after the structure was determined, to states of the dinuclear center as a whole. It soon emerged that the EPR signals correlated with particular catalytic properties. Fernandez et al.⁹³ showed that the Ni-C state corresponds to a catalytically *active* state, whereas the Ni-A and Ni-B states were inactive toward hydrogen.⁹³ These states will be described in section 4.1. A number of additional states were observed by EPR and FTIR, which were given additional suffixes, including “R” for reduced (and in some cases “r” for ready) and “S” for EPR-silent.

Redox titrations of these EPR-detectable species established the following: (a) one-electron reduction of the Ni-A and Ni-B states gave EPR-silent states; (b) Ni-B is two electrons more reduced than Ni-A; (c) Ni-C is two electrons more reduced than Ni-B; (d) one-electron reduction of Ni-C results in another EPR-silent state named as Ni-R (Ni-SR by some authors); (e) all these redox equilibria are pH-dependent; thus, protons as well as electrons are involved in these processes.^{91,94–101}

A valuable feature of the EPR spectra of hydrogenases is the spin coupling between paramagnetic centers, which leads to splitting or distortion of the spectra. These features differ from the complexities introduced by the superimposition of

multiple isolated paramagnets, which can be resolved by recording spectra at different microwave frequencies. To first order, the *g*-factor anisotropy scales with microwave frequency, but the magnitude of the splitting scales with magnetic field. An example of a spectrum showing the effects of spin–spin interactions is observed at temperatures below 10 K, termed the “split Ni-C” signal. Its presence correlates well with redox conditions where the NiFe center gives the Ni-C signal, and the proximal [4Fe-4S] cluster is reduced, leading to the conclusion that it arises from a dipolar coupling between them.¹⁰² This was confirmed by measurements at different microwave frequencies. The spectrum was simulated by a combination of exchange and dipolar interactions.¹⁰³ Another type of spectrum displaying the effects of spin–spin interactions has been observed in the oxidized state of some, but not all, Ni–Fe hydrogenases. This spectrum in the hydrogenase from *A. vinosum* was demonstrated to disappear during progressive reduction of the enzyme, with a simultaneous increase in the signal from the oxidized [3Fe-4S] cluster.¹⁰⁴ EPR spectra at multiple frequencies¹⁰⁵ indicated that it is due to interaction between the oxidized cluster and an unidentified paramagnet.¹⁰⁵ The redox properties of the signal were investigated by redox titrations; the potential of the interacting paramagnet did not correspond to that of the NiFe center, nor did it correlate with the state of activation of the enzyme. However, the midpoint potential of the interacting species showed a pH-dependence indicating a proton-dependent reduction.¹⁰⁶ The properties of this signal might be explained if there was an iron ion in the metal-binding site, corresponding to the magnesium-binding site in *D. gigas* hydrogenase (Figure 1a). Such an iron atom was observed in the structure of the Ni–Fe–Se hydrogenase of *Dm. baculatum*, and it was tentatively assigned as iron by anomalous dispersion.⁶⁹ No such spin–spin interaction would be expected in the latter enzyme, since there is no [3Fe-4S] cluster, but if there were such a center in the hydrogenase of *A. vinosum*, this might provide an explanation for the spin-coupled signals.

Bagley and co-workers showed that the FTIR bands due to the intrinsic diatomic ligands of the active site of *A. vinosum* Ni–Fe hydrogenase shift in frequency upon reducing/oxidizing the sample with H₂/O₂.⁴² This observation led to FTIR-spectroelectrochemical characterization of *D. gigas* hydrogenase, which allowed identification of all redox states of the active site, not only paramagnetic ones, and to determination of the redox and acid–base equilibria that relate them to each other.¹⁰⁷ It emerged that FTIR, observing the vibrational frequencies of the CN and CO ligands, monitors changes in the electron density of the active site Fe, while EPR principally monitors the electronic state of the Ni. As redox titrations by FTIR correspond, to within experimental error, with those done by EPR spectroscopy (Figure 3), it can be concluded that the bimetallic complex of the active site behaves as one electronic entity. Figure 4 shows the equilibria that correlate the different redox states of the active site that have been detected spectroscopically for “standard” Ni–Fe hydrogenases. The iron atom of the active site is low-spin Fe(II) in all states, as observed from ENDOR and EPR spectroscopy,^{108–109} which is in agreement with its coordination by the strong-field and π -accepting CO and σ -donating CN[−] ligands. Moreover, the frequency shifts observed in FTIR of the active site upon change of redox state are considerably smaller than those observed in model complexes for a Fe(II)/Fe(III) transition.¹¹⁰ Therefore, changes

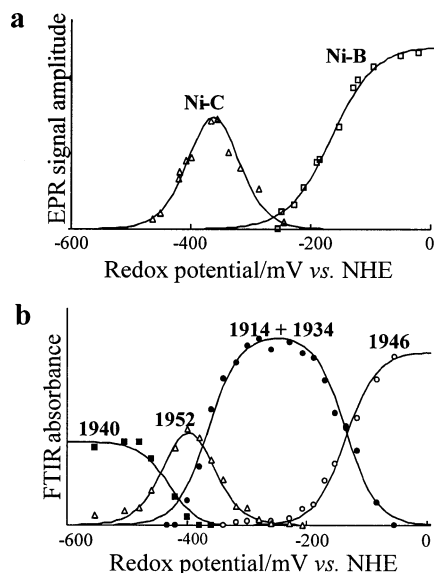


Figure 3. Redox titrations of the active site of *D. gigas* hydrogenase monitored by EPR (data from ref 91) and FTIR (data from ref 107): open triangle, Ni-C signal; open square, Ni-A signal; closed squares, 1940 cm^{-1} band; open triangles, 1952 cm^{-1} band; closed circles, 1914 + 1934 cm^{-1} band; open circles, 1946 cm^{-1} band. Reprinted from ref 304, Copyright 2005, with permission from Elsevier B.V.

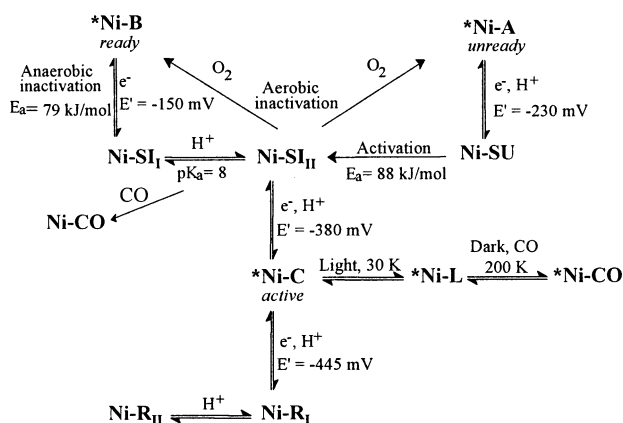


Figure 4. Scheme of the different redox states of the active site of standard Ni–Fe hydrogenases. The paramagnetic EPR-active states are marked with an asterisk. The formal redox potentials (at pH 8.0), energy barriers, and pK_a correspond to those measured by FTIR-spectroelectrochemistry of *D. gigas* hydrogenase in ref 107. Ni-A, Ni-B, Ni-SU, Ni-SI_I, Ni-SI_{II}, Ni-CO, and Ni-R are named in some references as Ni_u, Ni_r, Ni_u-S, Ni_r-S, Ni_a-S, Ni-S-CO, and Ni-SR, respectively.

of formal oxidation state in the active site should take place in the Ni atom, as expected from the redox titrations of the Ni-EPR signals. A different coordination of Fe in the active site of the Ni–Fe hydrogenase from *D. vulgaris* Miyazaki, consisting of two CO and one SO ligands, has been reported based on X-ray crystallography and mass spectrometry (pyrolysis-MS and TOF-SIMS) analysis; however, the FTIR and EPR spectra were essentially identical to the one reported for other standard Ni–Fe hydrogenases.^{111,112}

The EPR spectra of paramagnetic states of hydrogenases are typical of Ni(III) ions, although the spectra of Ni(I) are not too dissimilar.^{100,113} Nickel-K edge XAS spectra are consistent with the formal oxidation state of the Ni metal oscillating from Ni(III) in all EPR active states to Ni(II) in the EPR silent states.¹¹⁴ It is currently a matter of debate if the Ni(II) states are high spin or low spin.^{108,115–122}

More recently, FTIR-spectroelectrochemical experiments have been performed for other “standard” hydrogenases such as those from *D. fructosovorans*, *A. vinosum*, and *D. vulgaris* that have confirmed the previous results.^{123–125} Only slight differences in frequency values (Table 1), redox potentials, and pH-dependence have been observed, which clearly suggests that the structure and functionality of the active site in most Ni–Fe hydrogenases are equivalent. Thus, there is little evidence to support the early reports of important differences between Ni–Fe hydrogenases from *D. gigas*^{50,52} and *D. vulgaris*.^{111,126} The vibrational shifts and the intensities of the infrared bands of the diatomic ligands are related to the π -electron mobility or delocalization in the active site, which is the result of the electronic changes of its metal atoms and their interactions with the active site cavity. In a study to evaluate the influence of the protein background on the structure and functionality of the active site of *D. fructosovorans* Ni–Fe hydrogenase, it has been clearly demonstrated that the mutations modifying the hydrogen bonding of the CN^- ligands with neighboring amino acid residues induced modifications of the FTIR spectra.¹²⁷ The removal of a serine that is hydrogen bonded to cyanides (Figure 5) leads to a shift to lower frequencies, while the introduction of a new serine residue that could establish new hydrogen bonds produced shifts to higher frequencies. Similar frequency shifts have been reported for biomimetic Fe complexes upon hydrogen bonding of the cyanide ligands.²⁹ It is interesting to note that, whatever the mutation, the frequencies of the two CN^- ligands shifted in the same direction and with similar magnitude, indicating that the two CN^- oscillators remained coupled.

Some other redox states of the active site have been detected that are not functional. These include states of enzyme inhibited by carbon monoxide or enzyme irradiated by visible/near-ultraviolet light at low temperatures (see Figure 4). By EPR experiments, two Ni-CO (called Ni-S-CO by some authors) states have been proposed: one a paramagnetic state and the other EPR silent.^{128–129} Two Ni-CO states have been detected by FTIR, but both of them were shown to be EPR-silent, with the difference between them being the redox state of the proximal [4Fe-4S] cluster, which affects slightly the electron density in the active site.¹²³ Irradiation of Ni-C with visible light at low temperature allows detection of another redox state named as Ni-L, which is generally considered to be a Ni(I) state.^{112,130–132}

Light irradiation of a coordination complex may have a number of different consequences, including displacement of a ligand and electron transfer. It is now commonly considered that the light-sensitivity of the Ni-C state corresponds to the displacement of a hydrogen-containing species near the dinuclear [Ni–Fe] site.¹³³ One of these species has been proposed to be a bridging hydride between the nickel and the iron ions in the Ni-C state.¹³⁴ Besides, it has also been proposed that a proton transfer involving the terminal cysteine ligand of the nickel ion also accompanies the photoprocess. The cancellation of the exchange coupling with the proximal [4Fe-4S] cluster¹³⁴ suggested that the group that loses the proton during this process was the cysteine 65 thiol (in *D. gigas* numbering).^{108,135} This hypothesis is supported by the site-directed mutagenesis experiments conducted on glutamate 25 of *D. fructosovorans* hydrogenase. The substitution of this residue by an aspartate resulted in the loss of the photosensitivity of the reduced [Ni–Fe] center, associated with the presence of spectroscopic features

Table 1. Vibrational Frequencies (cm⁻¹) of the Diatomic Ligands of the Active Site at Different Redox States of Ni–Fe Hydrogenases Measured by FTIR^a

redox state	<i>A. vinosum</i> ^b		<i>D. gigas</i> ^c		<i>D. fructosovorans</i> ^d		<i>D. vulgaris</i> ^e	
	$\nu(\text{CO})$	$\nu(\text{CN})$	$\nu(\text{CO})$	$\nu(\text{CN})$	$\nu(\text{CO})$	$\nu(\text{CN})$	$\nu(\text{CO})$	$\nu(\text{CN})$
Ni-A	1945	2082, 2093	1947	2083, 2093	1947	2084, 2096	1956	2084, 2094
Ni-B	1943	2079, 2090	1946	2079, 2090	1946	2080, 2091	1955	2081, 2090
Ni-SU	1948	2088, 2100	1950	2089, 2099	1950	2091, 2101	1946	2075, 2086
Ni-SI _I	1910	2052, 2067	1914	2055, 2069	1913	2054, 2069	1922	2056, 2070
Ni-SI _{II}	1931	2073, 2084	1934	2075, 2086	1933	2074, 2087	1943	2075, 2086
Ni-C	1951	2073, 2085	1952	2073, 2086	1951	2074, 2086	1961	2074, 2085
Ni-R _I	1936	2059, 2072	1940	2060, 2073	1938	2060, 2074	1948	2061, 2074
Ni-R _{II}	1921	2048, 2064	1923	2050, 2060	1922	2051, 2067	1933	nd
Ni-R _{III}	1913	2043, 2058	nd	nd	nd	nd	1919	2050, 2065
Ni-CO	1929, 2060	2069, 2082	1932, 2056	2070, 2083	1931, 2055	2069, 2084	nd	nd
Ni-L	1898	2044, 2060	nd	nd	nd	nd	nd	nd

^a nd = not determined. ^b Data from refs 42 and 124. ^c Data from ref 107. ^d Data from ref 123. ^e Data from ref 125.

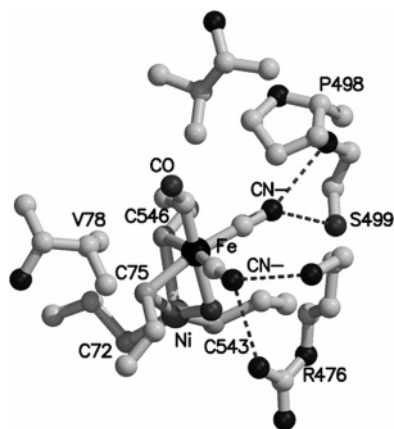


Figure 5. Scheme showing the active site of *D. fructosovorans* Ni–Fe hydrogenase and neighboring amino acid residues that have been exchanged by mutations. The dashed lines indicate putative hydrogen bonds. Coordinates were obtained from the crystal structure at 2.54 Å resolution of *D. gigas* hydrogenase (Brookhaven Protein Data Bank). Reprinted with permission from ref 127. Copyright 2003 Springer-Verlag.

comparable with the Ni-L signals. This observation suggests that the mutation induced modifications that maintain the active site in a conformation close to that of the illuminated state. It was then supposed that the shortening by one C–C bond of the lateral chain of glutamate brings the carboxylate closer to the cysteine 72 Ni-thiolate ligand (cysteine 65 in *D. gigas* numbering) by 0.5 Å, thereby preventing the protonation of that cysteine.¹³⁶ Beyond the illuminated state, this study shows that the EPR and FTIR signals are sensitive not only to the redox state of the Ni and Fe but also to the hydrogen-bond network that exists in the active site cavity, and that any modification, even at a remote distance, might influence the spectroscopic features.

Other studies of the redox states of the active site have been reported for “nonstandard” Ni–Fe hydrogenases such as Ni–Fe–Se hydrogenases, aerobic hydrogenases, and hyperthermophilic hydrogenases. In Ni–Fe–Se hydrogenases, a cysteine of the protein sequence is replaced by a selenocysteine.¹³⁷ EPR studies with the ⁷⁷Se-enriched hydrogenase of *Dm. baculatum*¹³⁸ and Ni and Se X-ray absorption spectroscopy of the same enzyme¹³⁹ demonstrated that the selenocysteine is coordinated to the Ni site. These suggestions were confirmed when the crystallographic structure was obtained, which showed that the selenocysteine replaces one of the terminal cysteines coordinated to the Ni atom. This selenocysteine corresponds to cysteine 530 in *D.*

gigas numbering, which is at H-bond distance from the proton-transfer gate glutamate 18.⁶⁹ This structural difference greatly affects the functionality of the active site, changing the activity kinetics and redox potentials of the states.^{140–141} For instance, oxidized states with paramagnetic Ni are seldom detected for *Dm. baculatum* and *D. vulgaris* Ni–Fe–Se hydrogenases, and the aerobically isolated enzyme is mostly EPR-silent. Moreover, the Ni–Fe–Se hydrogenases require little if any reductive activation in order to initiate H₂-production or H₂-uptake,^{142–144} although reduction with methyl viologen is required for H⁺/D⁺-exchange activity.¹⁴⁵ A Ni-C type signal is detected for reduced, active hydrogenase,^{142–144,146} and also a paramagnetic Ni-CO state.¹⁴⁷ However, the FTIR spectra of both oxidized and reduced samples are quite complex and dissimilar from those of “standard” Ni–Fe hydrogenases.¹¹⁷ High resolution ¹H electron nuclear double resonance (ENDOR) of deuterium exchanged Ni–Fe and Ni–Fe–Se hydrogenase took advantage of the replacement of a Ni sulfur ligand by selenium for the assignment of ENDOR signals to the six protons of the cysteines bound to nickel.¹⁴⁸

The oxygen-tolerant hydrogenases, particularly the cytoplasmic soluble hydrogenase from *Ralstonia eutropha* which uses NAD⁺ as its direct electron acceptor, are of great interest, owing to their stability and insensitivity to inhibition by O₂ and CO. So far, there is no crystallographic structure for a hydrogenase of this type, but although the amino-acid sequences indicate a Ni–Fe center, spectroscopic studies clearly suggest a different active site structure from those already determined. First of all, no significant EPR signals due to the Ni–Fe active site are detected for aerobically isolated or active soluble hydrogenase (SH or SHase).¹⁴⁹ Thus, the active site is probably Ni(II)–Fe(II) in most redox states; only after prolonged reduction of the hydrogenase does a Ni-C type signal start to appear.¹⁵⁰ Second, FTIR spectroscopy combined with chemical analysis suggests that there are three CN⁻ and one CO ligands coordinated to the Fe atom and a fourth CN⁻ coordinated to the Ni atom.¹⁵¹ Third, XAS studies point to coordination of Ni predominantly by hard (O,C) ligands rather than soft (S) ligands.^{152,153} FTIR-spectroelectrochemical studies of *R. eutropha* SHase by van der Linden et al. indicated that aerobically isolated enzyme was converted to an active state by reduction at –316 mV vs NHE and that this step is irreversible under anaerobic conditions. A more reduced state was obtained at –391 mV that was equivalent to hydrogenase reduced by 1 atm of H₂. This latter redox transition was reversible under anaerobic conditions.¹⁵² Figure 6 shows the scheme of the redox states

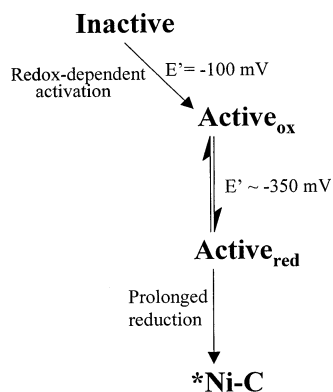


Figure 6. Redox states of the SH from *R. eutropha* detected by different spectroscopic techniques (FTIR, EPR, and XAS). The paramagnetic EPR-active state is marked with an asterisk.

of the active site of *R. eutropha* SHase according to the FTIR-spectroelectrochemical experiments and other redox controlled spectroscopic measurements.

The β -proteobacterium *R. eutropha* hosts two other oxygen-tolerant hydrogenases: the membrane-bound hydrogenase (sometimes referred to as MBH or MBHase) and the H₂-sensing regulatory hydrogenase (RH or RHase).¹⁵⁴ Hydrogen sensors, which have a regulatory function but little activity in H₂ production or consumption, have also been described for *Rhodobacter capsulatus* and *Bradyrhizobium japonicum*.⁶³ Since the early studies by EPR and redox titrations,¹⁵⁵ there have been few spectroscopic studies of the active site of MBHase, in comparison with many on the regulatory hydrogenase. Recently, an FTIR spectrum of MBHase, as isolated, has been reported, which also shows the typical CO and CN⁻ coordination of “standard” hydrogenases.¹⁵⁶

The active site of the RHase seems to be structurally similar to those of “standard” Ni–Fe hydrogenases although it is isolated as a dimer of heterodimers. Pierik et al. characterized the active states of RHase by FTIR and EPR.¹⁵⁷ They concluded from the FTIR experiments that the active site has one CO and two CN⁻ ligands, as in standard Ni–Fe hydrogenases.¹⁵⁷ Redox titration by FTIR-spectroelectrochemistry confirmed the existence of only two redox states: one comparable to Ni-SI in “standard” Ni–Fe hydrogenases and another reduced paramagnetic state similar to Ni-C. The formal midpoint redox potential E_m was estimated to be -322 mV vs NHE at pH 7.0, which is similar to those reported for the Ni-SI/Ni-C transition (A. L. De Lacey, unpublished results). An ENDOR and HYSORE study of the regulatory hydrogenase by Lubitz and co-workers concluded that a hydrogen exchangeable with D₂O or D₂ was in a bridging position between the active site metals in the reduced state,¹⁵⁸ a structural characteristic assigned also to the Ni-C state of “standard” Ni–Fe hydrogenases.^{112,122,135,159–161} An XAS study of the regulatory hydrogenase concluded that the active site Ni has fewer S ligands and more (O, N) ligands than “standard” hydrogenases.¹⁶² However, site-directed mutagenesis on RHase reported by Friedrich and co-workers indicated that the four cysteine residues adjacent to the Ni atom are indispensable for correct assembly of the protein, with three of them being indispensable for Ni-binding.⁵⁵ More recently, iron-EXAFS spectra of this sensor hydrogenase have suggested a new type of iron–sulfur cluster, which may be a [4Fe-3S-3O], in addition to two standard [2Fe-2S] clusters.¹⁶³

A complete EPR study has been reported for the Ni–Fe “sulfhydrogenase” from the hyperthermophilic Archaeobacterium *Pyrococcus furiosus*. Paramagnetic signals due to active site Ni were observed upon heat-induced reduction by an internal substrate, some of which are similar to those described for “standard” Ni–Fe hydrogenases, while others reflected temperature-dependent transitions between states.¹⁶⁴ FTIR spectra for reduced and oxidized samples of this hydrogenase have been reported, showing bands due to the CO and CN⁻ ligands of the active site. However, these spectra revealed a great deal of heterogeneity in the samples, which made interpretation difficult.¹¹⁷ On the other hand, EPR spectra of the hydrogenases from the hyperthermophilic bacterium *Aquifex aeolicus* were typical of the Ni-B and Ni-C states of standard hydrogenases, but not Ni-A.¹⁶⁵

3.2. Fe–Fe Hydrogenases

The different redox states of the active site of Fe–Fe hydrogenases, also named the H-cluster, were studied first by EPR spectroscopy. Two oxygen-sensitive hydrogenases, I and II, were purified anaerobically from *C. pasteurianum* and gave rhombic signals typical of $S = 1/2$ systems, with the highest g -value at 2.10, which were assigned to the active sites. Redox titrations showed that these signals disappeared upon reduction with an apparent formal potential of about -400 mV vs NHE at pH 8.0 to give diamagnetic states.¹⁶⁶ These redox states have been named H_{ox} and H_{red}, respectively. Hydrogenases, such as those from *D. vulgaris* and *D. desulfuricans*, which retain activity after aerobic purification,^{167–169} were found to comprise an inactive and diamagnetic state of the H-clusters; only after reductive treatment under anaerobic conditions did these hydrogenases become active, and the H_{ox} signal was detected. Patil et al. showed that during activation a transient rhombic EPR signal with the highest g -value at 2.06 appeared, reaching its maximum at about -110 mV at pH 7.0.¹⁶⁷ In addition, Pierik et al. reported that the reduction step from this transient state to H_{ox} was irreversible under anaerobic conditions.¹⁶⁸

Subsequent FTIR measurements showed that Fe–Fe hydrogenases contain low-spin Fe with CO and CN⁻ ligands in their H-cluster.^{170–171} The FTIR bands due to these ligands shift in frequency upon changes of the redox state of the hydrogenase (Table 2). In a recent publication, redox titrations followed by FTIR in a spectroelectrochemical cell were reported for *D. desulfuricans* hydrogenase.¹⁷² Figure 7 shows a scheme of the redox transitions of this hydrogenase starting from the aerobic inactive state, H_{inact} (also known as H_{ox}^{air}). The measured formal potentials in this work correlate reasonably well with those measured by EPR^{166–168} and with redox potential-controlled Mössbauer data¹⁷³ taking into account the differences in pH conditions and hydrogenase origin.

Reduction from diamagnetic H_{inact} to the transient paramagnetic state, H_{trans}, is a one-electron step^{168,172} and reversible.¹⁷² Mössbauer spectroscopy indicates that in both states the [Fe–Fe]_H subcluster is diamagnetic and that the reducing equivalent is used to reduce the [4Fe-4S]_H subcluster.¹⁷³ The presence of the strong CO and CN⁻ ligands in the [Fe–Fe]_H subcluster ensures that these Fe atoms are low-spin, and it is difficult to assign their oxidation state from the isomer shift parameter of Mössbauer spectra.¹⁷³ However, DFT calculations of models of the H_{inact} state support a Fe(II)–Fe(II) configuration of the [Fe–Fe]_H subcluster.^{174–175}

Table 2. Vibrational Frequencies (cm⁻¹) of the Diatomic Ligands of the Active Site at Different Redox States of Fe–Fe Hydrogenases Measured by FTIR^a

redox state	<i>D. vulgaris</i> ^b		<i>D. desulfuricans</i> ^c		<i>C. pasteurianum</i> I ^d	
	$\nu(\text{CO})$	$\nu(\text{CN})$	$\nu(\text{CO})$	$\nu(\text{CN})$	$\nu(\text{CO})$	$\nu(\text{CN})$
H _{inact}	1847, 1983, 2007	2087, 2106	1848, 1983, 2007	2087, 2106	nd	nd
H _{trans}	nd	nd	1836, 1977, 1983	2075, 2100	nd	nd
H _{ox}	1940, 1965	2079, 2095	1802, 1940, 1965	2079, 2093	1802, 1948, 1971	2072, 2086
H _{ox} -CO	1811, 1964, 1971, 2016	2088, 2096	1810, 1963, 1971, 2016	2088, 2096	1810, 1971, 1974, 2017	2077, 2096
H _{red}	1894, 1916, 1965	2041, 2079	1894, 1916, 1965	2040, 2079	nd	nd
H _{sred}	nd	nd	1883, 1932, 1955	nd	nd	nd

^a nd = not determined. ^b Data from ref 171. ^c Data from ref 172. ^d Data from ref 288.

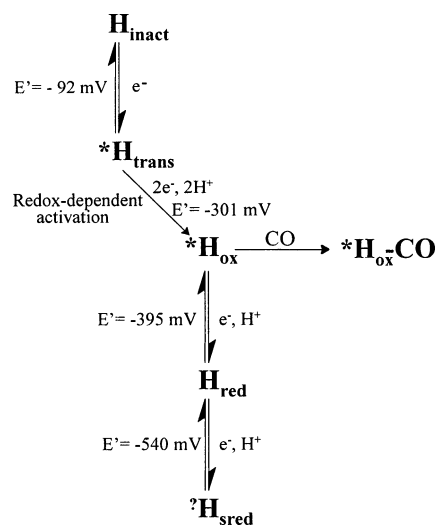


Figure 7. Scheme of the different redox states of the active site of Fe hydrogenases. The paramagnetic EPR-active states are marked with an asterisk (the EPR spectra of H_{sred} have not been reported). The formal redox potentials (at pH 8.0) correspond to those measured by FTIR-spectroelectrochemistry of *D. desulfuricans* Fe hydrogenase in ref 172.

Diferrous dithiolates with cyanide and carbonyl ligation that bear a structural and spectroscopic relationship to the H_{inact} state have been synthesized.^{176–177}

By an irreversible redox-dependent process, the H_{ox} state is obtained from the H_{trans} state. Mössbauer and ENDOR studies of *C. pasteurianum*¹⁷⁸ and *D. vulgaris*¹⁷⁹ Fe–Fe hydrogenases have indicated that in H_{ox} the [4Fe-4S]_H subcluster is diamagnetic and that the unpaired spin is centered at one Fe site of the [2Fe-2S] subcluster; thus, the subcluster is in a mixed-valence state, either Fe(II)–Fe(III) or Fe(II)–Fe(I). As the magnetic coupling between the cubane and diiron subclusters is low in this state, it was proposed that the paramagnetic atom was the Fe distal to the cubane.^{178–179} A FTIR characterization under redox potential control of *D. desulfuricans* hydrogenase allowed assignment of the infrared bands of the H_{ox} state to the different CO and CN⁻ ligands of the H cluster, and the authors proposed a distal Fe(I) and a proximal Fe(II) as the electronic configuration of the [2Fe-2S] subcluster.¹⁸⁰ FTIR characterization of biomimetic models of this subcluster^{181,182} and calculated vibrational frequencies from DFT studies^{174,175,183} have confirmed this electronic configuration.

Redox titrations followed by EPR^{166,168} or FTIR¹⁷² indicate that H_{red} is one electron more reduced than H_{ox}. The main structural difference between the two states is that, upon reduction, the bridging CO ligand shifts toward the distal Fe, acquiring a semibridging coordination *trans* to the vacant coordination site.¹⁸⁴ As H_{sred} is a diamagnetic state^{179,185–186}

and Mössbauer studies clearly indicated that the [4Fe-4S]_H subcluster is in the oxidized +2 state and that the two Fe atoms of the other subcluster are spectroscopically indistinguishable,^{178,179} there are two possible electronic configurations for the [2Fe-2S]_H subcluster: an antiferromagnetically coupled Fe(I)–Fe(I) state or a Fe(II)–Fe(II) state with a coordinated hydride. The first synthetic models reported for the diiron subcluster were stable dinuclear complexes Fe(I)–Fe(I),^{187–189} however, Fe(II)–Fe(II) complexes with a hydride ligand have been reported more recently.^{190–193} In addition, a diferrous complex featuring a semibridging CO ligand has also been reported.¹⁹⁴ Fe¹⁺Fe¹⁺ models were favored by DFT calculations reported by several authors,^{174,195,196} whereas Liu and Hu proposed that H_{red} was a mixture of Fe(I)–Fe(I) and Fe(II)–Fe(II)–H⁻ configurations based on the comparison of the calculated vibrational frequencies for models of both options with the experimental ones reported for *D. desulfuricans* Fe–Fe hydrogenase.¹⁷⁵

At very low redox potentials, a super-reduced state of the H-cluster, named H_{sred}, was detected by infrared spectroelectrochemistry. This state was not very stable and tended to decompose before it could be reoxidized to H_{red}. As no other data are available from other spectroscopic techniques, this reduction step cannot be ascribed to the cubane or diiron subclusters of the active site.¹⁷² A CO-inhibited state of the H-cluster was detected several years ago by EPR spectroscopy of various Fe–Fe hydrogenases.^{166,169} Mössbauer and ENDOR spectroscopic studies suggested that the CO-inhibited state has a similar electronic configuration to H_{ox},^{173,178} thus, we can consider the former also as a Fe(II)Fe(I) subcluster with an oxidized cubane subcluster and name it as H_{ox}-CO. DFT studies^{174–175} and FTIR characterization of synthetic models^{181,182} support this electronic configuration for the dinuclear iron subcluster. Nevertheless, a recent computational study proposed that the unpaired spin in H_{ox}-CO is significantly delocalized between the two Fe atoms.¹⁸³ Sulfur K-edge XAS measurements, combined with density functional calculations on a synthetic H-cluster model, suggested that there is extensive delocalization of frontier molecular orbitals of the iron and sulfur atoms of both subclusters.¹⁹⁷ In fact, EPR spectra of ⁵⁷Fe-enriched enzyme from *D. desulfuricans* in the H_{ox}-CO state are consistent with a magnetic hyperfine interaction of the unpaired spin with all six Fe atoms of the H cluster.¹⁹⁸

3.3. Fe–S-Cluster-free Hydrogenase (Hmd)

As for the iron atom of Ni–Fe hydrogenase's active site, and in contrast to the Fe–Fe hydrogenases, the iron of the cofactor of Hmd is not redox active and under all conditions tested remains EPR-silent. Spectroscopic data obtained by FTIR, Mössbauer, and XAS indicate that the iron is in a

low-spin state, although it is yet unknown if it is Fe(II) or Fe(I).¹⁹⁹

A CO-inhibited state and a CN-inhibited state have been observed by FTIR spectroscopy. These extrinsic ligands bind most probably to the H₂-reactive site of the iron atom.⁸²

4. Activation Processes

Most hydrogenases are not fully active when isolated aerobically, requiring a reductive process to become catalytically competent. The nature of this activation process depends on the structure of their active site, but in all cases, it involves a structural reorganization of the active site from a form stable in air to the form that is catalytically active for H₂-uptake/production.

4.1. Ni–Fe Hydrogenases

As mentioned above, standard Ni–Fe hydrogenases have several different oxidized states with different kinetic behavior: Fernandez et al.⁹³ postulated that the difference between the Ni-A and Ni-B states was associated with a difference in activation behavior. Ni–Fe hydrogenases, such as that from *D. gigas*, are isolated aerobically and are inactive in assays where H₂ is the reductant or in hydrogen–deuterium and hydrogen–tritium exchange assays.^{200–202} To restore the activity requires reducing conditions and the absence of O₂.²⁰³ A confusing feature of this reductive activation was the highly variable nature of the onset, rate, and extent of activation. There is often a lag of minutes or even hours before the enzyme starts to become active, and the extent of activation depends on the history of the enzyme sample. Moreover, once reductive activation has started, some of the hydrogenase activity reappears quickly, but restoration of full activity takes several hours at ambient temperatures. Fernandez et al.²⁰⁴ explained these effects in terms of a minimum of three forms of the enzyme: the *active* state, the *ready* state that becomes active quickly upon reduction, and the *unready* state that needs a long period of incubation under reducing conditions before becoming active. It was proposed that in the oxidized enzyme the H₂-binding site (now known to be the Ni–Fe center) is inactive or blocked, so that activation of the hydrogenase requires electron transfer into the H₂-binding site from elsewhere in the electron-transfer chain. According to this scheme, it would require the presence of only a few active hydrogenase molecules to start the reduction process, after which the activation would be autocatalytic. The reductant could be a low-potential electron-donor compound, or another electron source such as an electrode. In concentrated hydrogenase preparations, activation could be by intermolecular electron transfer between hydrogenase molecules or by residual traces of low-potential carriers such as cytochrome *c*₃ or ferredoxin from the bacterial source material. Otherwise, in the assay, the activating compound could be a reduced electron acceptor such as methyl viologen.

Fernandez et al.⁹³ showed that, for *D. gigas* Ni–Fe hydrogenase, the relative proportions of the Ni-A and Ni-B EPR signals correlated with the proportion of the enzyme in the unready and ready states. For both the ready and unready states, the first step of activation is the reduction of Ni(III) to Ni(II) as observed by EPR.^{91,93,99} Subsequent X-ray diffraction studies showed that the main structural difference between oxidized and reduced states of the active site is that, in the latter, the oxygen species that bridges the metals has

disappeared, and the Ni–Fe distance is 0.25 Å shorter. Therefore, it was assumed that reduction of the oxidized states triggered the removal of a bridging oxygen species, which allowed H₂ binding to the active site and catalytic turnover.⁶⁹ This was confirmed by an ¹⁷O ENDOR study in which the signal due to Ni-A labeled with ¹⁷O was lost upon reductive activation to Ni-C.²⁰⁵

FTIR-spectroelectrochemical studies of different hydrogenases have indicated that one-electron reduction of Ni-A and Ni-B leads to two different states: Ni-A leads to the Ni-SU (named Ni_a-S by other authors) state, and Ni-B leads to Ni-SI.^{107,123–125} Enzyme in the Ni-SI state is active, whereas the Ni-SU state is still inactive.^{107,206–209} The activation process represents a gradual, spontaneous conversion of the Ni-SU to the active Ni-SI state, a step that is rate-limiting and entropic.^{93,107,209} Two forms of the Ni-SI state are in pH equilibrium, as detected by FTIR (Figure 4).^{123–125} The unprotonated form is named Ni-SI_I (Ni_r-S by other authors), whereas the protonated form is named Ni-SI_{II} (Ni_a-S by other authors). It has been proposed, on the basis of the difference in vibrational frequencies of the diatomic ligands of the Fe atom, that the pH equilibrium involves protonation of a terminal cysteine of the Ni.^{107,125,210} Although crystal structures of these states have not been reported, some computational studies consider that one of the Ni-SI forms still has an oxygen ligand bound to the active site.^{211,212} However, there are experimental results which support that Ni-SI has lost the bridging oxygen ligand, whereas it is still present in Ni-SU. First of all, an X-ray absorption spectroscopic study of *A. vinosum* hydrogenase concluded that a Ni–O bond was present in Ni-SU, which disappeared in the four coordinated Ni-SI states of the active site.²¹³ Second, FTIR-spectroelectrochemical characterization of *D. fructosovorans* hydrogenase in the presence of carbon monoxide, which is a competitive inhibitor of hydrogenases, showed that extrinsic CO binds to Ni-SI but not to Ni-A, Ni-B, or Ni-SU. The interpretation of this result was that the inhibitor can only bind to the Ni atom when the bridging oxygen species is removed from the active site, thus leaving a vacant coordination site.¹²³ In addition, several theoretical studies support models of the Ni-SU and Ni-SI states with and without a bridging oxygen species, respectively.^{214–217} Therefore, it is generally considered that the “ready” behavior of Ni-B is due to fast removal of the bridging oxygen species upon reduction, whereas the “unready” behavior of Ni-A is due to slow removal of the bridging oxygen species upon reduction.

The early studies on the Ni–Fe hydrogenases used electron-transfer mediator dyes such as the low-potential methyl viologen (*E*_m –440 mV vs NHE), which presumably supplies electrons to the iron–sulfur clusters,⁹³ and the oxidant 2,6-dichloroindophenol (*E*_m +217 mV). In these experiments, it is difficult to control the rate of the reaction, and, at higher potentials, there is the likelihood of exposure to O₂. Recently, electrochemical studies by Armstrong's group, of hydrogenases adsorbed onto the surface of a carbon electrode in an anaerobic chamber, have provided an incisive method to control the applied redox potential and observe the activation and inactivation processes. The rate of diffusion of substrate molecules to the enzyme is controlled by the rotation rate of the electrode. Electrons are supplied by the electrode directly to the electron-transfer chain, in all states of the enzyme. The electric current is a measure of catalytic activity, and the driving force, voltage, can be altered at will.

Rapid changes in applied voltage can be used to measure the instantaneous activity of the enzyme, while chronoamperometry, in which a current is measured during the steady application of a voltage, can be used to follow activation and inactivation.^{218,219} In this way, it was shown that conversion of “ready” to “active” *A. vinosum* hydrogenase is rate-limited by the redox potential, which suggests that the reduction of Ni-B to Ni-SI is the slow step of the process.²⁰⁶ A contrast may be drawn with the “unready” hydrogenase, where an analogous study indicated that a fast and reversible electrochemical step precedes the rate-determining step of the activation process, independent of the redox potential.²⁰⁹ The latter result confirmed the previous FTIR-spectroelectrochemical study of *D. gigas* hydrogenase that showed that Ni-A could be reduced to Ni-SU in a reversible way and that the rate-limiting step of the activation process was conversion of Ni-SU to the active states, independent of redox potential and pH.¹⁰⁷ The redox titration of the Ni-A/Ni-SU couple followed by FTIR has also been reported for the *D. fructosovorans*, *A. vinosum*, and *D. vulgaris* Ni-Fe hydrogenases.^{123–125} The pH dependences of the formal measured redox potentials for these standard Ni-Fe hydrogenases are indicative of a one-electron/one-proton step, which is in agreement with the small shift in the frequencies of the CO and CN⁻ ligands, which means a small change in the electron density of the active site. One exception is the case of the *D. vulgaris* Miyazaki F hydrogenase, in which the shift of the CO and CN⁻ bands is larger and follows a different pattern than the other standard Ni-Fe hydrogenases. Therefore, Fitchner et al. suggested that this enzyme has a different electronic configuration for the Ni-SU state which could account for the faster activation process of Ni-A.¹²⁵

Kurkin et al. studied the activation of Ni-A and Ni-B with H₂ by stopped-flow FTIR spectroscopy.²⁰⁷ In that work, they observed that the Ni-A state was converted to the active states very slowly, whereas the latter converted quickly, after a lag phase of a few seconds, through which a specific reduction of the enzyme happens. In agreement with previous proposals, the authors concluded that H₂ was not able to reduce the active site directly in the Ni-A and Ni-SU states, whereas it did reduce the active site in the Ni-B state after a few seconds' lag phase.²⁰⁷ De Lacey et al. applied FTIR-spectroelectrochemistry to *D. gigas* hydrogenase in H₂O/D₂O and found that for the activation of Ni-A there is no significant kinetic effect of the solvent or the pH.²²⁰ This suggests that the rate-limiting step for Ni-A activation is not the protonation of the bridging ligand. The cause of the different kinetic behaviors of Ni-A and Ni-B has been interpreted in recent years as a difference of the nature of the oxygen species in both states. In a single-crystal EPR study on this enzyme, the *g*-tensors of the Ni-A and Ni-B states were determined as having a similar orientation and the authors proposed that the difference of the *g_y* values between Ni-A and Ni-B could be explained by a protonation of the bridging Ni-Fe ligand.²²¹ A single-crystal ENDOR study of the same enzyme in the Ni-B state detected a proton hyperfine tensor with an orientation compatible with the calculated one by DFT studies of oxidized active site models with a μ -hydroxo bridging ligand.²²² In the same work it was observed that this hyperfine coupling was either missing or decreased in magnitude in Ni-A, confirming a structural difference of the active site involving the bridging ligand. However, HYSORE spectroscopy and H/D exchange do

show an exchangeable proton in Ni-A that can be assigned to the bridging ligand, although in this case it has a different orientation than that in Ni-B or it is of a different type.²²³ Quantum calculations of EPR parameters of models of Ni-Fe hydrogenase active sites and comparison with experimental values suggested a hydroxo bridging ligand in Ni-B, and an oxo or peroxy ligand in Ni-A.^{224–225} The authors argued that the latter ligand would be removed from the active site with more difficulty. In a similar study reported by Stadler et al., the authors were in agreement with the Ni-B assignment but favored a hydroxo ligand for Ni-A instead of an oxo ligand because it modeled better the experimental paramagnetic and structural parameters.²¹⁶ Stadler et al. proposed that the difference in electronic structure between Ni-A and Ni-B could be explained by a different protonation level of a cysteine ligand of the Ni atom and that the kinetic barrier for Ni-A activation was caused by a different orientation of a nearby glutamate residue, which impeded fast removal of the bridging hydroxo ligand as a water molecule.²¹⁶ Bleijlevens et al., on the basis of the H/D hyperfine coupling of the EPR signals, proposed a bridging oxygen species between the metals in the Ni-A state, and a terminal hydroxo ligand to the Ni in Ni-B. This terminal ligand would be pointing toward the H₂-transport channel, which should facilitate its exit from the active site during activation.²²⁶ A difficulty with these proposals in which the Ni-A and Ni-B states both have a single bridging oxygen atom is that they do not explain why it is impossible to interconvert the states without prior reduction.

The proposal that hydrogenases in the Ni-A state have a peroxy bridging ligand was supported by a recent X-ray diffraction study of *D. fructosovorans*.²²⁷ In the Ni-B state, an oxygen species was clearly shown in the bridging position between the metals. A similar conclusion was drawn for the Ni-B state of *D. vulgaris* Miyazaki F hydrogenase.²²⁸ A recent further refinement of X-ray diffraction data from *D. gigas* and *D. fructosovorans* hydrogenases, mainly in the unready state, suggested that the bridging ligand in Ni-A is probably monatomic rather than diatomic.²²⁷ The protein molecules in the crystals were not in a homogeneous state, and clear featureless electron-density difference maps were only obtained when the bridging ligand was modeled as 70% (hydro-)peroxy and 30% (hydro-)oxo, which is consistent with the relative abundance of the Ni-A/Ni-B species as measured by EPR. In addition, the refinement data suggested partial oxidation of a bridging cysteine to sulfenic acid/sulfenate.²²⁷ Ogata et al. have also reported the crystallographic structure of *D. vulgaris* Miyazaki F hydrogenase in the Ni-A state with a diatomic bridging ligand, which was assigned to a dioxygen with one of the oxygen atoms oriented toward the H₂-transport channel. The authors suggested that this orientation is responsible for the blocking of the active site toward reaction with H₂ in the active site.²²⁸

Marine organisms such as *D. gigas* are sometimes exposed to air, which would be expected to convert their periplasmic hydrogenases to the unready state. If the activation of the unready states by reducing agents in vitro is very slow, taking many hours at ocean temperatures, it is a question as to how their hydrogenases become reactivated, if indeed they do. Based on these structural data, it has been proposed that the kinetic barrier of Ni-A is either due to the difficulty of the release of H₂O₂ from the active site^{227,229} or, alternatively, due to the reduction of a sulfenate to thiolate in one of the cysteine ligands and liberation of H₂O.²²⁹ Lamle et al. showed

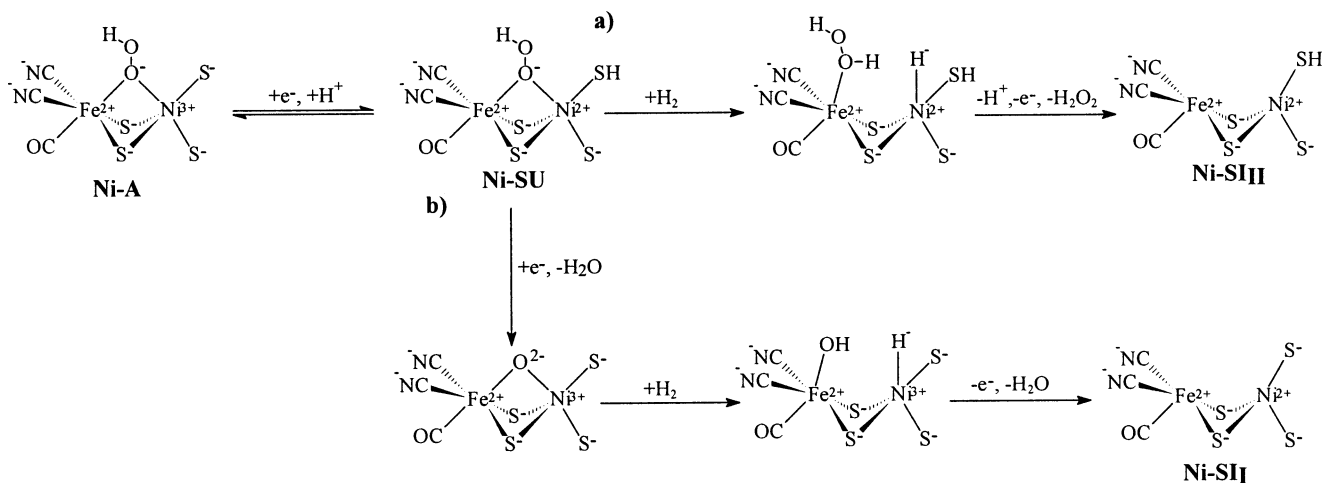


Figure 8. Simplified scheme of the possible mechanisms of activation of the active site of standard NiFe hydrogenases proposed by Jayapal et al. in ref 212 considering a hydroperoxo bridging ligand for Ni-A.

that *A. vinosum* hydrogenase could be reactivated more rapidly by H_2 or CO, in a complex multistep process. They proposed that the rate-limiting step is an internal rearrangement of the oxygen-containing species that allows its subsequent and fast displacement by H_2 or CO.²⁰⁹ In a recent computational study, the activation by H_2 was simulated, assuming a hydroperoxo bridging ligand in the Ni-A state and a hydroxo ligand for Ni-B. Two pathways of activation of Ni-A were considered, one in which H_2O_2 is liberated from the active site and another in which two H_2O molecules are liberated.²¹² It was concluded that the second mechanism had a transition state with a kinetic barrier more similar to the experimental results.^{107,204,229} Figure 8 shows the simplified scheme of both proposed mechanisms. Another recent computational study combined with quantum refinement of the previously reported crystallographic data of the “unready” oxidized states of *D. fructosovorans* suggests that in that structure there is a mixture of states of the active site. The best fit was obtained with a μ -hydroxo bridging ligand and partial oxidation of one terminal and one bridging ligand. Nevertheless, in this work a minor conformation with a bridging peroxo ligand was not excluded.²³⁰ The activation mechanism has also been studied for *Thiocapsa roseopericina* hydrogenase by kinetic measurements.^{231–232} These authors proposed that there is an autocatalytic step in the activation process.

The SHase of *R. eutropha*, despite being active in the presence of O_2 , needs to be activated when it is isolated in air. This activation process is different from those of “standard” Ni–Fe hydrogenases because, as mentioned before, there are no Ni-A nor Ni-B states in this hydrogenase and FTIR measurements indicated a different structure of the active site^{149,151} and XAS.^{152,153,233} Activation of aerobic SHase (in a heterotetrameric form) is rapid (within a few seconds) in the presence of sodium dithionite or catalytic amounts of NADH.^{234,235} Interestingly, the enzyme may be activated by NADPH as well as NADH, but only in a hexameric form of the enzyme that incorporates a dimer of subunits I_2 , which probably bears the NADPH binding site.²³⁶ In an FTIR-spectroelectrochemical cell, the active state of soluble H_2 ase was obtained by adjusting the potential of an aerobic sample to -316 mV, with this step being irreversible in the absence of O_2 .¹⁵⁰ This result is in general agreement with the titration of the activity for the same hydrogenase reported previously by Petrov et al.,²³⁴ although they

estimated a midpoint redox potential for activation of -100 mV. A mechanism for the activation process has been proposed, taking into account the structural characteristics of the active site of this hydrogenase, namely that the Fe atom has one CO and three CN^- ligands and the Ni atom has one additional CN^- , as deduced from FTIR spectroscopy,¹⁵¹ and that the Ni has predominant coordination by C or O ligands in the aerobically oxidized state, as deduced from XAS spectroscopy.¹⁵² According to this hypothesis, upon reductive activation with NADH, electrons are transferred to the Ni–Fe active site via a $[2Fe-2S]$ cluster and this causes removal of an oxygen species from terminal coordination to Ni, leaving a vacant site for hydrogen binding and cleavage.^{150,152,233,237}

4.2. Fe–Fe Hydrogenases

For those Fe–Fe hydrogenases that can be reductively activated, the rate of activation is much more rapid than that for most Ni–Fe hydrogenases.^{140–169} Redox titrations of these hydrogenases followed by different spectroscopic techniques have concluded that this activation step involves the reduction of the H_{trans} state to the H_{ox} state^{167,168,172,173} and that this step is irreversible under anaerobic conditions.^{168–172} From the Mössbauer characterization of *D. vulgaris* hydrogenase, Pereira et al.¹⁷³ concluded that in this activation step there was not a net reduction of the H cluster; hence, they proposed a conformational change during conversion that promoted the transfer of one electron from the $[4Fe-4S]_H$ subcluster to the $[2Fe]_H$ subcluster.²³⁸ Other authors have proposed that in the inactive states a ligand is terminally bound to the distal Fe of the $[2Fe]_H$ subcluster that is removed upon reduction, leaving a vacant site for H_2 binding during catalytic turnover. DFT calculations by Cao and Hall showed that a $Fe(II)-Fe(II)$ site with a terminal H_2O ligand is very stable and proposed that this is a good model for H_{inact} because that coordination blocked the active site. Upon reduction to $Fe(II)-Fe(I)$, the calculations indicated that the water molecule dissociated and H_{ox} was formed.¹⁷⁴ However, in this work, models for the H_{trans} state were not studied. Similar theoretical studies by Liu and Hu favored instead a terminal hydroxo ligand as a better candidate for H_{inact} than a water or a dioxygen ligand because in the former case the predicted CO vibrational frequencies were nearer to the experimental ones, and in addition, it allowed upon reduction an intermediate $Fe(II)-Fe(I)-(OH)$ spin-polarized state that models

H_{trans} .¹⁷⁵ Another DFT study has proposed a thermodynamically favorable activation pathway that involves, first, protonation of the putative hydroxo ligand of H_{inact} , subsequent removal of H_2O from the active site, and finally, a mono-electronic reduction of the dinuclear iron site to form H_{ox} .²³⁹ However, this study does not take into consideration the experimental evidence of the existence of the H_{trans} intermediate. In a recent study of the activation process of *D. desulfuricans* hydrogenase by FTIR-spectroelectrochemistry and light-induced reduction in the presence of extrinsic CO, the reduction of H_{inact} to H_{trans} was reported to weaken the coordination of an unidentified terminal ligand to the distal Fe, which was removed upon further reduction to H_{ox} .¹⁷² As both H_{trans} and H_{ox} are paramagnetic states and their redox titration step could be fitted to a two-electron Nernstian process, the authors proposed that the activation step involved a redox-dependent chemical change, such as a two-electron reduction of a Cys-SOH (sulfenic acid) in H_{trans} to a Cys-SH in H_{ox} . An alternative explanation postulated in this work for the activation process was the possibility of reduction of a disulfide bond involving one or two of the thiol ligands of the H cluster.¹⁷² A very recent kinetic analysis of the hydrogen oxidation activity of aerobically isolated *D. vulgaris* (Hildenborough) Fe-Fe hydrogenase suggested that activation by hydrogen is cooperative: a first hydrogen molecule binds to the active site with low affinity and then a second one binds to the active site with high affinity and is oxidized at a high rate.²⁴⁰

5. Inactivation Processes

Compared to other enzymes, which often undergo considerable conformational changes on binding of the substrates, hydrogenases are rigid proteins with a multilayered structure consisting of sheets of β -strands and α -helices (Figure 1a). The only parts that are expected to move are the side chains of amino acids involved in transfer of hydrons to the active site. Even here, much of the movement of hydrons is predicted to occur through bound water molecules in the protein structure.²⁴¹ Therefore, hydrogenases are well suited enzymes to investigate the mechanism of their inactivation by external agents, since in most of the cases, their molecular structure remains stable during deactivating/reactivating treatments.

5.1. Ni-Fe Hydrogenases

5.1.1. Inactivation by O_2

The fact that Ni-Fe hydrogenases become deactivated by trace amounts of O_2 has been known for several decades.²⁴² Depending on the conditions of exposure to the gas, different ratios of the “unready” Ni-A and “ready” Ni-B states are obtained.^{52,93,205,207,228,229,243,244} The mechanism of these inactivation processes is still not well understood.²⁴⁵ Van der Zwaan and co-workers showed that oxidation of active *A. vinosum* hydrogenase with $^{17}O_2$ caused the appearance of a mixture of Ni-A and Ni-B EPR spectra, each of which showed broadening due to ^{17}O hyperfine coupling.²⁴⁶ More recently, Carepo et al. reported that oxidation with air of a *D. gigas* hydrogenase solution in $H_2^{17}O$, and in the Ni-C state, gave Ni-A with an ^{17}O label, as observed by ENDOR spectroscopy.²⁰⁵ These results showed that molecular oxygen reacts directly with the active site and at least one oxygen atom binds tightly in the vicinity of the Ni atom. Thus, an oxygenic species formed by reaction of O_2 at the active site

can be exchanged by H_2O or OH^- from the solvent before it binds to the Ni atom. This exchange is previous to Ni-A formation because the authors found that no solvent-exchange effect was observed by incubation of Ni-A in $H_2^{17}O$. A stopped-flow FTIR study of *A. vinosum* hydrogenase showed that Ni-B was formed by reaction of the Ni-R or the Ni-C states with excess O_2 , whereas some Ni-A was formed and Ni-SI detected as a transient if the O_2 concentration was decreased. The authors interpreted these results as indicating that O_2 can react directly at the active site or at the distal iron sulfur cluster, with the latter reaction being faster. According to this, when there is low amount of O_2 , the active site is oxidized to Ni-SI via the iron-sulfur clusters before it reacts with O_2 , and in this case, the hydrogenase has two reducing equivalents that lead to peroxide formation and finally to the Ni-A state. In the case that there is an excess of O_2 , the Ni-C and Ni-R states would react directly with O_2 with enough reducing equivalents to form H_2O or OH^- , leading to the formation of the Ni-B state. This hypothesis has found support in several electrochemical and crystallographic studies of different Ni-Fe hydrogenases. Lamle et al.²²⁹ studied the potential dependences and kinetics of the aerobic interconversions of *A. vinosum* hydrogenase adsorbed on a carbon electrode. This work showed that the “unready” (Ni-A) state was formed preferentially when O_2 reacted with the hydrogenase at high redox potentials, which should favor partial reduction of O_2 at the active site, whereas the “ready” (Ni-B) state was formed when O_2 reacted with the hydrogenase at lower redox potentials, which should favor complete reduction of O_2 to water. According to this, a H_2O or OH^- species would be available for binding directly to the active site during Ni-B formation, whereas two possibilities exist for Ni-A formation: (i) a peroxide or superoxide ion formed by partial reduction of O_2 binds directly to the active site as a bridging ligand or (ii) the peroxide or superoxide oxidizes a cysteine ligand of the active site to an S-oxide or sulfenate species and subsequently a hydroxide formed binds to the active site as a bridge between the two metals. A similar study performed by Leger and co-workers with *D. fructosovorans* hydrogenase concluded that inactivation by O_2 is a bimolecular process with a pH-independent rate constant of $3 \times 10^4 \text{ s}^{-1} \text{ M}^{-1}$ at 40 °C and 1 atm H_2 pressure. The reaction rate did not depend greatly on the H_2 pressure, which indicates that H_2 needs not to be released from the active enzyme before O_2 reacts with the active site, and therefore, it can attack any of the active states (Ni-R, Ni-C, or Ni-SI). For this enzyme, a mixture of both Ni-A and Ni-B was always obtained upon oxidation under the conditions studied.²⁴⁷

As mentioned above, the most recent X-ray diffraction data of Ni-Fe hydrogenases in the oxidized states point to a monatomic oxygen species bridging the two metals in Ni-B, whereas, for Ni-A, a diatomic oxygen species was favored as bridging ligand.^{227–228} These results would in principle support option i for the mechanism of Ni-A formation. However, in crystals of the putative Ni-A state, significant electron density at some of the active site cysteine ligands that could be refined to S-oxide/sulfenate species suggests that mechanism ii may take place at least in part of the hydrogenase sample. In fact, Volbeda et al. did emphasize that in the crystals there was a considerable proportion of hydrogenase molecules in which the nickel was EPR-silent; in the study of Ogata et al., the amount of EPR-silent hydrogenase in the putative Ni-A crystal was not estimated.

Therefore, more spectroscopic characterization of the pure Ni-A and the “unready” EPR-silent states is necessary in order to clarify the mechanisms of O₂ inactivation of Ni–Fe hydrogenases.

The stability of different types of hydrogenases to O₂ inactivation is variable and depends on the form of the enzyme and on previous oxidizing and reducing treatments. Morozov et al. reported that *T. roseopersicina* hydrogenase becomes O₂-tolerant when immobilized on an electrode, in spite of being very O₂-sensitive in solution;²⁴⁸ no explanation was offered by the authors for this effect. The SHase from *R. eutropha*, which is usually oxygen-tolerant, is irreversibly deactivated by O₂ after it has been previously incubated in the presence of reductants such as H₂ or NADH.^{150,151,249} FTIR spectroscopy showed that this reductive treatment removed irreversibly the CN[−] ligand of the Ni atom of the active site; thus, the authors concluded that these ligands protected the active site from O₂.¹⁵¹ Interestingly, bacteria that metabolize H₂ under aerobic conditions have been found to bear an additional *hypX* gene. A *hypX*[−] mutant of *R. eutropha* grew slowly under standard aerobic conditions, and the purified hydrogenase did not contain the extra nickel-bound CN, suggesting that, in the cell, the third cyanide is provided by the HypX protein.²⁵⁰ The SHase from the HypX[−] strain is highly sensitive to oxygen inactivation during turnover conditions in the presence of low concentrations of NADH. In the presence of an excess of NADH, the enzyme is not deactivated by oxygen, as enough electrons are available to reduce directly O₂ into H₂O.²⁵⁰ The lack of the third cyanide in HypX[−] soluble H₂ase, clearly showed by FTIR spectroscopic studies, demonstrates that this ligand is responsible for the O₂-resistance of soluble H₂ase. A possible explanation would be that the Ni coordination position occupied by the cyanide is not available for oxygen reaction. The enhanced O₂-sensitivity of a mutant of SHase in which Leucine118 was substituted by phenylalanine was attributed to steric hindrance by the bulky phenylalanine that may block the incorporation of the extra ligand.⁵⁴

The oxygen tolerance of *R. eutropha* MBHase has been studied by protein film voltammetry, which showed that this enzyme maintained a significant amount of H₂-uptake activity in the presence of high levels of O₂ and 100% of activity recovery was measured upon removal of O₂.¹⁵⁶ This low O₂-sensitivity has been exploited for developing a membraneless hydrogen–oxygen fuel cell with MBHase as the anode catalyst²⁵¹ and laccase as the cathode catalyst. The MBHase has a FTIR spectrum similar to “standard” Ni–Fe hydrogenases instead of to the SHase; that is, there is no additional CN[−] ligand on the Ni site.²⁵¹ Thus, the O₂-tolerance of the MBHase cannot be explained in the same way as that of the soluble H₂ase. It seems that it could be due rather to a combination of a slower rate of inactivation by O₂ with fast activation by H₂, as observed with hydrogenase I from *Aquifex aeolicus*.²⁵²

The RHases from *R. eutropha*²⁵³ and *Rhodobacter capsulatus*^{145,254} are not deactivated at all by O₂. Electrochemical measurements showed that, unusually, the regulatory hydrogenase reacts reversibly with O₂ even during turnover and continues to catalyze H₂ oxidation in the presence of O₂.¹⁵⁶ This property has been assumed to be due to a narrower gas channel for H₂ transportation. In standard Ni–Fe hydrogenases, molecular modeling indicated that the connection of the gas channel with the active site cavity is controlled by two conserved hydrophobic amino acids,

usually valine and leucine, in the large subunits. In oxygen tolerant hydrogenases, represented by the RHase of *R. eutropha*, the HupUV proteins from *Rd. capsulatus*,²⁵⁵ and *Bradyrhizobium japonicum*,²⁵⁶ valine and leucine, are replaced by the more bulky residues isoleucine and phenylalanine, respectively.²⁵⁷ It was proposed that these residues might play the role of a molecular sieve, limiting access of O₂ to the active site. To investigate this theoretical consideration experimentally, mutagenesis experiments were conducted on the RHase from *R. eutropha* and HupUV from *Rd. capsulatus*. The isoleucine and phenylalanine were substituted by the valine and leucine.^{258,259} In each case, the resulting mutated hydrogenases were inhibited by O₂, demonstrating that the nature of the amino-acid residues that form the gas channel is very important for O₂-sensitivity.

5.1.2. Anaerobic Inactivation by Increased Redox Potential

A characteristic feature of Ni–Fe hydrogenases is that their activity in H₂-oxidation drops, even under strict anaerobic conditions, at high overpotentials. This effect was initially observed by two independent research groups in 1985 for *D. gigas* hydrogenase: (i) Fernandez et al. reported that anaerobic oxidation of active enzyme with dichloroindophenol gave “ready” enzyme;²⁰⁴ (ii) Mege and Bourdillon showed that the electroenzymatic oxidation of H₂ by *D. gigas* hydrogenase immobilized on a glassy carbon electrode, with methyl viologen as redox mediator, decreased at high redox potentials and that the inactivation process corresponded to a reversible Nernstian one-electron/one-proton step taking place at potentials 280 mV more positive than the H⁺/H₂ couple.²⁶⁰ FTIR-spectroelectrochemical characterization of the same enzyme combined with isotope exchange activity measurements showed that this anaerobic inactivation corresponded to the oxidation of the Ni-SI state of the active site to the Ni-B state and that this process followed first-order kinetics with a high kinetic barrier.¹⁰⁷ This same process has been studied by the same technique for wild type *D. fructosovorans* Ni–Fe hydrogenase, and the influence of amino acid substitutions around the active site on the first-order rate constant and the Arrhenius activation energy was examined.¹²⁷ The anaerobic interconversions between the active and inactive states of *A. vinosum* hydrogenase were studied by chronoamperometric measurements of the enzyme immobilized on an electrode. The measurements showed that the kinetics of oxidative inactivation were independent of redox potential, consistent with a controlled chemical event. As Ni-B has a μ -hydroxo bridging ligand and Ni-SI probably has not, the authors suggested that the rate-limiting step of Ni-SI oxidation is the incorporation of OH[−] into the active site.²⁰⁶ Support for this proposed mechanism came from FTIR-spectroelectrochemistry, which showed a primary kinetic solvent isotope effect for the anaerobic oxidation of *D. gigas* hydrogenase.²²⁰ In the same work, it was reported that a glutamate residue near to the active site had a role in this process, possibly by taking a proton from a water molecule to allow its binding to the active site as a hydroxide species (Figure 9). FTIR-spectroelectrochemical studies of the Ni-SI/Ni-B transition have been recently performed for the *A. vinosum*¹²⁴ and *D. vulgaris* Miyazaki F¹²⁵ hydrogenases. Similar results were obtained to those of *D. gigas* hydrogenase, although a clear pH-dependent effect of the kinetics of Ni-SI oxidation was observed for *A. vinosum*, which is not measured with the *D. gigas* enzyme, and the

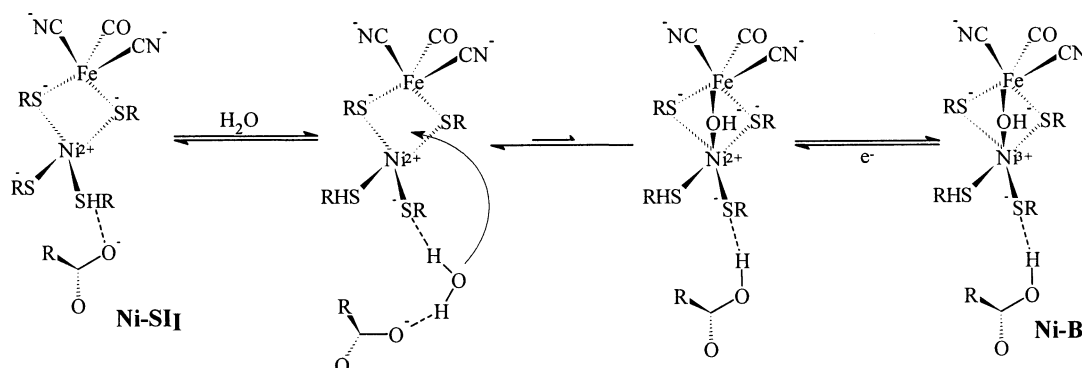


Figure 9. Possible mechanism of anaerobic inactivation of the active site of standard Ni–Fe hydrogenases taking into account the role of the carboxylic group of glutamic 25 amino acid (*D. fructosovorans* numeration).

oxidation kinetics of Ni-SI are relatively rapid in the *D. vulgaris* enzyme even at low temperatures.

Anaerobic inactivation of a nonstandard Ni–Fe hydrogenase, the MBHase from *R. eutropha*, was observed by protein film voltammetry experiments. This process took place at a potential 150 mV more positive than that for the standard Ni–Fe hydrogenases. So far, there are no spectroscopic data to ascertain if this corresponds to oxidation to a state of the active site equivalent to the Ni-B state.¹⁵⁶

5.1.3. Inhibition by Carbon Monoxide

CO is a competitive inhibitor of most Ni–Fe hydrogenases, as the effect is reversed upon increase of H₂ pressure.^{140,242} Direct spectroscopic evidence of CO binding to Ni ion at the catalytic active site of Ni–Fe hydrogenase was first obtained by EPR measurements of active enzyme under a ¹³CO atmosphere.²⁴⁶ The FTIR band of extrinsic CO bound to the active site was also identified by the isotopic shift measured under a ¹³CO atmosphere.^{41,123} Multiple-scattering analysis of the EXAFS data from *A. vinosum* [Ni–Fe] hydrogenase deactivated with CO also revealed the presence of Ni(II)–CO with CO bound as a terminal ligand.¹¹⁴ Almost simultaneously it was reported that the nickel L-edge soft X-ray spectrum of CO-inhibited *D. gigas* hydrogenase is consistent with CO binding to Ni and has the features of a Ni(II) high-spin state.¹¹⁷ FTIR data and DFT calculated spectra of CO-inhibited *D. fructosovorans* hydrogenase suggest that the extrinsic CO was only weakly bound to the Ni atom in a terminal mode, as no vibrational coupling with the structural CO ligand of the Fe atom was observed; moreover, the vibration frequency of the extrinsic CO was considerably higher than that expected for CO tightly bound to a metal.¹²³ Definitive proof of the binding mode of the CO inhibitor came from the X-ray structure of related [Ni–Fe] hydrogenase from *D. vulgaris* Miyazaki F activated with H₂ and further treated with CO, which showed a CO molecule terminally bound to Ni with a bent conformation.²⁶¹

FTIR-spectroelectrochemistry experiments were conducted with a *D. fructosovorans* hydrogenase in a saturated solution of CO. In these experiments, evidence was obtained that Ni–Fe hydrogenases in the inactive states Ni-A, Ni-B, and Ni-SU do not bind extrinsic CO. CO binding to the active site took place only after reductive activation of the enzyme to the Ni-SI forms, presumably when the bridging oxygen species had been removed from the active site. In addition, in this work it was shown that CO-inhibition blocked electron and proton transfer at the active site, although reduction at the proximal [4Fe-4S] cluster was detected.¹²³ The kinetics of CO binding to the Ni–Fe site in the hydrogenase from

A. vinosum was investigated by stopped-flow infrared spectroscopy by Albracht, Thorneley, and co-workers.²⁰⁸ Active enzyme in the redox states Ni-SI or Ni-R, in which the nickel is Ni(II), reacted much faster with CO than enzyme in the redox state Ni-C, in which the nickel is shown by EPR to be Ni(III), confirming the previous finding that replacement of H[−] by CO is easier with Ni(II) than with Ni(III).¹²⁹ A DFT study on different models of the paramagnetic CO-inhibited state of the active site concluded that a structure with the extrinsic CO coordinated to Ni(I) in an axial position gave the best fit of calculated EPR parameters to the experimental data.²¹¹ Another DFT study on the active site structure of CO-inhibited Ni–Fe hydrogenase, which is EPR-silent but detectable by FTIR, concluded that only with high-spin Ni(II) were the calculated ν_{CO} frequencies similar to those obtained experimentally.¹²² The kinetics of CO inhibition of *D. fructosovorans* Ni–Fe hydrogenase immobilized on an electrode were studied by Leger et al. using chronoamperometry under steady-state mass transport conditions. This work showed that CO-inhibition is fast and reversible and that CO binds only to the Ni-SI state.²⁴⁷

Ni–Fe–Se hydrogenases are generally more sensitive to CO inhibition than Ni–Fe hydrogenases.²⁶² Sorgenfrei et al. measured the EPR spectrum of active F₄₂₀-nonreducing hydrogenase from *Methanococcus voltae* in the presence of either CO or ¹³CO. The data suggested that, in this Ni–Fe–Se hydrogenase, extrinsic CO was bound to the Ni atom opposite to the selenium atom.¹⁴⁷

A few Ni–Fe hydrogenases are resistant to CO inhibition, such as the CO-induced hydrogenase from *Rhodospirillum rubrum*²⁶³ and the hyperthermophilic hydrogenase from *Pyrococcus furiosus*.²⁶⁴ The O₂-tolerant hydrogenases from *R. eutropha* are also completely insensitive to CO.^{151,250,253} Only after prolonged reduction of the SHase by NADH or sodium dithionite is a Ni-C state detected by EPR spectroscopy. At this stage, the hydrogenase becomes sensitive to CO and the EPR spectrum changes to an apparent Ni-CO signal.²⁶⁵ It has been proposed recently that this is due to loss of the extra CN[−] ligand to form an active site structure similar to those of “standard” Ni–Fe hydrogenases. It was suggested that the cysteine ligands of the Ni atom are chemically modified to sulfenates in SHase but are reduced to thiolates, yielding a more conventional active site structure.¹⁵⁰ SHase that has lost the CN[−] ligand of the Ni, as shown by FTIR, is sensitive to O₂ but not to CO,^{151,250} indicating that the requirements for reaction of the active site with O₂ and CO are different. The MBHase, which appears from FTIR spectroscopy to have normal CO and CN[−] coordination, is also completely insensitive to CO-

inhibition even though O_2 can reach the active site.²⁵¹ For this reason, the *R. eutropha* MBHase has been used as catalyst for the anode of a CO-insensitive biological fuel cell.²⁶⁶

5.1.4. Other Inhibitors

NO inhibits the D_2/H^+ exchange activity of *D. gigas* Ni–Fe and *Dm. baculatum* Ni–Fe–Se hydrogenases.²⁶² The irreversible inactivation of the membrane-bound Ni–Fe hydrogenase of *Azotobacter vinelandii* by NO was investigated by Hyman and Arp, who concluded that the NO binding site is different from the H_2 activation center and suggested that NO destroys iron sulfur clusters essential for the catalysis rather than the active site.²⁶⁷

Acetylene is also known as an inhibitor of [Ni–Fe] hydrogenases, competitive with H_2 and CO,²⁶⁸ which indicates that the binding of these three gases is mutually exclusive.²⁰² Arp et al. have obtained experimental evidence of acetylene binding to the large subunit of the enzyme,²⁶⁹ that in Ni–Fe hydrogenases accommodates the bimetallic active site,⁵² but the site of binding is unknown. By contrast, the H_2 -sensor hydrogenase from *R. eutropha* is insensitive to C_2H_2 ,²⁵³ perhaps its gas channel is too narrow for access.

Cyanide has been reported to be an irreversible inhibitor of a Ni–Fe hydrogenase isolated from *A. vinelandii*, in an oxidized state that is formed in the presence of H_2 and O_2 ,²⁷⁰ however, cyanide (as KCN) does not inhibit the active, anaerobically isolated enzyme.²⁷¹ Diaryl iodonium salts have been shown to inhibit the hydrogenase complex of *Rd. capsulatus*.²⁷²

Transition metals ions such as Cu(II) and Hg(II) inhibit the growth of bacteria such as *D. desulfuricans*, interfering with their hydrogen metabolism.²⁷³ EPR and UV–visible spectroscopy studies on *D. gigas* hydrogenase deactivated by Cu^{2+} salts suggested that the loss of catalytic activity was due to the destruction of a [3Fe-4S] cluster in the electron-transfer chain.²⁷⁴ A similar deactivating effect, by Hg(II), has been reported to occur to the Ni–Fe hydrogenase from *D. vulgaris*.^{275,276} Cu(II) and Hg(II) irreversibly inhibit the hydrogenase from *T. roseopersicina*.²⁷⁷ Nedoluzhko et al.²⁷⁸ have reported that Pb(II) can act as electron donor to the hydrogenase but is also an irreversible inhibitor.

Sulfide, the metabolic product of bacterial sulfate reduction, is an inhibitor of some hydrogenases.¹²⁴ Bleijlevens et al. showed that adding Na_2S to active *A. vinosum* hydrogenase and subsequent oxidation produced an inactive state which was EPR-silent and had an FTIR spectrum different from the Ni-A, Ni-B, and Ni-SU states. Reductive activation of this sample was possible, albeit slowly, but required lower redox potentials than those for Ni-A. Recently, this Na_2S inhibition effect and reductive reactivation has been shown for several standard Ni–Fe hydrogenases by protein film voltammetry.²⁷⁹ These results are understood in terms of the X-ray crystal structure of *D. vulgaris* Miyazaki F hydrogenase in the oxidized state, in which a sulfur species was assigned as a bridging ligand between both metals of the active site.¹²⁶ This observation offers a possible explanation as to why formation of H_2S is detected upon reductive activation of this hydrogenase.²⁸⁰

5.2. Fe–Fe Hydrogenases

The Fe–Fe hydrogenases of sulfate-reducing bacteria from the genus *Desulfovibrio* reveal that hydrogenases are more

sensitive to inhibition by O_2 , CO, and NO than are the Ni–Fe and Ni–Fe–Se hydrogenases.¹⁴⁰

5.2.1. Inactivation by O_2

Active Fe–Fe hydrogenases become irreversibly deactivated in contact with O_2 , and the EPR signals of the H-cluster disappear, presumably because O_2 reacts with and destroys the H-cluster.¹⁶⁶ However, the hydrogenases from *D. vulgaris* (Hildenborough)²⁸¹ and *D. desulfuricans*¹⁶⁹ have an oxidized inactive state that is air-stable; they can be activated quickly under reductive conditions, but this process cannot be reversed in the presence of O_2 . Recently, the reactivity toward O_2 of *D. desulfuricans* hydrogenase immobilized on a carbon electrode was studied by protein film voltammetry. This work confirmed the previous studies performed with enzyme in solution. In particular, injection of O_2 to active enzyme completely inhibited H_2 -uptake activity in a irreversible way, whereas if O_2 was injected at high redox potentials, in which the enzyme activity was suppressed by anaerobic oxidation, part of the activity could be restored upon reduction at low redox potentials.¹⁵⁶

5.2.2. Anaerobic Inactivation

Van Dijk et al. reported in 1983 that an inactive but air-stable state of *D. vulgaris* (Hildenborough) hydrogenase could be obtained from the active states under certain conditions, which included anaerobiosis and the use of dichloroindophenol as oxidant. This anaerobic inactivation did not take place by oxidation with cytochrome *c*; the enzyme remained active under those conditions even though cytochrome *c* has a similar midpoint redox potential to dichloroindophenol.²⁸¹ The authors' suggestion that anaerobic inactivation requires an obligatory two-electronic oxidation step, since dichloroindophenol is usually a $n = 2$ oxidant, whereas cytochrome *c* is a $n = 1$ oxidant, seems unlikely, since dichloroindophenol may also be an $n = 1$ oxidant, generating a radical.²⁸² Redox titrations of Fe–Fe hydrogenases monitored by EPR¹⁶⁸ or FTIR spectroscopy¹⁷² showed that anaerobic oxidation to the air-stable state (H_{inact}) did not take place. The reduction step from the inactive H_{trans} state to the active H_{ox} state fitted better to a two-electron process.¹⁷² Therefore, it is possible that the anaerobic inactivation process is rate-limited by a two-electron oxidation of H_{ox} to H_{trans} . Protein film voltammetry experiments of *D. desulfuricans* hydrogenase did show anaerobic inactivation at high redox potentials. In this case, no redox mediators were used, since electrons were exchanged directly at the electrode, allowing simultaneous transfer of two electrons.^{156,283}

5.2.3. Inhibition by CO

Fe–Fe hydrogenases are strongly inhibited by CO in a competitive manner.^{169,284} Of the known hydrogenases, this class is the most sensitive to CO: a 50% decrease in the H^+/D_2 exchange activity of the Fe–Fe periplasmic hydrogenase from *D. vulgaris* is obtained with concentrations of CO as low as $0.1 \mu M$ in solution.¹⁴⁰ As mentioned above, CO binding to the active site of Fe–Fe hydrogenases gives a characteristic spectrum in EPR and FTIR that corresponds to the H_{ox} -CO state. The crystallographic study of *C. pasteurianum* hydrogenase in this state concluded that a single exogenous molecule of CO binds to the vacant coordination site of the distal Fe atom of the H cluster, which is the putative substrate binding site, since CO is a competi-

tive inhibitor.²⁸⁵ EPR spectra of crystals of this CO-inhibited enzyme exhibited the characteristic signal of the H_{ox} -CO state described for Fe-Fe hydrogenases in solution.²⁸⁶ Fe-carbonyls are characteristically photosensitive, and X-ray diffraction data were obtained after irradiation of the CO-inhibited crystal with a helium/neon laser. The calculated electron density difference maps $F_o(\text{illuminated}) - F_o(\text{dark})$ revealed changes in electron density at the H cluster where the exogenous CO is bonded.²⁸⁷ The results were interpreted as a photodissociation of the terminal ligand trans to the bridging CO ligand. This indicates that the putative extrinsic CO ligand is chemically more labile than the intrinsic CO ligands, probably because the latter ones are trans to π -donor thiol ligands.²⁸⁷ An FTIR-spectroelectrochemical study of CO and ^{13}C O binding to *D. desulfuricans* hydrogenase indicated that extrinsic CO vibrationally couples with the terminal CO ligand of the distal Fe atom, in agreement with the crystal structure of H_{ox} -CO.¹⁸⁰ In the Fe-Fe hydrogenases, the vibrational frequency of extrinsic CO is lower than that in the Ni-Fe hydrogenases, which suggests that extrinsic CO binds to a stronger π -accepting metal in the former than in the latter.^{41,123} This explains why Fe-Fe hydrogenases have a lower K_i for CO than Ni-Fe hydrogenases: the structure of the active sites of the Fe-Fe hydrogenases allows a stronger binding of extrinsic CO. FTIR studies of the CO-inhibited form of *C. pasteurianum* I Fe-Fe hydrogenase confirmed the results reported for the *D. desulfuricans* hydrogenase and concluded that the intrinsic CO ligands are not bound to the same Fe atom of the active site; otherwise, only two CO bands would be observed in the CO-inhibited state.²⁸⁸ A theoretical study of the FTIR data of the CO-inhibited state has contradicted the crystallographically deduced model and suggested that the vacant coordination site of the distal Fe is occupied by the intrinsic CN ligand of the Fe atom and that the extrinsic CO is *trans* to a bridging thiolate.²⁸⁹ In this work, however, no account was taken of the influence of the protein environment, which probably controls the sites of cyanide binding by hydrogen bonding to polar residues. For this reason, these terminal ligands were assigned as CN^- ligands.⁷¹ In a recent FTIR study of CO inhibition in *D. desulfuricans* hydrogenase, it was shown that exogenous CO does not bind the H_{inact} state but it is able to bind to the H_{trans} state, which suggests that in this state the putative H_2O or OH^- terminal ligand of the distal Fe atom is more weakly bound in the H_{trans} state.¹⁷²

An interesting phenomenon of Fe-Fe hydrogenases is the light-sensitivity of their different states. Photoirradiation of the CO-inhibited state at cryogenic temperatures produced two species with different infrared spectra. Irradiation at temperatures below 150 K produced the photolysis of exogenous CO, and the expulsion of exogenous CO was gradually followed by the loss of the bridging CO ligand of the active site at temperatures below 80 K.²⁸⁸ Fiedler and Brunold have discussed the different possible structures of the photodissociated states based on computational studies.¹⁸³ Recently, it has been shown by EPR¹⁹⁸ and FTIR¹⁷² spectroscopy that the light inactivation of the active states of Fe-Fe hydrogenases is due to a kind of cannibalization; some of the enzyme molecules have their H cluster destroyed by the light, and the released CO then binds to the H cluster of other molecules forming the H_{ox} -CO state. Destruction of clusters may also explain why the EPR spectrum of *C. pasteurianum* hydrogenase exposed to O_2 strongly resembled that of the CO-inhibited form.¹⁶⁶

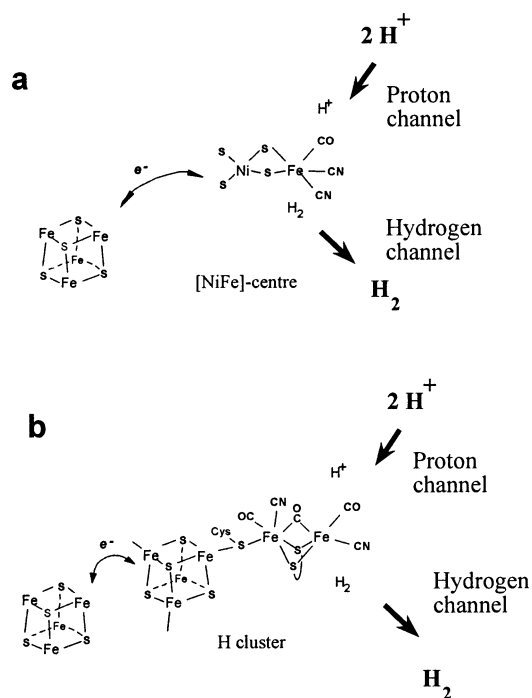


Figure 10. Scheme of the different steps involved in the catalytic cycle of Ni-Fe hydrogenases (a) and Fe-Fe hydrogenases (b).

5.2.4. Other Inhibitors

Fe-Fe hydrogenase from *D. desulfuricans* was shown to be inhibited by Cu(II) but only in the presence of ascorbate.¹⁶⁹ The hydrogenase from *D. vulgaris*²⁷⁵ as well as the one involved in the reduction of 2,4,6-trinitrotoluene by hydrogen in *C. acetobutylicum*²⁷⁶ are deactivated by Hg(II).

Nitrites are inhibitors of Fe-Fe hydrogenases and to a lesser extent of Ni-Fe-Se hydrogenases, but they do not inhibit Ni-Fe hydrogenases.²⁶²

6. Catalytic Cycle

The first studies of catalytic H_2 activation by bacterial whole cells in the presence of deuterium revealed a heterolytic splitting of D_2 , in contrast to the homolytic mechanism believed to occur on platinum and other noble metals.²⁹⁰ The use of the hydrogen-exchange assay to study the activity and function of hydrogenases, either *in vivo* using whole cells or with purified hydrogenases, has been reviewed by P. Vignais.²⁰² Another approach has been the detection of hydrogen species in the catalytic metal clusters by ENDOR^{158,226} and electron spin envelope modulation (ESEEM)^{291–292} in those states of hydrogenases in which the metal center has an odd number of electrons.

It is possible to divide the hydrogenase catalytic cycle into five steps, which are, in the direction of H_2 -oxidation: (i) diffusion of hydrogen molecules from the surface of the protein to the active site through the gas channels, (ii) heterolytic splitting of the hydrogen molecule after binding to the bimetallic active site, (iii) intramolecular electron transfer from the active site to the distal redox cluster, (iv) proton transfer from the active site to the water solvent, and (v) intermolecular electron transfer from the distal cluster to the redox partner (cytochrome, ferredoxin, redox mediators, or electrode surface) (Figure 10). As mentioned above, steps iii and iv take place by different paths through the protein.

(i) Diffusion of Hydrogen Molecules to the Active Site.

In the X-ray structure of *D. gigas* hydrogenase, the active site is located about 3.0 nm from the molecular surface, a distance over which H₂ molecules have to diffuse.⁵⁰ Determination of the structure at 0.254 nm resolution revealed the existence of hydrophobic cavities that connect the active site of Ni–Fe hydrogenases with the molecule surface. Determination of the crystal structure in high-pressure xenon showed a channel network that would function in gas exchange with the surface. Molecular dynamics simulations showed that diffusion of H₂ molecules to the active site would not be rate-limiting at the observed rate of catalysis.²⁹³ A more recent study aimed at analyzing possible pathways of H₂ entering inside the Ni–Fe hydrogenase of *D. gigas* by using molecular dynamics simulations in explicit solvent and molecular hydrogen also concluded that hydrogen easily permeates the protein and moves preferentially in channels to the Ni side of the active site. After identification of the potential regions involved in the control of hydrogen access to the active site, mutations that could improve the H₂ access to the active site were tested *in silico*. A simulated mutation of valine 67 to alanine indicated an increase of H₂ concentration in the protein and a lower effective distance from the active site.²⁹⁴ Another computational investigation on Fe–Fe hydrogenases has examined the H₂ exit path from the buried catalytic site to the external surface and the way that it allows the inhibitor O₂ to reach the active site.²⁹⁵ The authors found that, besides hydrophobic channels, the small H₂ and O₂ molecules can diffuse inside the protein through defined packing defects, predicted from the dynamic motion of the protein structure at a time scale of nanoseconds. Further simulations predicted different pathways for diffusion of H₂ and O₂ to the active site of Fe–Fe hydrogenase and the surface. Whereas O₂ crosses the protein through defined channels, H₂ molecules spread out in the protein and take many different exits.²⁹⁶

(ii) Heterolytic Splitting of a Hydrogen Molecule after Binding to the Bimetallic Active Site. The key reaction in the activation of H₂ is the heterolytic cleavage to a proton and a hydride. In a protein, there are many basic groups that can initially accept the proton, which can be passed down the proton-transfer pathway. This reaction is responsible for the H₂/HD isotope exchange reaction mentioned previously. The heterolytic cleavage reaction must take place at a center such as an organometallic compound to bind the hydride for long enough for catalysis to take place. This is a very unusual event, and the only enzymes that catalyze it efficiently are hydrogenases. Indeed, it appears to be the principal mechanism in biochemistry for metabolism of hydrogen, since even sensor proteins for detecting the concentration of H₂ use dinuclear centers similar to the Ni–Fe hydrogenases. A few enzymes are known that can produce H₂ as a side reaction, namely nitrogenase,²⁹⁷ carbon monoxide dehydrogenase,²⁹⁸ and pyruvate:ferredoxin oxidoreductase,²⁹⁹ but these enzymes do not consume hydrogen reversibly. What the hydrogenases, including the one that contains no iron–sulfur clusters, have in common is a low-valent iron ion coupled to carbonyl, and in most cases cyanide ligands. It seems a reasonable presumption that this site is involved at some stage in binding of the hydride.

The detailed steps of the hydrogenase catalytic activity have proved to be rather difficult to observe and as a result have been a matter of much theoretical debate.^{32,245,300–304} However, we can make a few general observations.

We start from the premise that hydride is bound to the enzyme, possibly on the low-valent iron atom. It must next simultaneously transfer two reducing equivalents to an electron acceptor in order to release the second proton. The difficulty is that most carriers in biological electron-transfer chains accept electrons one at a time. Only a select group of carriers is able to accomplish the feat of accepting two electrons and donating them singly to the next acceptor. Among these are certain organic redox cofactors, such as flavins, quinones, and pterins, which can undergo reduction by two hydrogen atoms and donate two electrons by stabilizing an intermediate radical species, such as FAD/FADH•/FADH₂. Some metal ions, such as molybdenum, which can take up three oxidation states, Mo(VI)/Mo(V)/Mo(IV), are also well suited to this function, but probably not at a sufficiently low potential. In the active sites of hydrogenases, the possibilities for these sorts of transactions are nickel, which can undergo oxidation–reduction between states Ni(III)/Ni(II)/Ni(I) by steps which are close in potential, and, in principle, iron, as Fe(III)/Fe(II)/Fe(I) or as clusters of iron atoms undergoing two such transitions.

(iii) Intramolecular Electron Transfer from the Active Site to the Distal Redox Cluster. In a different direction from the gas channels, a chain of iron sulfur clusters, separated by distances less than 1.5 nm (see Figure 1), provides an electron-transfer pathway from the H₂-splitting site to the site on the surface where electron acceptors bind. Chains of carriers in electron-transfer chains are now known in many redox enzymes and allow rapid electron transfer across considerable distances.³⁰⁵ The rate would be expected to be rapid with equipotential carriers. However, a surprising finding was the presence of a high-potential center (–70 mV in *D. gigas* and +65 mV in *D. fructosovorans* hydrogenases) in the middle of a low-potential (–340 mV) electron pathway of Ni–Fe hydrogenase.

To investigate the role of the [3Fe-4S] cluster in the intramolecular electron transfer, Pro-238 of *D. fructosovorans* hydrogenase (P239 in *D. gigas* numbering), which occupies the position of a potential additional ligand to the intermediate Fe–S cluster, was replaced by a cysteine residue. The mutation resulted in a functional enzyme that maintained its structural integrity and exhibited a decrease in the midpoint potential of the modified center from +65 mV to –250 mV.³⁰⁶ In spite of the 315 mV decrease of the center redox potential, the effect of the mutation on the catalytic activity was rather limited whatever the electron acceptor.

Later, a membrane-bound Ni–Fe hydrogenase was isolated from *Methanosarcina barkeri*, which is probably involved in a proton-pumping mechanism and has three [4Fe-4S] clusters of similar low redox potential.³⁰⁷ In another study conducted on *Methanococcus voltae* Ni–Fe–Se hydrogenase, the medial [4Fe-4S] center was transformed into a [3Fe-4S] center, which resulted in an increase in midpoint potential of 400 mV, from –370 mV in the wild-type enzyme to +60 mV for the mutant [3Fe-4S] cluster, which is similar to that of *D. fructosovorans* hydrogenase.³⁰⁸ In that case, the activity was affected only when the natural electron acceptor, F420, was tested. It therefore appears that, despite the apparently unfavorable ΔG° values deduced from potentiometric experiments, the intramolecular electron transfer between the [3Fe-4S] center and the [4Fe-4S] centers is rapid enough to be nonlimiting in hydrogenase activity.³⁰⁹ These studies clearly raise the question of the relevance of the measured redox potential in the description of the electron

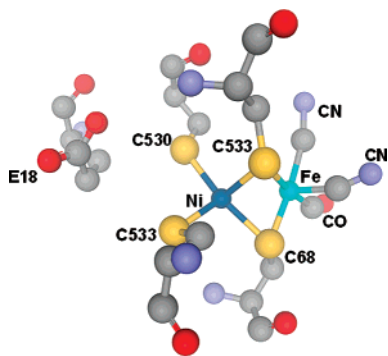


Figure 11. Zoomed view of the active site of *D. gigas* NiFe hydrogenase including amino acid glutamic 18.

transfer in proteins. The midpoint potential of the [3Fe-4S] cluster, as measured by equilibrium redox titrations, would be different from the actual potential determined from the states of reduction of the electron carriers.

(iv) Proton Transfer from the Active Site to the Water Solvent. A third pathway between the surface and the active site is required for transfer of protons involved in the hydrogenase reaction. Within an electron-transfer protein, it is important to maintain charge neutrality between different redox species; otherwise, the free energy changes involved become substantial. In the case of hydrogenases, this appears to be accomplished by the cotransport of hydrogen ions in parallel with electron transfer. It is interesting that the proteins of the respiratory chain, in particular Complex I, NADH:ubiquinone reductase, show ancestral relationships in their structure to the hydrogenases.³¹⁰ These complexes also catalyze concerted transfers of electrons and protons, in this case with transfer of protons across a membrane. In principle, the protein matrix provides the groups that will accept or donate protons from and to the active site, but once again, there seem to be specific and conserved pathways to facilitate this transfer.

One possible pathway involves water molecules coordinating the conserved divalent metal ion, which in *D. vulgaris* hydrogenase (Figure 1a) is a magnesium ion¹²⁶ and in *Dm. baculatum* hydrogenase is an Fe(II) ion.⁶⁹ Possible proton pathways on Ni-Fe hydrogenases have been evaluated by site-directed mutagenesis experiments. The first study was conducted on *R. eutropha* soluble NAD-reducing hydrogenase. A set of two histidines and one glutamate extending on about 13 Å from the Ni ligand cysteine-461 (C533 in *D. gigas* numbering) were mutated. The resulting enzymes exhibited a 75–95% decrease in activity, suggesting that the proton transfer was actually impaired.⁵³ It was not possible at that time to perform spectroscopic experiments on the mutated hydrogenases to determine the real impact of the mutations. A more recent study conducted on *D. fructosovorans* hydrogenase targeted the conserved glutamate-25 (18 in *D. gigas* numbering) located at 3 Å from the Ni ligand cysteine-543 (C530 in *D. gigas* numbering), exactly in the opposite direction as the previous study (Figure 11). This residue was chosen because it is the most disordered along with C543,^{50,311} suggesting a possible motion that might imply an active role in the proton transfer. The substitution of the carboxylate group of glutamate 25 by the non-protonatable amide group from a glutamine resulted in a complete loss of activity, even though all the prosthetic groups of the enzyme involved in electron transfer or hydrogen splitting were still perfectly constituted and functional.¹³⁶ Therefore, this glutamate appears to be the

proton-transfer gate during the catalytic cycle of the Ni-Fe hydrogenase, through which the protons are entering or exiting the active site. A recent DFT study of proton and electron transfers to and from the active site has also concluded that this glutamate residue has an essential role in catalysis.¹⁶⁰ Beyond glutamate 25, there are numerous other proton-carrying groups, including several water molecules, aspartates, glutamates, and histidines, so the pathway becomes rapidly diffused. It is moreover likely that a network of pathways exists, as observed by Massanz,⁵³ to make sure that this essential component of the hydrogenase activity does not fail.

(v) Intermolecular Electron Transfer from the Distal Cluster to the Redox Partner. The intermolecular electron-transfer steps between the hydrogenases and their respective electron-transfer partners have also attracted attention. Molecular modeling of the electrostatic surface characteristics of the Ni-Fe hydrogenase from *D. desulfuricans* ATCC 27774 hydrogenase and its physiological electron-transfer partner, a tetraheme cytochrome *c*₃, indicated an electrostatic interaction between the proteins involving the zone around the distal [4Fe-4S] cluster and the region surrounding heme IV in cytochrome *c*₃.³¹¹ An extensive investigation of the parameters that control cytochrome *c*₃ interaction with Ni-Fe hydrogenases from *Desulfovibrio* revealed a highly efficient electron transfer between hydrogenase and cytochrome *c*₃ (second-order rate constant *k* about 10⁹ M⁻¹ s⁻¹). The thermodynamic parameters of their interaction were determined by isothermal calorimetric titrations. The results indicated that the driving force for the complex formation was a positive entropy change; the net increase of entropy and enthalpy was associated with proton release in combination with water molecule exclusion. In another study, no complex formation was detected at high ionic strength, confirming that electrostatic forces play an important stabilizing effect on the complex between the two proteins.³¹² In another study, much lower association rates were found with the hydrogenase from *D. norvegicum*.³¹³

In a recent work, the electron-transfer mechanism between ¹⁵N-labeled cytochrome *c*₃ and *D. vulgaris* (Miyazaki F) Ni-Fe hydrogenase has been studied by NMR. The results suggest that heme 3 is the electron gate to ferrous *c*₃. In the same study, site-directed mutagenesis of individual lysine residues to uncharged methionine increased the *K*_m of the electron-transfer kinetics, which indicates that the positive charges of the lysines around heme 4 are involved in the formation of the complex between the region of the [4Fe-4S] cluster of the hydrogenase that is responsible for reduction of the cytochrome.³¹⁴

The crystal structure of *D. gigas* Ni-Fe hydrogenase indicates that the distal [4Fe-4S] cluster, that is the nearest to the protein surface, is surrounded by several glutamate residues.⁵⁰ The surface electrostatic potential distribution obtained from the crystal structure indicates the existence of a strong dipole moment in the enzyme molecule, with the distal [4Fe-4S] cluster located in the negative region of the protein surface where the docking of cytochrome *c*₃ to the hydrogenase molecule takes place (Figure 12).³¹⁵ This distal [4Fe-4S] cluster has an unusual His(Cys)₃ ligation (Figure 13). Replacement of this histidine by a cysteine or a glycine did not affect the correct assembly of the distal [4Fe-4S] cluster, but the H₂-oxidation activity of the mutant hydrogenases was reduced to less than 3% of that of the wild type. Similar decreases in H₂-oxidation rates were

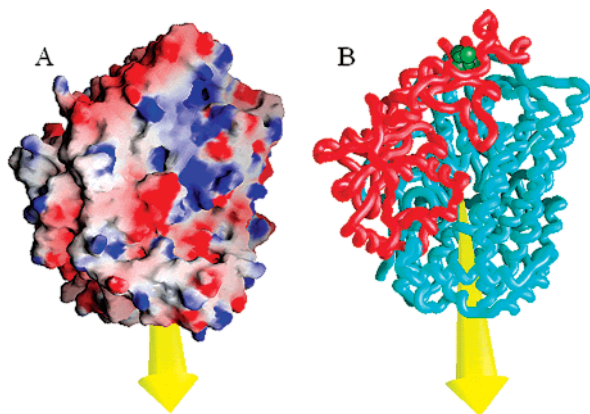


Figure 12. 3D-structure of *D. gigas* hydrogenase obtained from the Brookhaven Protein Data Bank. (A) Surface electrostatic-potential distribution: negative regions (red), positive regions (blue), direction of the dipole moment (yellow arrow). (B) Position of the distal 4Fe4S cluster (green), large subunit (cyan), and small subunit (red) relative to the dipole moment. The direction and magnitude (564 debyes) of the dipole moment of the crystal structure were calculated with GRASP software. Reprinted with permission from ref 315. Copyright 2005 American Chemical Society.

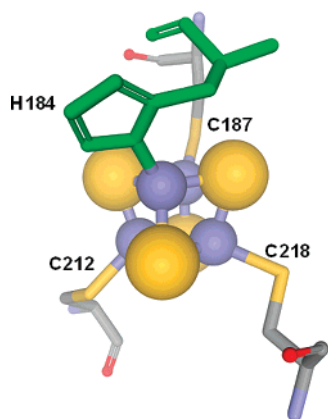


Figure 13. Zoomed view of the distal [4Fe-4S] center of *D. gigas* Ni-Fe hydrogenase. The histidine 184 is highlighted in green. The numbers of the cysteine ligands are indicated.

observed with soluble electron acceptors and with the enzyme directly adsorbed onto an electrode. These results suggest that a short distance between Fe-S clusters in biological redox chains may not always be sufficient to support rapid intramolecular electron transfer and that the nature of the protein amino acid ligands plays an important role in facilitating electron transfer.³¹⁶

The physiological redox electron partner of the Fe-Fe hydrogenase from *D. desulfuricans* is cytochrome c_{533} . A structural model of their complex has been obtained from a combination of NMR experiments and docking calculations.³¹⁷ According to this model, the cytochrome interacts with the small subunit of the hydrogenase; the closest contacts are between a cysteine ligand of the distal cluster of the hydrogenase and another cysteine ligand of the heme in the cytochrome. The model indicates that these cysteines, facing each other, are the site of electron transfer between hydrogenase and cytochrome.

6.1. Catalytic Mechanism at the Active Site

The mechanism of heterolytic cleavage of H_2 at the active site and the reverse reaction of H_2 production from protons and electrons is the most intriguing aspect of the catalytic

function of Ni-Fe and Fe-Fe hydrogenases. Therefore, nature has been able to develop two different ways to accomplish this chemical process without using noble metals. The crystallographic structures of active and inhibited forms of hydrogenases combined with spectroscopic data of the different redox states of the active site have given hints of the catalytic cycle. Theoretical methods, particularly density functional theory (DFT), and the chemistry of biomimetic models of both types of active site have complemented this information for determination of the mechanisms of the catalytic cycle at the active site of hydrogenases and the most probable structures of the redox states that participate in it.

6.1.1. Ni-Fe Hydrogenases

As discussed above, the redox states of the active site that correspond to catalytically competent enzyme are three: Ni-R, Ni-C, and Ni-SI. Kinetic data of the H_2 -production and oxidation activities of several Ni-Fe hydrogenases can be fitted to three-step mechanisms that involve these three with redox potentials similar to those obtained by spectroscopic redox titrations.^{231,318,319} Both Ni-R and Ni-SI have different subforms that differ in their protonation levels of the active site (Figure 4), and not all of them may participate in the catalytic cycle. Some authors consider that only Ni-SI_{II} is catalytically competent, arguing that Ni-SI_I may still have a hydroxo/aquo ligand in the active site and, therefore, is an inactive state.^{207,245} However, there is no spectroscopic evidence of a structural difference of this sort between the two forms of Ni-SI, and the shift of the vibrational frequencies observed between the FTIR spectra of both subforms fits quite well to a different level of protonation of one of the terminal cysteines of the Ni atom.²¹⁰ Taking into account the broad pH range in which Ni-Fe hydrogenases are active (especially for H_2 -activation), it is quite possible that the catalytic cycle can work with different levels of protonation.³¹⁹ Other authors have pointed out that a catalytic cycle can be described involving only the Ni-C and Ni-R, as they are the only two states that are in thermodynamic equilibrium with H_2 .^{208,241} This is quite possible for the case of the H_2 -production activity, which takes place in a medium of low redox potential, but in the case of H_2 -oxidation activity, the driving force is a high-redox potential medium (either imposed at an electrode or due to the presence of the redox-acceptor partner), which suggests that Ni-SI may be a stable intermediate of the reaction. In any case, there is general agreement in considering Ni-C the key intermediate of the catalytic cycle because there is sufficient experimental and theoretical data for the presence of a bridging hydride ligand in this state, consistent with heterolytic cleavage of H_2 at the active site.^{112,122,158-161,320} However, as mentioned above, it is not agreed if the EPR-silent intermediates of the catalytic reaction Ni-SI and Ni-R correspond to low spin or high spin Ni(II) states.^{108,117,121-122}

Another controversial point of the catalytic cycle concerns the role of the two metal ions of the dinuclear center in binding and heterolytic cleavage. Some authors favor Ni as the binding place of the substrate and a more relevant function on hydride formation because the crystal structures indicate that the gas transport channel of the enzyme ends there and that the competitive inhibitor binds terminally to Ni.^{241,261} Moreover, experimental and theoretical studies of biomimetic Ni(II) complexes have shown that base-assisted heterolytic cleavage of H_2 takes place with formation of a hydride ligand bound to the metal.³²¹⁻³²⁵ It has been proposed

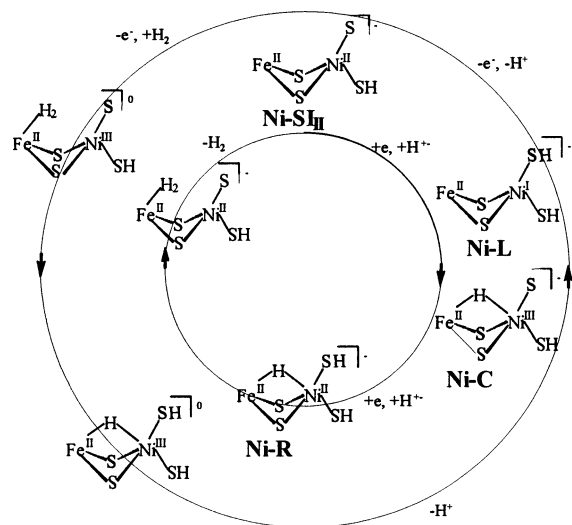


Figure 14. Simplified scheme of the catalytic cycle mechanism proposed for standard Ni–Fe hydrogenases in ref 122. The outer circle represents the H₂-oxidation pathway (counterclockwise direction), whereas the inner circle represents the H₂-production pathway (clockwise direction). The structures between the circles are common to both pathways.

that this hydride acceptor ability is enhanced when the coordination of the Ni complex corresponds to a distorted tetrahedron,³²² which is the coordination around Ni in the crystal structures of Ni–Fe hydrogenases.^{50,69,326} Conversely, other authors have favored the Fe atom as the binding place of H₂ based on DFT calculations of the intermediates and transition steps of the catalytic cycle (Figure 14)^{122,160} and on the high affinity of low spin d⁶ metals for H₂.^{29,301}

There are numerous candidates for the base that accepts the proton formed during the heterolytic cleavage, but there is currently no experimental support for any of them. They include a terminal cysteine ligand of the Ni atom (Figure 14), because of the high dynamic disorder of the S atom of this residue in the crystallographic structures.^{69,311} A DFT study²³⁸ calculated the energy barrier for heterolytic cleavage assisted by a terminal S ligand to be similar to the activation energy measured for the H₂-uptake activity of hydrogenase by direct electrochemistry, 55 kJ/mol.³²⁷ Another DFT study by Siegbahn pointed out that a bridging cysteine of the active site may also act as a base during the catalytic cycle.¹⁶⁰ A water molecule bound to the Fe in the Ni-SI has also been proposed,²¹¹ although to date there is no experimental evidence of this coordination in that state.

In a recent DFT study, Pardo et al. have proposed a catalytic mechanism for Ni–Fe hydrogenases that involves different pathways for H₂-production and H₂-oxidation,¹²² which is shown in Figure 14 in a simplified scheme. The inner cycle of the scheme corresponds to the H₂-production pathway (clockwise direction). In this case, the starting point is the Ni-SI_{II} state that in a one-electron/one-proton step is reduced to a Ni(I)–Fe(II) transient intermediate, which is not detected by spectroscopy during turnover conditions but could be similar to the Ni-L state detected by photodissociation of Ni-C at low temperatures.^{112,129,132} The existence of this transient intermediate in the catalytic cycle has also been proposed by other authors and may explain the H₂/D₂ exchange activity of Ni–Fe hydrogenases.²⁰² The Ni-L transient state evolves quickly to form the stable Ni-C intermediate, which in a second one-electron/one-proton step forms Ni-R. There is no direct experimental evidence of the

nature of the hydrogen species bound to the Ni-R state, although the frequency shifts of the diatomic ligands of the active site observed by FTIR when reducing Ni-C to Ni-R suggest that the latter state retains the bridging hydride ligand.²⁴¹ In fact, most DFT studies propose this coordination for Ni-R.^{121,122,160,211} The final steps of the H₂-production reaction could be formation of a H₂ ligand on the Fe and its release via the gas-transport channel. The reverse reaction pathway, H₂-oxidation, is represented in the outer cycle in the counterclockwise direction. The first step involves binding of H₂ to the Fe atom of the Ni-SI_{II} state. Pardo et al. calculated that the subsequent heterolytic cleavage step had a lower kinetic barrier if the Ni atom was previously oxidized to Ni(III). However, Siegbahn has concluded from a similar study that this cleavage step is more favorable with a Ni(II)–Fe(II) oxidation level if the net charge of the model of the active site used is different.¹⁶⁰ In the same work it was concluded that including atoms of amino acid residues surrounding the active site in the DFT calculations did not impede H₂-binding to the Fe atom. After heterolytic cleavage and transfer of one proton, the Ni-C state is formed; this then forms the transient intermediate similar to Ni-L that is quickly oxidized to the Ni-SI_{II} state (Figure 14).

The effect of substitution of a sulfur atom coordinating the Ni atom by selenium in the models of the active site of Ni–Fe hydrogenases has been studied by DFT. In that study it was concluded that the main effect was due to the increased acidity of Se relative to S, which could improve proton transfer from the active site.¹⁶⁰ This may explain the different catalytic properties of Ni–Fe–Se hydrogenases, although other authors have suggested that other differences in the protein environment of the active site may tune the catalytic properties of these particular hydrogenases.¹⁴⁴

6.1.2. Fe–Fe Hydrogenases

The redox potential-controlled spectroscopic studies^{167–168,172} indicate that only two of the states of the active site detected can be stable intermediates of the catalytic cycle, taking into account the redox potential range in which Fe–Fe hydrogenases turn over H₂.^{156,328,329} These two redox states are H_{ox} and H_{red}; the former can be considered the state at which H₂ binds for heterolytic cleavage, and the latter one can be considered the state that is capable of proton reduction for the reverse reaction, i.e., H₂ production. As there is a one-electron difference between the two states and two electrons are implicated in this reaction, the participation of the iron–sulfur clusters for providing or accepting an additional electron is compulsory during the catalytic cycle. A combined crystallographic and FTIR study suggested that the main structural change in the active site during turnover is the movement of the μ -CO ligand in H_{ox} toward the distal Fe of the active site, thus giving a semibridging mode in H_{red}.¹⁸⁴ This bridging CO ligand is *trans* to the coordination position of the distal Fe, in its active state, that is either vacant or weakly bound to a solvent molecule. This site has been proposed as the site for substrate binding during catalytic turnover.^{45,72} This hypothesis has additional support from the crystallographic structure of the CO-inhibited state, showing that the competitive inhibitor CO binds to that vacant site.^{285,287} In contrast to Ni–Fe hydrogenases, there is no direct spectroscopic evidence of a hydride species bound to the active site, although an intermediate species with a bound hydride would be expected in the catalytic cycle because HD-production is measured at faster rates than H₂-production

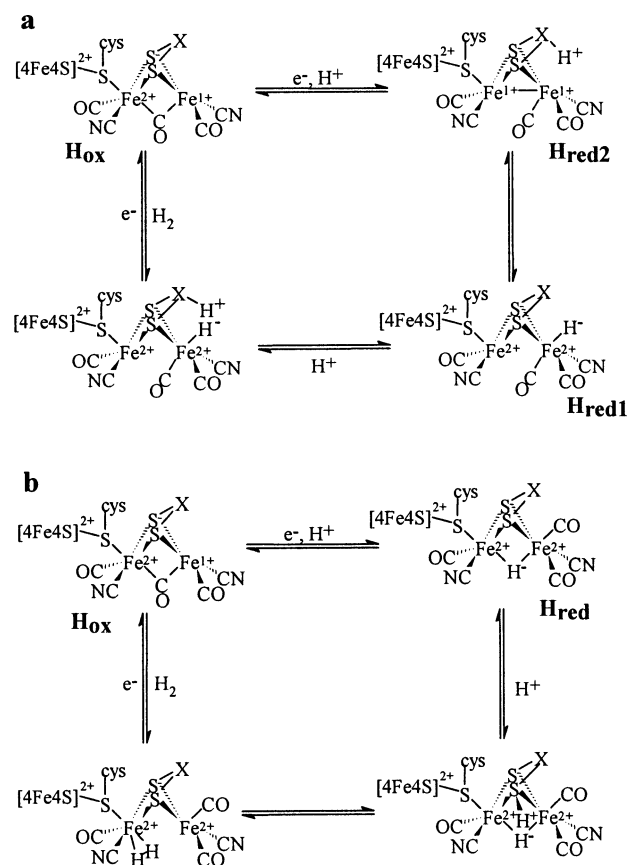


Figure 15. Possible catalytic cycle mechanisms for Fe-Fe hydrogenases.

during D_2/H^+ isotope-exchange activity assays of Fe-Fe hydrogenases.¹⁴⁰ Several authors have proposed that binding of H_2 to the distal Fe, which has the bridging CO ligand in the *trans* position, increases its acidity, thereby favoring its heterolytic cleavage and terminal binding of a hydride to this site (Figure 15a).^{72,174,287,330–331} The heterolytic cleavage step may be assisted through proton extraction by the putative amine group of the organic ligand that forms a bridge between both Fe atoms.^{35,131,184,332} According to this mechanism, simultaneously with the heterolytic cleavage of H_2 , an electron is ceded to the iron-sulfur cluster electron-transport chain, leading to formation of the intermediate state Fe(II)-Fe(II)-(H⁻), which has been proposed as one of the configurations of the H_{red} state (H_{red1} in Figure 15a).¹⁷⁵ This state is isoelectronic with the proposed intermediate Fe(I)-Fe(I), which has also been suggested for the H_{red} state (H_{red2} in Figure 15a).^{174–175,195–196} This electron-rich dinuclear iron intermediate could be the starting point for proton reduction in the reverse reaction, as shown in Figure 15a. The H_{ox} state may be formed in the catalytic cycle by the release of H_2 from the active site (H_2 -production activity) or by cession of an electron of the H_{red2} state to the iron-sulfur clusters (H_2 -oxidation activity). The shift of one of the CO ligands of the active site from bridging to semibridging coordination and *vice versa* during the catalytic cycle has been rationalized as a way of tuning the electronic distribution in both Fe atoms in order to allow reversibility of the enzymatic activity.^{45,333}

Alternative mechanisms have been proposed in which the binding site for H_2 is the proximal Fe and that lead to formation of a bridging hydride intermediate (Figure 15b).^{36,245,334–335} This hypothesis is supported by the low-

energy barrier for the heterolytic cleavage by this method and the high stability of the bridging hydride intermediate, as shown by the chemistry of biomimetic dinuclear iron complexes^{191,336–339} and DFT calculations.^{196,334–335} In this mechanism, the H_{red} state would correspond to the bridging hydride intermediate (Figure 15b). There is no need to postulate that the secondary amine in the putative bridging azapropandithiol acts as a proton acceptor, since one of the thiolates of this ligand or one of the CN⁻ ligands could perform this function.^{36,196,334–335} However, it has been argued by other authors that a possible role of the bridging CO ligand is to prevent formation of a hydride in that position by steric effects,^{333,340} and a combined electronic absorption spectroscopy/DFT study of an Fe(I)-Fe(I) complex suggests that the shift of the bridging CO ligand toward the distal Fe in the H_{red} increases the nucleophilicity of this atom via polarization of the electron density of the Fe-Fe bond.³⁴⁰ This electronic effect should promote protonation at the vacant coordination site of the distal Fe instead of the Fe-Fe bond.^{333,340} Van der Vlugt et al.¹⁹³ have reported the synthesis of the first di-ferrous species bearing a terminal hydride ligand. It produced H_2 upon reaction with Brønsted acids, whereas equivalent $\mu-H^-$ compounds did not because they were too stable. Therefore, the mechanism of the catalytic cycle with the terminal hydride intermediate (Figure 15a) fits better with the experimental results obtained with enzyme and functional biomimetic complexes. Nevertheless, the possibility of a bridging hydride intermediate cannot be excluded because the energy barriers calculated for this mechanism are similar to those of the terminal hydride mechanism.^{196,334–335}

6.1.3. Fe-S Cluster-free Hydrogenases (Hmd)

This hydrogenase, by contrast with other known hydrogenases, does not catalyze the reduction of dyes such as methyl viologen with H_2 even in the presence of methenyl- H_4MPT^+ .⁷⁴ However, it catalyzes the reversible reduction of N^5, N^{10} -methenyl- H_4MPT^+ with H_2 to N^5, N^{10} -methylene- H_4MPT and a proton in the absence of any added electron acceptors.⁷³ It also catalyzes the interconversion of *para*- H_2 and *ortho*- H_2 in the presence of methenyl- H_4MPT^+ , a reaction that is suppressed in D_2O .⁷⁵ The formation of HD and D_2 , rather than conversion of *para*- H_2 to *ortho*- H_2 , was observed, indicating that, after the heterolytic splitting of the hydrogen molecule, the dissociation of the exchangeable proton is faster than the reformation of H_2 .⁷⁶ NMR studies with labeled methenyl- H_4MPT^+ have shown that Hmd catalyzes the Re-site stereospecific transfer of a hydride from H_2 to methenyl- H_4MPT^+ .³⁴¹

Before it was known that the enzyme contains an iron-carbonyl center, an unusual catalytic mechanism was proposed by Thauer and co-workers, formulated by analogy with the superacid mechanism elucidated by Olah for the formation of carbocations and H_2 from alkanes.^{74,76} However, now that the iron-carbonyl cofactor in Hmd has been identified, one can envisage the formation of a hydride at this center in an analogous way to the Ni-Fe and Fe-Fe hydrogenases, followed by a transfer of the hydride from the iron site to the cation radical of 5,10-methenyl- H_4MPT^+ (Figure 16). This transfer would occur inside the protein and would not necessarily lead to hydrogen isotope exchange with the surrounding water. However, the reaction would be reversible, and since the 5,10-methenyl- H_4MPT^+ cation has an exchangeable proton, release of the cation in isotopically

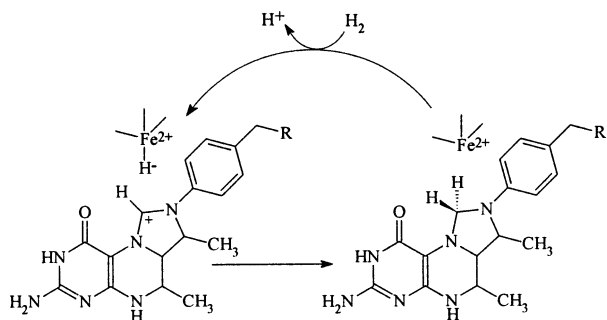


Figure 16. Proposed reaction catalyzed by the iron-sulfur-free hydrogenase, N^5,N^{10} -methylene-tetrahydromethanopterin dehydrogenase.

labeled water would incorporate hydrogen isotopes stereospecifically into the product, as observed.

7. Concluding Remarks

The hydrogenases have evolved to consume or produce hydrogen under a challenging range of conditions. Even though the Fe-Fe and Ni-Fe hydrogenases are not phylogenetically related, the common feature that can be postulated as responsible for hydrogenase activity is the conserved low-spin Fe coordinated to CN and CO. The existence of at least two different types of hydrogenases is the result of a convergent evolution, which means that two enzymes of different origins have been selected to carry out the same reaction. We may wonder what in evolution has led to such phenomenon. Oxygen apparition in the atmosphere about two billions years ago might be a plausible explanation. Nevertheless, it is not yet possible to determine which enzyme is the oldest and which had been selected when oxygen appeared. In any case, oxygen is a strong inhibitor of most hydrogenases. Ni-Fe hydrogenases are the most widespread, and enzymes of this group only have been identified as oxygen-tolerant. Two main strategies have been adopted to operate in the presence of oxygen: exclusion of O_2 from the active site by restricting the gas channels, or having a catalytic center partially blocked by additional ligands. These mechanisms have the added benefit of protecting the active sites from CO, which is produced metabolically in anaerobic environments. Many microorganisms are, at different times, exposed to both aerobic and anaerobic environments. Again, the problem of oxygen can be dealt with in a number of ways. Under aerobic conditions, the hydrogenases are converted to a dormant state but are arranged in such a way that it can be reactivated under reducing conditions. Each of these options involves a compromise between resistance to inactivation and catalytic efficiency.

8. List of Abbreviations

DFT	density functional theory
ENDOR	electron-nuclear double resonance
EPR	electron paramagnetic resonance
ESEEM	electron spin envelope modulation
FAD	flavin adenine dinucleotide
FTIR	Fourier-transform infrared
Hmd	H_2 -forming methylene- H_4 MPT dehydrogenase, or Fe-S cluster-free hydrogenase
HYSCORE	hyperfine sublevel correlation spectroscopy
MBHase	membrane-bound hydrogenase
MPT	methanopterin
MS	mass spectrometry
NAD	nicotinamide adenine dinucleotide

NADP	nicotinamide adenine dinucleotide phosphate
NHE	normal hydrogen electrode
RHase	regulatory hydrogenase
SHase	soluble hydrogenase
TOF-SIMS	time-of-flight-secondary ion mass spectrometry
XAS	X-ray absorption spectroscopy

9. Acknowledgments

A.L.L. and V.M.F. are grateful to Alejandro Ballesteros for helpful assistance and thank the Spanish Ministerio de Educación y Ciencia for financial support (Project CTQ2006-12097/BQU). M.R. acknowledges financial support from the CNRS (Grant G5RD-CT-2002-00750), the European Union (Competitive and Sustainable Growth Program), and the French Ministry of Research (ACI-ECD program).

10. References

- Barreto, L.; Makihira, A.; Riahi, K. *Int. J. Hydrogen Energy* **2003**, *28*, 267.
- Cammack, R.; Frey, M.; Robson, R. *Hydrogen as a Fuel: Learning from Nature*; Taylor & Francis: London and New York, 2001.
- Klass, D. L. *Biomass for Renewable Energy, Fuel and Chemicals*; Academic Press: San Diego, 1998.
- Melis, A.; Zhang, L. P.; Forestier, M.; Ghirardi, M. L.; Seibert, M. *Plant Physiol.* **2000**, *122*, 127.
- Woodward, J.; Orr, M.; Cordray, K.; Greenbaum, E. *Nature* **2000**, *405*, 1014.
- Ghirardi, M. L.; Zhang, J. P.; Lee, J. W.; Flynn, T.; Seibert, M.; Greenbaum, E.; Melis, A. *Trends Biotechnol.* **2000**, *18*, 506.
- Greenbaum, E.; Blankinship, S. L.; Lee, J. W.; Ford, R. M. *J. Phys. Chem. B* **2001**, *105*, 3605.
- Melis, A.; Happe, T. *Plant Physiol.* **2001**, *127*, 740.
- Chornet, E.; Czernik, S. *Nature* **2002**, *418*, 928.
- Tamagnini, P.; Axelsson, R.; Lindberg, P.; Oxelfelt, F.; Wunschiers, R.; Lindblad, P. *Microbiol. Mol. Biol. Rev.* **2002**, *66*, 1.
- Happe, T.; Hemschemeier, A.; Winkler, M.; Kaminski, A. *Trends Plant Sci.* **2002**, *7*, 246.
- Hallenbeck, P. C.; Benemann, J. R. *Int. J. Hydrogen Energy* **2002**, *27*, 1185.
- Tsygankov, A. A.; Fedorov, A. S.; Kosourov, S. N.; Rao, K. K. *Biotechnol. Bioeng.* **2002**, *80*, 777.
- Kalia, V. C.; Lal, S.; Ghai, R.; Mandal, M.; Chauhan, A. *Trends Biotechnol.* **2003**, *21*, 152.
- Schutz, K.; Happe, T.; Troshina, O.; Lindblad, P.; Leitao, E.; Oliveira, P.; Tamagnini, P. *Planta* **2004**, *218*, 350.
- Dante, R. C.; Armenta, S.; Gutierrez, M.; Celis, J. *Int. J. Hydrogen Energy* **2004**, *29*, 1219.
- Cournac, L.; Guedeny, G.; Peltier, G.; Vignais, P. M. *J. Bacteriol.* **2004**, *186*, 1737.
- Mertens, R.; Liese, A. *Curr. Opin. Biotechnol.* **2004**, *15*, 343.
- Penfold, D. W.; Macaskie, L. E. *Biotechnol. Lett.* **2004**, *26*, 1879.
- Franchi, E.; Tosi, C.; Scolla, G.; Della Penna, G.; Rodriguez, F.; Pedroni, P. M. *Mar. Biotechnol.* **2004**, *6*, 552.
- Kanai, T.; Imanaka, H.; Nakajima, A.; Uwamori, K.; Omori, Y.; Fukui, T.; Atomi, H.; Imanaka, T. *J. Biotechnol.* **2005**, *116*, 271.
- Prince, R. C.; Khesghi, H. S. *Crit. Rev. Microbiol.* **2005**, *31*, 19.
- Kruse, O.; Rupprecht, J.; Bader, K. P.; Thomas-Hall, S.; Schenk, P. M.; Finazzi, G.; Hankamer, B. *J. Biol. Chem.* **2005**, *280*, 34170.
- Yoshida, A.; Nishimura, T.; Kawaguchi, H.; Inui, M.; Yukawa, H. *Appl. Environ. Microbiol.* **2005**, *71*, 6762.
- Benemann, J. R.; Beresenson, J. A.; Kaplan, N. O.; Kamen, M. D. *Proc. Natl. Acad. Sci. U.S.A.* **1973**, *70*, 2317.
- Jones, A. K.; Sillery, E.; Albracht, S. P. J.; Armstrong, F. A. *J. Chem. Res., Synop.* **2001**, 297.
- Vincent, K. A.; Cracknell, J. A.; Parkin, A.; Armstrong, F. A. *Dalton Trans.* **2005**, 3397.
- Alonso-Lomillo, M. A.; Rüdiger, O.; Maroto-Valiente, A.; Velez, M.; Rodriguez-Ramos, I.; Munoz, F. J.; Fernandez, V. M.; De Lacey, A. L. Hydrogenase-Coated Carbon Nanotubes for Efficient H_2 Oxidation. *Nano Lett.* **2007**, *7*, 1603.
- Darensbourg, M. Y.; Lyon, E. J.; Smece, J. J. *Coord. Chem. Rev.* **2000**, *206*, 533.
- Evans, D. J. *J. Chem. Res., Synop.* **2001**, 297.
- Alper, J. *Science* **2003**, *299*, 1686.
- Evans, D. J.; Pickett, C. J. *Chem. Soc. Rev.* **2003**, *32*, 268.

- (33) Tard, C.; Liu, X. M.; Ibrahim, S. K.; Bruschi, M.; De Gioia, L.; Davies, S. C.; Yang, X.; Wang, L. S.; Sawers, G.; Pickett, C. J. *Nature* **2005**, *433*, 610.
- (34) Sun, L. C.; Akermark, B.; Ott, S. *Coord. Chem. Rev.* **2005**, *249*, 1653.
- (35) Liu, X. M.; Ibrahim, S. K.; Tard, C.; Pickett, C. J. *Coord. Chem. Rev.* **2005**, *249*, 1641.
- (36) Bruschi, M.; Zampella, G.; Fantucci, P.; De Gioia, L. *Coord. Chem. Rev.* **2005**, *249*, 1620.
- (37) Bouwman, E.; Reedijk, J. *Coord. Chem. Rev.* **2005**, *249*, 1555.
- (38) Artero, V.; Fontecave, M. *Coord. Chem. Rev.* **2005**, *249*, 1518.
- (39) Tye, J. W.; Hall, M. B.; Darensbourg, M. Y. *Proc. Natl. Acad. Sci. U.S.A.* **2005**, *102*, 16911.
- (40) Armstrong, F. A.; Albracht, P. J. *Philos. Trans. R. Soc. London, A* **2005**, *363*, 937.
- (41) Bagley, K. A.; Van Garderen, C. J.; Chen, M.; Duin, E. C.; Albracht, S. P. J.; Woodruff, W. H. *Biochemistry* **1994**, *33*, 9229.
- (42) Bagley, K. A.; Duin, E. C.; Roseboom, W.; Albracht, S. P. J.; Woodruff, W. H. *Biochemistry* **1995**, *34*, 5527.
- (43) Best, S. P. *Coord. Chem. Rev.* **2005**, *249*, 1536.
- (44) Adams, M. W. W.; Stiefel, E. I. *Curr. Opin. Chem. Biol.* **2000**, *4*, 214.
- (45) Nicolet, Y.; Cavazza, C.; Fontecilla-Camps, J. C. *J. Inorg. Biochem.* **2002**, *91*, 1.
- (46) LeGall, J.; DerVartanian, D. V.; Spilker, E.; Lee, J. P.; Peck, H. D. *Biochim. Biophys. Acta* **1971**, *234*, 525.
- (47) Thauer, R. K.; Fuchs, G.; Kaufer, B.; Schnitker, U. *Eur. J. Biochem.* **1974**, *45*, 343.
- (48) Cammack, R.; Fernandez, V. M.; Schneider, K. *The Bioinorganic Chemistry of Nickel*; VCH Publishers: New York, 1988; p 167.
- (49) Niviere, V.; Hatchikian, C.; Cambillau, C.; Frey, M. *J. Mol. Biol.* **1987**, *195*, 969.
- (50) Volbeda, A.; Charon, M. H.; Piras, C.; Hatchikian, E. C.; Frey, M.; Fontecilla-Camps, J. C. *Nature* **1995**, *373*, 580.
- (51) Hatchikian, E. C.; Bruschi, M.; LeGall, J. *Biochem. Biophys. Res. Commun.* **1978**, *82*, 451.
- (52) Volbeda, A.; Garcia, E.; Piras, C.; De Lacey, A. L.; Fernandez, V. M.; Hatchikian, E. C.; Frey, M.; Fontecilla-Camps, J. C. *J. Am. Chem. Soc.* **1996**, *118*, 12989.
- (53) Massanz, C.; Friedrich, B. *Biochemistry* **1999**, *38*, 14330.
- (54) Burgdorf, T.; De Lacey, A. L.; Friedrich, B. *J. Bacteriol.* **2002**, *184*, 6280.
- (55) Winter, G.; Buhrke, T.; Jones, A. K.; Friedrich, B. *Arch. Microbiol.* **2004**, *182*, 138.
- (56) Happe, R. P.; Roseboom, W.; Pierik, A. J.; Albracht, S. P. J.; Bagley, K. A. *Nature* **1997**, *385*, 126.
- (57) Pierik, A. J.; Roseboom, W.; Happe, R. P.; Bagley, K. A.; Albracht, S. P. J. *J. Biol. Chem.* **1999**, *274*, 3331.
- (58) Buhrke, T.; Brecht, M.; Lubitz, W.; Friedrich, B. *J. Biol. Inorg. Chem.* **2002**, *7*, 897.
- (59) Blokesch, M.; Paschos, A.; Theodoratou, E.; Bauer, A.; Hube, M.; Huth, S.; Bock, A. *Biochem. Soc. Trans.* **2002**, *30*, 674.
- (60) Reissmann, S.; Hochleitner, E.; Wang, H. F.; Paschos, A.; Lottspeich, F.; Glass, R. S.; Bock, A. *Science* **2003**, *299*, 1067.
- (61) Roseboom, W.; Blokesch, M.; Bock, A.; Albracht, S. P. J. *FEBS Lett.* **2005**, *579*, 469.
- (62) Casalat, L.; Rousset, M. *Trends Microbiol.* **2001**, *9*, 228.
- (63) Vignais, P. M.; Billoud, B.; Meyer, J. *FEMS Microbiol. Rev.* **2001**, *25*, 455.
- (64) Mulrooney, S. B.; Hausinger, R. P. *FEMS Microbiol. Rev.* **2003**, *27*, 239.
- (65) Winter, G.; Buhrke, T.; Lenz, O.; Jones, A. K.; Forger, M.; Friedrich, B. *FEBS Lett.* **2005**, *579*, 4292.
- (66) Magalon, A.; Bock, A. *J. Biol. Chem.* **2000**, *275*, 21114.
- (67) Theodoratou, E.; Paschos, A.; Magalon, A.; Fritsche, E.; Huber, R.; Bock, A. *Eur. J. Biochem.* **2000**, *267*, 1995.
- (68) Patil, D. S. *Methods Enzymol.* **1994**, *243*, 68.
- (69) Garcin, E.; Vernede, X.; Hatchikian, E. C.; Volbeda, A.; Frey, M.; Fontecilla-Camps, J. C. *Structure* **1999**, *7*, 557.
- (70) Peters, J. W.; Lanzilotta, W. N.; Lemon, B. J.; Seefeldt, L. C. *Science* **1998**, *282*, 1853.
- (71) Nicolet, Y.; Piras, C.; Legrand, P.; Hatchikian, C. E.; Fontecilla-Camps, J. C. *Struct. Folding Des.* **1999**, *7*, 13.
- (72) Nicolet, Y.; Lemon, B. J.; Fontecilla-Camps, J. C.; Peters, J. W. *Trends Biochem. Sci.* **2000**, *25*, 138.
- (73) Zirngibl, C.; Hedderich, R.; Thauer, R. K. *FEBS Lett.* **1990**, *261*, 112.
- (74) Thauer, R. K.; Klein, A. R.; Hartmann, G. C. *Chem. Rev.* **1996**, *96*, 3031.
- (75) Klein, A. R.; Fernandez, V. M.; Thauer, R. K. *FEBS Lett.* **1995**, *368*, 203.
- (76) Hartmann, G. C.; Santamaria, E.; Fernandez, V. M.; Thauer, R. K. *J. Biol. Inorg. Chem.* **1996**, *1*, 446.
- (77) Lyon, E. J.; Shima, S.; Buurman, G.; Chowdhuri, S.; Batschauer, A.; Steinbach, K.; Thauer, R. K. *Eur. J. Biochem.* **2004**, *271*, 195.
- (78) Shima, S.; Lyon, E. J.; Thauer, R. K.; Mienert, B.; Bill, E. *J. Am. Chem. Soc.* **2005**, *127*, 10430.
- (79) Buurman, G.; Shima, S.; Thauer, R. K. *FEBS Lett.* **2000**, *485*, 200.
- (80) Shima, S.; Lyon, E. J.; Sordel-Klippert, M. S.; Kauss, M.; Kahnt, J.; Thauer, R. K.; Steinbach, K.; Xie, X. L.; Verdier, L.; Griesinger, C. *Angew. Chem., Int. Ed.* **2004**, *43*, 2547.
- (81) Pilak, O.; Mamat, B.; Vogt, S.; Hagemeyer, C. H.; Thauer, R. K.; Shima, S.; Vonnheim, C.; Warkentin, E.; Ermler, U. *J. Mol. Biol.* **2006**, *358*, 798.
- (82) Lyon, E. J.; Shima, S.; Boecher, R.; Thauer, R. K.; Grevels, F. W.; Bill, E.; Roseboom, W.; Albracht, S. P. J. *J. Am. Chem. Soc.* **2004**, *126*, 14239.
- (83) Korbas, M.; Vogt, S.; Meyer-Klaucke, W.; Bill, E.; Lyon, E. J.; Thauer, R. K.; Shima, S. *J. Biol. Chem.* **2006**, *281*, 30804.
- (84) Siegbahn, P. E. M.; Blomberg, M. R. A. *Chem. Rev.* **2000**, *100*, 421.
- (85) Loscher, S.; Zebger, I.; Andersen, L. K.; Hildebrandt, P.; Meyer-Klaucke, W.; Haumann, M. *FEBS Lett.* **2005**, *579*, 4287.
- (86) Pickett, C. J.; Best, S. P. *Coord. Chem. Rev.* **2005**, *249*, 1517.
- (87) Capon, J. F.; Gloaguen, F.; Schollhammer, P.; Talarmin, J. *Coord. Chem. Rev.* **2005**, *249*, 1664.
- (88) Matias, P. M.; Pereira, I. A. C.; Soares, C. M.; Carrondo, M. A. *Prog. Biophys. Mol. Biol.* **2005**, *89*, 292.
- (89) Albracht, S. P. J. *Hydrogen as a Fuel: Learning from Nature*; Taylor & Francis: London and New York, 2001; p 110.
- (90) Albracht, S. P. J.; Graf, E. G.; Thauer, R. K. *FEBS Lett.* **1982**, *140*, 311.
- (91) Cammack, R.; Patil, D.; Aguirre, R.; Hatchikian, E. C. *FEBS Lett.* **1982**, *142*, 289.
- (92) LeGall, J.; Ljungdahl, P. O.; Moura, I.; Peck, H. D., Jr.; Xavier, A. V.; Moura, J. J. G.; Teixeira, M.; Huynh, B. H.; DerVartanian, D. V. *Biochem. Biophys. Res. Commun.* **1982**, *106*, 610.
- (93) Fernandez, V. M.; Hatchikian, E. C.; Patil, D.; Cammack, R. *Biochim. Biophys. Acta* **1986**, *883*, 145.
- (94) Teixeira, M.; Moura, I.; Xavier, A. V.; DerVartanian, D. V.; LeGall, J.; Peck, H. D., Jr.; Huynh, B. H.; Moura, J. J. G. *Eur. J. Biochem.* **1983**, *130*, 481.
- (95) Cammack, R.; Patil, D. S.; Hatchikian, E. C.; Fernandez, V. M. *Biochim. Biophys. Acta* **1987**, *912*, 98.
- (96) Coremans, J. M. C. C.; van der Zwaan, J. W.; Albracht, S. P. J. *Biochim. Biophys. Acta* **1989**, *997*, 256.
- (97) Teixeira, M.; Moura, I.; Xavier, A. V.; Moura, J. J. G.; LeGall, J.; DerVartanian, D. V.; Peck, H. D., Jr.; Huynh, B. H. *J. Biol. Chem.* **1989**, *264*, 16435.
- (98) Coremans, J. M. C. C.; Van Garderen, C. J.; Albracht, S. P. J. *Biochim. Biophys. Acta* **1992**, *1119*, 148.
- (99) Coremans, J. M. C. C.; van der Zwaan, J. W.; Albracht, S. P. J. *Biochim. Biophys. Acta* **1992**, *1119*, 157.
- (100) Roberts, L. M.; Lindahl, P. A. *Biochemistry* **1994**, *33*, 14339.
- (101) Roberts, L. M.; Lindahl, P. A. *J. Am. Chem. Soc.* **1995**, *117*, 2565.
- (102) Cammack, R.; Patil, D. S.; Fernandez, V. M. *Biochem. Soc. Trans.* **1985**, *13*, 572.
- (103) Guigliarelli, B.; More, C.; Fournel, A.; Asso, M.; Hatchikian, E. C.; Williams, R.; Cammack, R.; Bertrand, P. *Biochemistry* **1995**, *34*, 4781.
- (104) Albracht, S. P. J.; Kalkman, M. L.; Slater, E. C. *Biochim. Biophys. Acta* **1983**, *724*, 309.
- (105) Surerus, K. K.; Chen, M.; van der Zwaan, J. W.; Rusnak, F. M.; Kolk, M.; Duin, E. C.; Albracht, S. P. J.; Munck, E. *Biochemistry* **1994**, *33*, 4980.
- (106) Cammack, R.; Rao, K. K.; Serra, J.; Llama, M. J. *Biochimie* **1986**, *68*, 93.
- (107) De Lacey, A. L.; Hatchikian, E. C.; Volbeda, A.; Frey, M.; Fontecilla-Camps, J. C.; Fernandez, V. M. *J. Am. Chem. Soc.* **1997**, *119*, 7181.
- (108) Dole, F.; Fournel, A.; Magro, V.; Hatchikian, E. C.; Bertrand, P.; Guigliarelli, B. *Biochemistry* **1997**, *36*, 7847.
- (109) Huyett, J. E.; Carepo, M.; Pamplona, A.; Franco, R.; Moura, I.; Moura, J. J. G.; Hoffman, B. M. *J. Am. Chem. Soc.* **1997**, *119*, 9291.
- (110) Lai, C. H.; Lee, W. Z.; Miller, M. L.; Reibenspies, J. H.; Darensbourg, D. J.; Darensbourg, M. Y. *J. Am. Chem. Soc.* **1998**, *120*, 10103.
- (111) Higuchi, Y.; Toujou, F.; Tsukamoto, K.; Yagi, T. *J. Inorg. Biochem.* **2000**, *80*, 205.
- (112) Foerster, S.; Stein, M.; Brecht, M.; Ogata, H.; Higuchi, Y.; Lubitz, W. *J. Am. Chem. Soc.* **2003**, *125*, 83.
- (113) Moura, J. J. G.; Teixeira, M.; Moura, I.; Le Gall, J. *The Bioinorganic Chemistry of Nickel*; VCH Publishers: New York, 1988; p 191.
- (114) Davidson, G.; Choudhury, S. B.; Gu, Z. J.; Bose, K.; Roseboom, W.; Albracht, S. P. J.; Maroney, M. J. *Biochemistry* **2000**, *39*, 7468.
- (115) Fan, C.; Houseman, A. L. P.; Doan, P.; Hoffman, B. M. *J. Phys. Chem.* **1993**, *97*, 3017.
- (116) Bagyinka, C.; Whitehead, J. P.; Maroney, M. J. *J. Am. Chem. Soc.* **1993**, *115*, 3576.

- (117) Wang, H. X.; Ralston, C. Y.; Patil, D. S.; Jones, R. M.; Gu, W.; Verhagen, M.; Adams, M.; Ge, P.; Riordan, C.; Marganian, C. A.; Mascharak, P.; Kovacs, J.; Miller, C. G.; Collins, T. J.; Brooker, S.; Croucher, P. D.; Wang, K.; Stiefel, E. I.; Cramer, S. P. *J. Am. Chem. Soc.* **2000**, *122*, 10544.
- (118) Fan, H. J.; Hall, M. B. *J. Am. Chem. Soc.* **2002**, *124*, 394.
- (119) Gu, W. W.; Jacquamet, L.; Patil, D. S.; Wang, H. X.; Evans, D. J.; Smith, M. C.; Millar, M.; Koch, S.; Eichhorn, D. M.; Latimer, M.; Cramer, S. P. *J. Inorg. Biochem.* **2003**, *93*, 41.
- (120) Loschen, C.; Frenking, G. *Inorg. Chem.* **2004**, *43*, 778.
- (121) Bruschi, M.; De Gioia, L.; Zampella, G.; Reiher, M.; Fantucci, P.; Stein, M. *J. Biol. Inorg. Chem.* **2004**, *9*, 873.
- (122) Pardo, A.; De Lacey, A. L.; Fernandez, V. M.; Fan, H. J.; Fan, Y. B.; Hall, M. B. *J. Biol. Inorg. Chem.* **2006**, *11*, 286.
- (123) DeLacey, A. L.; Stadler, C.; Fernandez, V. M.; Hatchikian, E. C.; Fan, H. J.; Li, S. H.; Hall, M. B. *J. Biol. Inorg. Chem.* **2002**, *7*, 318.
- (124) Bleijlevens, B.; van Broekhuizen, F. A. A.; De Lacey, A. L.; Roseboom, W.; Fernandez, V. M.; Albracht, S. P. J. *J. Biol. Inorg. Chem.* **2004**, *9*, 743.
- (125) Fichtner, C.; Laurich, C.; Bothe, E.; Lubitz, W. *Biochemistry* **2006**, *45*, 9706.
- (126) Higuchi, Y.; Yagi, T.; Yasuoka, N. *Structure* **1997**, *5*, 1671.
- (127) DeLacey, A. L.; Fernandez, V. M.; Rousset, M.; Cavazza, C.; Hatchikian, E. C. *J. Biol. Inorg. Chem.* **2003**, *8*, 129.
- (128) van der Zwaan, J. W.; Albracht, S. P. J.; Fontijn, R. D.; Roelofs, Y. B. M. *Biochim. Biophys. Acta* **1986**, *872*, 208.
- (129) Happe, R. P.; Roseboom, W.; Albracht, S. P. J. *Eur. J. Biochem.* **1999**, *259*, 602.
- (130) Boison, G.; Schmitz, O.; Schmitz, B.; Bothe, H. *Curr. Microbiol.* **1998**, *36*, 253.
- (131) Fan, H. J.; Hall, M. B. *J. Am. Chem. Soc.* **2001**, *123*, 3828.
- (132) Fichtner, C.; van Gastel, M.; Lubitz, W. *Phys. Chem. Chem. Phys.* **2003**, *5*, 5507.
- (133) Medina, M.; Hatchikian, E. C.; Cammack, R. *Biochim. Biophys. Acta* **1996**, *1275*, 227.
- (134) Dole, F.; Medina, M.; More, C.; Cammack, R.; Bertrand, P.; Guigliarelli, B. *Biochemistry* **1996**, *35*, 16399.
- (135) De Gioia, L.; Fantucci, P.; Guigliarelli, B.; Bertrand, P. *Inorg. Chem.* **1999**, *38*, 2658.
- (136) Dementin, S.; Burlat, B.; De Lacey, A. L.; Pardo, A.; Adryanczyk-Perrier, G.; Guigliarelli, B.; Fernandez, V. M.; Rousset, M. *J. Biol. Chem.* **2004**, *279*, 10508.
- (137) Voordouw, G.; Strang, J. D.; Wilson, F. R. *J. Bacteriol.* **1989**, *171*, 3881.
- (138) He, S. H.; Teixeira, M.; LeGall, J.; Patil, D. S.; Moura, I.; Moura, J. J. G.; DerVartanian, D. V.; Huynh, B. H.; Peck, H. D., Jr. *J. Biol. Chem.* **1989**, *264*, 2678.
- (139) Eidsness, M. K.; Scott, R. A.; Prickril, B. C.; DerVartanian, D. V.; LeGall, J.; Moura, I.; Moura, J. J. G.; Peck, H. D., Jr. *Proc. Natl. Acad. Sci. U.S.A.* **1989**, *86*, 147.
- (140) Fauque, G.; Peck, H. D., Jr.; Moura, J. J. G.; Huynh, B. H.; Berlier, Y.; DerVartanian, D. V.; Teixeira, M.; Przybyla, A. E.; Lespinat, P. A.; Moura, I.; LeGall, J. *FEMS Microbiol. Rev.* **1988**, *54*, 299.
- (141) Berlier, Y.; Lespinat, P. A.; Dimon, B. *Anal. Biochem.* **1990**, *188*, 427.
- (142) Teixeira, M.; Fauque, G.; Moura, I.; Lespinat, P. A.; Berlier, Y.; Prickril, B.; Peck, H. D., Jr.; Xavier, A. V.; LeGall, J.; Moura, J. J. G. *Eur. J. Biochem.* **1987**, *167*, 47.
- (143) Teixeira, M.; Moura, I.; Fauque, G.; Czechowski, M.; Berlier, Y.; Lespinat, P. A.; LeGall, J.; Xavier, A. V.; Moura, J. J. G. *Biochimie* **1986**, *68*, 75.
- (144) Valente, F. M. A.; Oliveira, A. S. F.; Gnad, N.; Pacheco, I.; Coelho, A. V.; Xavier, A. V.; Teixeira, M.; Soares, C. M.; Pereira, I. A. C. *J. Biol. Inorg. Chem.* **2005**, *10*, 667.
- (145) Vignais, P. M.; Courmact, L.; Hatchikian, E. C.; Elsen, S.; Serebryakova, L.; Zorin, N.; Dimon, B. *Int. J. Hydrogen Energy* **2002**, *27*, 1441.
- (146) Sorgenfrei, O.; Duin, E. C.; Klein, A.; Albracht, S. P. J. *Eur. J. Biochem.* **1997**, *247*, 681.
- (147) Sorgenfrei, O.; Duin, E. C.; Klein, A.; Albracht, S. P. J. *J. Biol. Chem.* **1996**, *271*, 23799.
- (148) Muller, A.; Tscherny, I.; Kappl, R.; Hatchikian, E. C.; Huttermann, J.; Cammack, R. *J. Biol. Inorg. Chem.* **2002**, *7*, 177.
- (149) Happe, R. P.; Roseboom, W.; Egert, G.; Friedrich, C. G.; Massanz, C.; Friedrich, B.; Albracht, S. P. J. *FEBS Lett.* **2000**, *466*, 259.
- (150) Van der Linden, E.; Burgdorf, T.; De Lacey, A. L.; Buhrke, T.; Scholte, M.; Fernandez, V. M.; Friedrich, B.; Albracht, S. P. J. *J. Biol. Inorg. Chem.* **2006**, *11*, 247.
- (151) Van der Linden, E.; Burgdorf, T.; Bernhard, M.; Bleijlevens, B.; Friedrich, B.; Albracht, S. P. J. *J. Biol. Inorg. Chem.* **2004**, *9*, 616.
- (152) Burgdorf, T.; Loscher, S.; Liebisch, P.; Van der Linden, E.; Galender, M.; Lenzian, F.; Meyer-Klaucke, W.; Albracht, S. P. J.; Friedrich, B.; Dau, H.; Haumann, M. *J. Am. Chem. Soc.* **2005**, *127*, 576.
- (153) Muller, A.; Erkens, A.; Schneider, K.; Muller, A.; Nolting, H. F.; Sole, V. A.; Henkel, G. *Angew. Chem., Int. Ed. Engl.* **1997**, *36*, 1747.
- (154) Kleihues, L.; Lenz, O.; Bernhard, M.; Buhrke, T.; Friedrich, B. *J. Bacteriol.* **2000**, *182*, 2716.
- (155) Schneider, K.; Patil, D. S.; Cammack, R. *Biochim. Biophys. Acta* **1983**, *748*, 353.
- (156) Vincent, K. A.; Parkin, A.; Lenz, O.; Albracht, S. P. J.; Fontecilla-Camps, J. C.; Cammack, R.; Friedrich, B.; Armstrong, F. A. J. *J. Am. Chem. Soc.* **2005**, *127*, 18179.
- (157) Pierik, A. J.; Schmelz, M.; Lenz, O.; Friedrich, B.; Albracht, S. P. J. *FEBS Lett.* **1998**, *438*, 231.
- (158) Brecht, M.; van Gastel, M.; Buhrke, T.; Friedrich, B.; Lubitz, W. *J. Am. Chem. Soc.* **2003**, *125*, 13075.
- (159) Stein, M.; Lubitz, W. *Phys. Chem. Chem. Phys.* **2001**, *3*, 5115.
- (160) Siegbahn, P. E. M. *Adv. Inorg. Chem.* **2004**, *56*, 101.
- (161) Foerster, S.; van Gastel, M.; Brecht, M.; Lubitz, W. *J. Biol. Inorg. Chem.* **2005**, *10*, 51.
- (162) Haumann, M.; Porthun, A.; Buhrke, T.; Liebisch, P.; Meyer-Klaucke, W.; Friedrich, B.; Dau, H. *Biochemistry* **2003**, *42*, 11004.
- (163) Buhrke, T.; Loscher, S.; Lenz, O.; Schlodder, E.; Zebger, I.; Andersen, L. K.; Hildebrandt, P.; Meyer-Klaucke, W.; Dau, H.; Friedrich, B.; Haumann, M. *J. Biol. Chem.* **2005**, *280*, 19488.
- (164) Silva, P. J.; de Castro, B.; Hagen, W. R. *J. Biol. Inorg. Chem.* **1999**, *4*, 284.
- (165) Brugna-Guiral, M.; Tron, P.; Nitschke, W.; Stetter, K. O.; Burlat, B.; Guigliarelli, B.; Bruschi, M.; Giudici-Ortoniconi, M. T. *Extremophiles* **2003**, *7*, 145.
- (166) Adams, M. W. W. *Biochim. Biophys. Acta* **1990**, *1020*, 115.
- (167) Patil, D. S.; Moura, J. J. G.; He, S. H.; Teixeira, M.; Prickril, B. C.; DerVartanian, D. V.; Peck, H. D., Jr.; LeGall, J.; Huynh, B. H. *J. Biol. Chem.* **1988**, *263*, 18732.
- (168) Pierik, A. J.; Hagen, W. R.; Redeker, J. S.; Wolbert, R. B. G.; Boersma, M.; Verhagen, M. F. J. M.; Grande, H. J.; Veeger, C.; Mutsaers, P. H. A.; Sands, R. H.; Dunham, W. R. *Eur. J. Biochem.* **1992**, *209*, 63.
- (169) Hatchikian, E. C.; Forget, N.; Fernandez, V. M.; Williams, R.; Cammack, R. *Eur. J. Biochem.* **1992**, *209*, 357.
- (170) van der Spek, T. M.; Arendsen, A. F.; Happe, R. P.; Yun, S. Y.; Bagley, K. A.; Stufkens, D. J.; Hagen, W. R.; Albracht, S. P. J. *Eur. J. Biochem.* **1996**, *237*, 629.
- (171) Pierik, A. J.; Hulstein, M.; Hagen, W. R.; Albracht, S. P. J. *Eur. J. Biochem.* **1998**, *258*, 572.
- (172) Roseboom, W.; De Lacey, A. L.; Fernandez, V. M.; Hatchikian, E. C.; Albracht, S. P. J. *J. Biol. Inorg. Chem.* **2006**, *11*, 102.
- (173) Pereira, A. S.; Tavares, P.; Moura, I.; Moura, J. J. G.; Huynh, B. H. *J. Am. Chem. Soc.* **2001**, *123*, 2771.
- (174) Cao, Z.; Hall, M. B. *J. Am. Chem. Soc.* **2001**, *123*, 3734.
- (175) Liu, Z. P.; Hu, P. *J. Am. Chem. Soc.* **2002**, *124*, 5175.
- (176) Boyke, C. A.; Rauchfuss, T. B.; Wilson, S. R.; Rohmer, M. M.; Benard, M. *J. Am. Chem. Soc.* **2004**, *126*, 15151.
- (177) Boyke, C. A.; van der Vlugt, J. I.; Rauchfuss, T. B.; Wilson, S. R.; Zampella, G.; De Gioia, L. *J. Am. Chem. Soc.* **2005**, *127*, 11010.
- (178) Popescu, C. V.; Munck, E. *J. Am. Chem. Soc.* **1999**, *121*, 7877.
- (179) Fritz, G.; Griesshaber, D.; Seth, O.; Kroneck, P. M. H. *Biochemistry* **2001**, *40*, 1317.
- (180) De Lacey, A. L.; Stadler, C.; Cavazza, C.; Hatchikian, E. C.; Fernandez, V. M. *J. Am. Chem. Soc.* **2000**, *122*, 11232.
- (181) Razavet, M.; Davies, S. C.; Hughes, D. L.; Pickett, C. J. *Chem. Commun.* **2001**, 847.
- (182) Razavet, M.; Borg, S. J.; George, S. J.; Best, S. P.; Fairhurst, S. A.; Pickett, C. J. *Chem. Commun.* **2002**, 700.
- (183) Fiedler, A. T.; Brunold, T. C. *Inorg. Chem.* **2005**, *44*, 9322.
- (184) Nicolet, Y.; De Lacey, A. L.; Vernede, X.; Fernandez, V. M.; Hatchikian, E. C.; Fontecilla-Camps, J. C. *J. Am. Chem. Soc.* **2001**, *123*, 1596.
- (185) Telsler, J.; Benecky, M. J.; Adams, M. W. W.; Mortenson, L. E.; Hoffman, B. M. *J. Biol. Chem.* **1986**, *261*, 13536.
- (186) Rusnak, F. M.; Adams, M. W. W.; Mortenson, L. E.; Munck, E. *J. Biol. Chem.* **1987**, *262*, 38.
- (187) Le Cloirec, A.; Best, S. P.; Borg, S.; Davies, S. C.; Evans, D. J.; Hughes, D. L.; Pickett, C. J. *Chem. Commun.* **1999**, 2285.
- (188) Lyon, E. J.; Georgakaki, I. P.; Reibenspies, J. H.; Darensbourg, M. Y. *Angew. Chem., Int. Ed.* **1999**, *38*, 3178.
- (189) Schmidt, M.; Contakes, S. M.; Rauchfuss, T. B. *J. Am. Chem. Soc.* **1999**, *121*, 9736.
- (190) Zhao, X.; Georgakaki, I. P.; Miller, M. L.; Yarbrough, J. C.; Darensbourg, M. Y. *J. Am. Chem. Soc.* **2001**, *123*, 9710.
- (191) Zhao, X.; Georgakaki, I. P.; Miller, M. L.; Mejia-Rodriguez, R.; Chiang, C. Y.; Darensbourg, M. Y. *Inorg. Chem.* **2002**, *41*, 3917.
- (192) Georgakaki, I. P.; Miller, M. L.; Darensbourg, M. Y. *Inorg. Chem.* **2003**, *42*, 2489.
- (193) van der Vlugt, J. I.; Rauchfuss, T. B.; Whaley, C. M.; Wilson, S. R. *J. Am. Chem. Soc.* **2005**, *127*, 16012.

- (194) van der Vlugt, J. I.; Rauchfuss, T. B.; Wilson, S. R. *Chem.—Eur. J.* **2006**, *12*, 90.
- (195) Bruschi, M.; Fantucci, P.; De Gioia, L. *Inorg. Chem.* **2003**, *42*, 4773.
- (196) Zhou, T. J.; Mo, Y. R.; Liu, A. M.; Zhou, Z. H.; Tsai, K. R. *Inorg. Chem.* **2004**, *43*, 923.
- (197) Schwab, D. E.; Tard, C.; Brecht, E.; Peters, J. W.; Pickett, C. J.; Szilagy, R. K. *Chem. Commun.* **2006**, 3696.
- (198) Albracht, S. P. J.; Roseboom, W.; Hatchikian, E. C. *J. Biol. Inorg. Chem.* **2006**, *11*, 88.
- (199) Shima, S.; Thauer, R. K. *Chem. Rec.* **2007**, *7*, 37.
- (200) Berlier, Y. M.; Fauque, G.; Lespinat, P. A.; LeGall, J. *FEBS Lett.* **1982**, *140*, 185.
- (201) Hallahan, D. L.; Fernandez, V. M.; Hatchikian, E. C.; Cammack, R. *Biochim. Biophys. Acta* **1986**, *874*, 72.
- (202) Vignais, P. M. *Coord. Chem. Rev.* **2005**, *249*, 1677.
- (203) Lissolo, T.; Pulvin, S.; Thomas, D. J. *Biol. Chem.* **1984**, *259*, 11725.
- (204) Fernandez, V. M.; Hatchikian, E. C.; Cammack, R. *Biochim. Biophys. Acta* **1985**, *832*, 69.
- (205) Carepo, M.; Tierney, D. L.; Brondino, C. D.; Yang, T. C.; Pamplona, A.; Telsler, J.; Moura, I.; Moura, J. J. G.; Hoffman, B. M. *J. Am. Chem. Soc.* **2002**, *124*, 281.
- (206) Jones, A. K.; Lamle, S. E.; Pershad, H. R.; Vincent, K. A.; Albracht, S. P. J.; Armstrong, F. A. *J. Am. Chem. Soc.* **2003**, *125*, 8505.
- (207) Kurkin, S.; George, S. J.; Thorneley, R. N. F.; Albracht, S. P. J. *Biochemistry* **2004**, *43*, 6820.
- (208) George, S. J.; Kurkin, S.; Thorneley, R. N. F.; Albracht, S. P. J. *Biochemistry* **2004**, *43*, 6808.
- (209) Lamle, S. E.; Albracht, S. P. J.; Armstrong, F. A. *J. Am. Chem. Soc.* **2005**, *127*, 6595.
- (210) Niu, S. Q.; Thomson, L. M.; Hall, M. B. *J. Am. Chem. Soc.* **1999**, *121*, 4000.
- (211) Stein, M.; Lubitz, W. *J. Inorg. Biochem.* **2004**, *98*, 862.
- (212) Jayapal, P.; Sundararajan, M.; Hillier, I. H.; Burton, N. A. *Phys. Chem. Chem. Phys.* **2006**, *8*, 4086.
- (213) Ishii, M.; Takishita, S.; Iwasaki, T.; Peerapornpisal, Y.; Yoshino, J.; Kodama, T.; Igarashi, Y. *Biosci. Biotechnol. Biochem.* **2000**, *64*, 492.
- (214) Li, S. H.; Hall, M. B. *Inorg. Chem.* **2001**, *40*, 18.
- (215) Fan, H. J.; Hall, M. B. *J. Biol. Inorg. Chem.* **2001**, *6*, 467.
- (216) Stadler, C.; Lacey, A. L.; Montet, Y.; Volbeda, A.; Fontecilla-Camps, J. C.; Conesa, J. C.; Fernandez, V. M. *Inorg. Chem.* **2002**, *41*, 4424.
- (217) Stein, M.; Lubitz, W. *Curr. Opin. Chem. Biol.* **2002**, *6*, 243.
- (218) Pershad, H. R.; Duff, J. L. C.; Heering, H. A.; Duin, E. C.; Albracht, S. P. J.; Armstrong, F. A. *Biochemistry* **1999**, *38*, 8992.
- (219) Lamle, S. E.; Vincent, K. A.; Halliwell, L. M.; Albracht, S. P. J.; Armstrong, F. A. *Dalton Trans.* **2003**, 4152.
- (220) De Lacey, A. L.; Pardo, A.; Fernandez, V. M.; Dementin, S.; Adryanczyk-Perrier, G.; Hatchikian, E. C.; Rousset, M. *J. Biol. Inorg. Chem.* **2004**, *9*, 636.
- (221) Trofanchuk, O.; Stein, M.; Gessner, C.; Lenzian, F.; Higuchi, Y.; Lubitz, W. *J. Biol. Inorg. Chem.* **2000**, *5*, 36.
- (222) van Gastel, M.; Stein, M.; Brecht, M.; Schroder, O.; Lenzian, F.; Bittl, R.; Ogata, H.; Higuchi, Y.; Lubitz, W. *J. Biol. Inorg. Chem.* **2006**, *11*, 41.
- (223) van Gastel, M.; Fichtner, C.; Neese, F.; Lubitz, W. *Biochem. Soc. Trans.* **2005**, *33*, 7.
- (224) Stein, M.; van Lenthe, E.; Baerends, E. J.; Lubitz, W. *J. Am. Chem. Soc.* **2001**, *123*, 5839.
- (225) Stein, M.; Lubitz, W. *Phys. Chem. Chem. Phys.* **2001**, *3*, 2668.
- (226) Bleijlevens, B.; Faber, B. W.; Albracht, S. P. J. *J. Biol. Inorg. Chem.* **2001**, *6*, 763.
- (227) Volbeda, A.; Martin, L.; Cavazza, C.; Matho, M.; Faber, B. W.; Roseboom, W.; Albracht, S. P. J.; Garcin, E.; Rousset, M.; Fontecilla-Camps, J. C. *J. Biol. Inorg. Chem.* **2005**, *10*, 591.
- (228) Ogata, H.; Hirota, S.; Nakahara, A.; Komori, H.; Shibata, N.; Kato, T.; Kano, K.; Higuchi, Y. *Structure* **2005**, *13*, 1635.
- (229) Lamle, S. E.; Albracht, S. P. J.; Armstrong, F. A. *J. Am. Chem. Soc.* **2004**, *126*, 14899.
- (230) Soderhjelm, P.; Ryde, U. *J. Mol. Struct.: THEOCHEM* **2006**, *770*, 199.
- (231) Osz, J.; Bagyinka, C. *Biophys. J.* **2005**, *89*, 1984.
- (232) Osz, J.; Bodo, G.; Branca, R. M. M.; Bagyinka, C. *Biophys. J.* **2005**, *89*, 1957.
- (233) Loscher, S.; Burgdorf, T.; Buhrke, T.; Friedrich, B.; Dau, H.; Haumann, M. *Biochem. Soc. Trans.* **2005**, *33*, 25.
- (234) Petrov, R. R.; Utkin, I. B.; Popov, V. O. *Arch. Biochem. Biophys.* **1989**, *268*, 287.
- (235) Schneider, K.; Erkens, A.; Muller, A. *Naturwissenschaften* **1996**, *83*, 78.
- (236) Burgdorf, T.; Van der Linden, E.; Bernhard, M.; Yin, Q. Y.; Back, J. W.; Hartog, A. F.; Muijsers, A. O.; de Koster, C. G.; Albracht, S. P. J.; Friedrich, B. *J. Bacteriol.* **2005**, *187*, 3122.
- (237) Loscher, S.; Burgdorf, T.; Zebger, I.; Hildebrandt, P.; Dau, H.; Friedrich, B.; Haumann, M. *Biochemistry* **2006**, *45*, 11658.
- (238) Niu, S.; Hall, N. B. *Inorg. Chem.* **2001**, *40*, 6201.
- (239) Motiu, S.; Dogaru, D.; Gogonea, V. *Int. J. Quantum Chem.* **2007**, *107*, 1248.
- (240) van Haaster, D. J.; Jongejan, J. A.; Hagedoorn, P. L.; Hagen, W. R. *Int. J. Hydrogen Energy* **2006**, *31*, 1432.
- (241) Volbeda, A.; Fontecilla-Camps, J. C. *Coord. Chem. Rev.* **2005**, *249*, 1609.
- (242) Hallahan, D. L.; Fernandez, V. M.; Hatchikian, E. C.; Hall, D. O. *Biochimie* **1986**, *68*, 49.
- (243) Albracht, S. P. J. *Biochim. Biophys. Acta* **1994**, *1188*, 167.
- (244) Agrawal, A. G.; van Gastel, M.; Gartner, W.; Lubitz, W. *J. Phys. Chem. B* **2006**, *110*, 8142.
- (245) Armstrong, F. A. *Curr. Opin. Chem. Biol.* **2004**, *8*, 133.
- (246) van der Zwaan, J. W.; Coremans, J. M. C. C.; Bouwens, E. C. M.; Albracht, S. P. J. *Biochim. Biophys. Acta* **1990**, *1041*, 101.
- (247) Leger, C.; Dementin, S.; Bertrand, P.; Rousset, M.; Guigliarelli, B. *J. Am. Chem. Soc.* **2004**, *126*, 12162.
- (248) Morozov, S. V.; Voronin, O. G.; Karyakina, E. E.; Zorin, N. A.; Cosnier, S.; Karyakin, A. A. *Electrochem. Commun.* **2006**, *8*, 851.
- (249) Petrov, R. R.; Utkin, I. B.; Popov, V. O. *Arch. Biochem. Biophys.* **1989**, *268*, 298.
- (250) Bleijlevens, B.; Buhrke, T.; Van der Linden, E.; Friedrich, B.; Albracht, S. P. J. *J. Biol. Chem.* **2004**, *279*, 46686.
- (251) Vincent, K. A.; Cracknell, J. A.; Lenz, O.; Zebger, I.; Friedrich, B.; Armstrong, F. A. *Proc. Natl. Acad. Sci. U.S.A.* **2005**, *102*, 16951.
- (252) Guiral, M.; Tron, P.; Belle, V.; Aubert, C.; Leger, C.; Guigliarelli, B.; Giudici-Orticoni, M. T. *Int. J. Hydrogen Energy* **2006**, *31*, 1424.
- (253) Bernhard, M.; Buhrke, T.; Bleijlevens, B.; De Lacey, A. L.; Fernandez, V. M.; Albracht, S. P. J.; Friedrich, B. *J. Biol. Chem.* **2001**, *276*, 15592.
- (254) Vignais, P. M.; Dimon, B.; Zorin, N. A.; Tomiyama, M.; Colbeau, A. *J. Bacteriol.* **2000**, *182*, 5997.
- (255) Elsen, S.; Colbeau, A.; Chabert, J.; Vignais, P. M. *J. Bacteriol.* **1996**, *178*, 5174.
- (256) Black, L. K.; Fu, C.; Maier, R. J. *J. Bacteriol.* **1994**, *176*, 7102.
- (257) Volbeda, A.; Montet, Y.; Vernede, X.; Hatchikian, E. C.; Fontecilla-Camps, J. C. *Int. J. Hydrogen Energy* **2002**, *27*, 1449.
- (258) Duche, O.; Elsen, S.; Cournac, L.; Colbeau, A. *FEBS J.* **2005**, *272*, 3899.
- (259) Buhrke, T.; Lenz, O.; Krauss, N.; Friedrich, B. *J. Biol. Chem.* **2005**, *280*, 23791.
- (260) Mege, R. M.; Bourdillon, C. *J. Biol. Chem.* **1985**, *260*, 14701.
- (261) Ogata, H.; Mizoguchi, Y.; Mizuno, N.; Miki, K.; Adachi, S.; Yasuoka, N.; Yagi, T.; Yamauchi, O.; Hirota, S.; Higuchi, Y. *J. Am. Chem. Soc.* **2002**, *124*, 11628.
- (262) Berlier, Y.; Fauque, G. D.; LeGall, J.; Choi, E. S.; Peck, H. D., Jr.; Lespinat, P. A. *Biochem. Biophys. Res. Commun.* **1987**, *146*, 147.
- (263) Fox, J. D.; Kerby, R. L.; Roberts, G. P.; Ludden, P. W. *J. Bacteriol.* **1996**, *178*, 1515.
- (264) Silva, P. J.; van den Ban, E. C. D.; Wassink, H.; Haaker, H.; de Castro, B.; Robb, F. T.; Hagen, W. R. *Eur. J. Biochem.* **2000**, *267*, 6541.
- (265) Erkens, A.; Schneider, K.; Muller, A. *J. Biol. Inorg. Chem.* **1996**, *1*, 99.
- (266) Vincent, K. A.; Cracknell, J. A.; Clark, J. R.; Ludwig, M.; Lenz, O.; Friedrich, B.; Armstrong, F. A. *Chem. Commun.* **2006**, 5033.
- (267) Hyman, M. R.; Arp, D. J. *Biochim. Biophys. Acta* **1991**, *1076*, 165.
- (268) Hyman, M. R.; Arp, D. J. *Biochemistry* **1987**, *26*, 6447.
- (269) Sun, J. H.; Hyman, M. R.; Arp, D. J. *Biochemistry* **1992**, *31*, 3158.
- (270) Sun, J. H.; Arp, D. J. *Arch. Biochem. Biophys.* **1991**, *287*, 225.
- (271) Seefeldt, L. C.; Arp, D. J. *J. Bacteriol.* **1989**, *171*, 3298.
- (272) Magnani, P.; Doussiere, J.; Lissolo, T. *Biochim. Biophys. Acta* **2000**, *1459*, 169.
- (273) Sani, R. K.; Peyton, B. M.; Brown, L. T. *Appl. Environ. Microbiol.* **2001**, *67*, 4765.
- (274) Fernandez, V. M.; Rua, M. L.; Reyes, P.; Cammack, R.; Hatchikian, E. C. *Eur. J. Biochem.* **1989**, *185*, 449.
- (275) Kamachi, T.; Uno, S.; Hiraishi, T.; Okura, I. *J. Mol. Catal. A: Chem.* **1995**, *96*, 329.
- (276) Kutty, R.; Bennett, G. N. *J. Ind. Microbiol. Biotechnol.* **2006**, *33*, 368.
- (277) Zadorny, O. A.; Zorin, N. A.; Gogotov, I. N. *Biochemistry (Moscow)* **2000**, *65*, 1287.
- (278) Nedoluzhko, A. I.; Shumilin, I. A.; Mazhorova, L. E.; Popov, V. O.; Nikandrov, V. V. *Bioelectrochemistry* **2001**, *53*, 61.
- (279) Vincent, K. A.; Belsey, N. A.; Lubitz, W.; Armstrong, F. A. *J. Am. Chem. Soc.* **2006**, *128*, 7448.
- (280) Higuchi, Y.; Yagi, T. *Biochem. Biophys. Res. Commun.* **1999**, *255*, 295.
- (281) van Dijk, C.; van Berkel-Arts, A.; Veeger, C. *FEBS Lett.* **1983**, *156*, 340.
- (282) Clark, W. M. *The Oxidation-Reduction Potentials of Organic Systems*; Krieger Pub. Co.: Huntington, NY, 1972.

- (283) Parkin, A.; Cavazza, C.; Fontecilla-Camps, J. C.; Armstrong, F. A. *J. Am. Chem. Soc.* **2006**, *128*, 16808.
- (284) Adams, M. W. W. *J. Biol. Chem.* **1987**, *262*, 15054.
- (285) Lemon, B. J.; Peters, J. W. *Biochemistry* **1999**, *38*, 12969.
- (286) Bennett, B.; Lemon, B. J.; Peters, J. W. *Biochemistry* **2000**, *39*, 7455.
- (287) Lemon, B. J.; Peters, J. W. *J. Am. Chem. Soc.* **2000**, *122*, 3793.
- (288) Chen, Z. J.; Lemon, B. J.; Huang, S.; Swartz, D. J.; Peters, J. W.; Bagley, K. A. *Biochemistry* **2002**, *41*, 2036.
- (289) Zilberman, S.; Stiefel, E. I.; Cohen, M. H.; Car, R. *Inorg. Chem.* **2006**, *45*, 5715.
- (290) Krasna, A. I. *Enzyme Microb. Technol.* **1979**, *1*, 165.
- (291) Sorgenfrei, O.; Linder, D.; Karas, M.; Klein, A. *Eur. J. Biochem.* **1993**, *213*, 1355.
- (292) Hagen, W. R.; van den Berg, W. A. M.; van Dongen, W. M. A. M.; Reijerse, E. J.; van Kan, P. J. M. *J. Chem. Soc., Faraday Trans.* **1998**, *94*, 2969.
- (293) Montet, Y.; Amara, P.; Volbeda, A.; Vernede, X.; Hatchikian, E. C.; Field, M. J.; Frey, M.; Fontecilla-Camps, J. C. *Nat. Struct. Biol.* **1997**, *4*, 523.
- (294) Teixeira, V. H.; Baptista, A. M.; Soares, C. M. *Biophys. J.* **2006**, *91*, 2035.
- (295) Cohen, J.; Kim, K.; King, P.; Seibert, M.; Schulten, K. *Structure* **2005**, *13*, 1321.
- (296) Cohen, J.; Kim, K.; Posewitz, M.; Ghirardi, M. L.; Schulten, K.; Seibert, M.; King, P. *Biochem. Soc. Trans.* **2005**, *33*, 80.
- (297) Fisher, K.; Lowe, D. J.; Thorneley, R. N. F. *Biochem. J.* **1991**, *279*, 81.
- (298) Ensign, S. A.; Ludden, P. W. *J. Biol. Chem.* **1991**, *266*, 18395.
- (299) Menon, S.; Ragsdale, S. W. *Biochemistry* **1996**, *35*, 15814.
- (300) Siegbahn, P. E. M.; Blomberg, M. R. A.; Pavlov, M. W. N.; Crabtree, R. H. *J. Biol. Inorg. Chem.* **2001**, *6*, 460.
- (301) Maroney, M. J.; Bryngelson, P. A. *J. Biol. Inorg. Chem.* **2001**, *6*, 453.
- (302) Frey, M. *ChemBioChem* **2002**, *3*, 153.
- (303) Volbeda, A.; Fontecilla-Camps, J. C. *Dalton Trans.* **2003**, 4030.
- (304) De Lacey, A. L.; Fernandez, V. M.; Rousset, M. *Coord. Chem. Rev.* **2005**, *249*, 1596.
- (305) Page, C. C.; Moser, C. C.; Dutton, P. L. *Nature* **1999**, *402*, 47.
- (306) Rousset, M.; Montet, Y.; Guigliarelli, B.; Forget, N.; Asso, M.; Bertrand, P.; Fontecilla-Camps, J. C.; Hatchikian, E. C. *Proc. Natl. Acad. Sci. U.S.A.* **1998**, *95*, 11625.
- (307) Kurkin, S.; Meuer, J.; Koch, J.; Hedderich, R.; Albracht, S. P. J. *Eur. J. Biochem.* **2002**, *269*, 6101.
- (308) Bingemann, R.; Klein, A. *Eur. J. Biochem.* **2000**, *267*, 6612.
- (309) Bertrand, P.; Dole, F.; Asso, M.; Guigliarelli, B. *J. Biol. Inorg. Chem.* **2000**, *5*, 682.
- (310) Sazanov, L. A.; Hinchliffe, P. *Science* **2006**, *311*, 1430.
- (311) Matias, P. M.; Soares, C. M.; Saraiva, L. M.; Coelho, R.; Morais, J.; Le Gall, J.; Carrondo, M. A. *J. Biol. Inorg. Chem.* **2001**, *6*, 63.
- (312) Pieulle, L.; Morelli, X.; Gallice, P.; Lojou, E.; Barbier, P.; Czjzek, M.; Bianco, P.; Guerlesquin, F.; Hatchikian, E. C. *J. Mol. Biol.* **2005**, *354*, 73.
- (313) Aubert, C.; Brugna, M.; Dolla, A.; Bruschi, M.; Giudici-Ortoni, M. T. *Biochim. Biophys. Acta* **2000**, *1476*, 85.
- (314) Yahata, N.; Saitoh, T.; Takayama, Y.; Ozawa, K.; Ogata, H.; Higuchi, Y.; Akutsu, H. *Biochemistry* **2006**, *45*, 1653.
- (315) Rüdiger, O.; Abad, J. M.; Hatchikian, E. C.; Fernandez, V. M.; De Lacey, A. L. *J. Am. Chem. Soc.* **2005**, *127*, 16008.
- (316) Dementin, S.; Belle, V.; Bertrand, P.; Guigliarelli, B.; Adryanczyk-Perrier, G.; De Lacey, A. L.; Fernandez, V. M.; Rousset, M.; Leger, C. *J. Am. Chem. Soc.* **2006**, *128*, 5209.
- (317) Morelli, X.; Czjzek, M.; Hatchikian, E. C.; Bornet, O.; Fontecilla-Camps, J. C.; Palma, N. P.; Moura, J. J. G.; Guerlesquin, F. *J. Biol. Chem.* **2000**, *275*, 23204.
- (318) De Lacey, A. L.; Moiroux, J.; Bourdillon, C. *Eur. J. Biochem.* **2000**, *267*, 6560.
- (319) Leger, C.; Jones, A. K.; Roseboom, W.; Albracht, S. P. J.; Armstrong, F. A. *Biochemistry* **2002**, *41*, 15736.
- (320) De Gioia, L.; Fantucci, P.; Guigliarelli, B.; Bertrand, P. *Int. J. Quantum Chem.* **1999**, *73*, 187.
- (321) Sellmann, D.; Geipel, F.; Moll, M. *Angew. Chem., Int. Ed.* **2000**, *39*, 561.
- (322) Curtis, C. J.; Miedaner, A.; Ciancanelli, R.; Ellis, W. W.; Noll, B. C.; DuBois, M. R.; DuBois, D. L. *Inorg. Chem.* **2003**, *42*, 216.
- (323) Sellmann, D.; Prakash, R.; Heinemann, F. W. *Eur. J. Inorg. Chem.* **2004**, 1847.
- (324) Liu, P.; Rodriguez, J. A. *J. Am. Chem. Soc.* **2005**, *127*, 14871.
- (325) Zampella, G.; Bruschi, M.; Fantucci, P.; De Gioia, L. *J. Am. Chem. Soc.* **2005**, *127*, 13180.
- (326) Higuchi, Y.; Ogata, H.; Miki, K.; Yasuoka, N.; Yagi, T. *Structure* **1999**, *7*, 549.
- (327) Leger, C.; Jones, A. K.; Albracht, S. P. J.; Armstrong, F. A. *J. Phys. Chem. B* **2002**, *106*, 13058.
- (328) Fernandez, V. M.; Munilla, R.; Ballesteros, A. *Arch. Biochem. Biophys.* **1982**, *215*, 129.
- (329) Butt, J. N.; Filipiak, M.; Hagen, W. R. *Eur. J. Biochem.* **1997**, *245*, 116.
- (330) Liu, Z. P.; Hu, P. *J. Chem. Phys.* **2002**, *117*, 8177.
- (331) Zampella, G.; Greco, C.; Fantucci, P.; De Gioia, L. *Inorg. Chem.* **2006**, *45*, 4109.
- (332) Tsuda, M.; Dino, W. A.; Kasai, H. *Solid State Commun.* **2005**, *133*, 589.
- (333) Darensbourg, M. Y.; Lyon, E. J.; Zhao, X.; Georgakaki, I. P. *Proc. Natl. Acad. Sci. U.S.A.* **2003**, *100*, 3683.
- (334) Bruschi, M.; Fantucci, P.; De Gioia, L. *Inorg. Chem.* **2002**, *41*, 1421.
- (335) Zhou, J.; Mo, Y. R.; Zhou, Z. H.; Tsal, K. *Inorg. Chem.* **2005**, *44*, 4941.
- (336) Gloaguen, F.; Lawrence, J. D.; Schmidt, M.; Wilson, S. R.; Rauchfuss, T. B. *J. Am. Chem. Soc.* **2001**, *123*, 12518.
- (337) Borg, S. J.; Behrsing, T.; Best, S. P.; Razavet, M.; Liu, X. M.; Pickett, C. J. *J. Am. Chem. Soc.* **2004**, *126*, 16988.
- (338) Brown, S. D.; Mehn, M. P.; Peters, J. C. *J. Am. Chem. Soc.* **2005**, *127*, 13146.
- (339) Schwartz, L.; Eilers, G.; Eriksson, L.; Gogoll, A.; Lomoth, R.; Ott, S. *Chem. Commun.* **2006**, 520.
- (340) Fiedler, A. T.; Brunold, T. C. *Inorg. Chem.* **2005**, *44*, 1794.
- (341) Schleucher, J.; Schwörer, B.; Thauer, R. K.; Griesinger, C. *J. Am. Chem. Soc.* **1995**, *117*, 2941.

CR0501947